AD-A189 727 MICROMECHANICS MODELS FOR UNSATURATED SATURATED AND DRY SANDS(U) WISCONSIN UNIV-MADISON J K JEVAPALAN ET AL 25 JAN 88 AFOSR-TR-88-0154 AFOSR-84-0090 1/3

UNCLASSIFIED F/G 8/10 NL

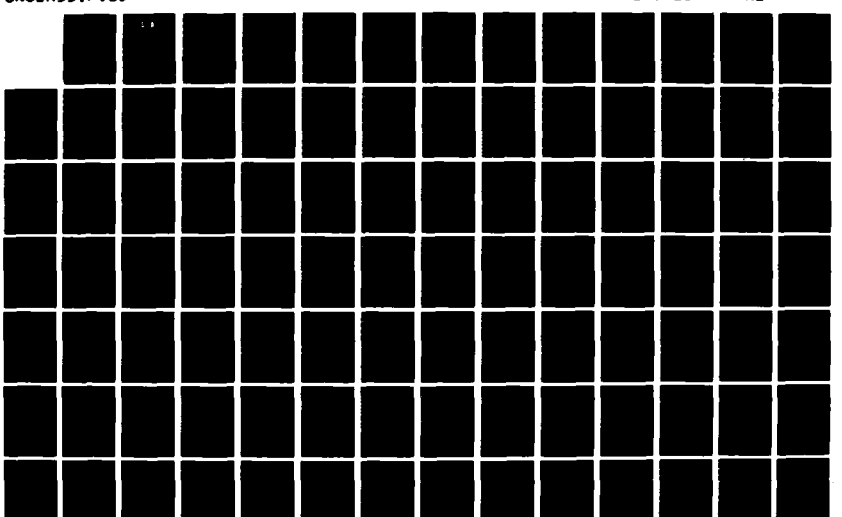

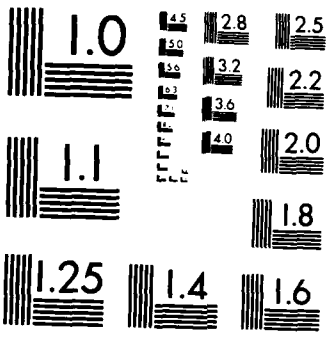

AD-A189 727

MENTATION PAGE

Form Approved
OMB No. 0704-0188

UNCLASSIFIED	1b. RESTRICTIVE MARKINGS
2a. SECURITY CLASSIFICATION AUTHORITY	3. DISTRIBUTION/AVAILABILITY OF REPORT: Approved for Public Release; Distribution Unlimited
2b. DECLASSIFICATION/DOWNGRADING SCHEDULE	
4. PERFORMING ORGANIZATION REPORT NUMBER(S)	5. MONITORING ORGANIZATION REPORT NUMBER(S): AFOSR-TR- 88-0134
6a. NAME OF PERFORMING ORGANIZATION: University of Wisconsin	6b. OFFICE SYMBOL (If applicable):
6c. ADDRESS (City, State, and ZIP Code): 2304 Engineering Building, University of Wisconsin, Madison 53706.	7a. NAME OF MONITORING ORGANIZATION: AFOSR/NA
8a. NAME OF FUNDING/SPONSORING ORGANIZATION: AFOSR	8b. OFFICE SYMBOL (If applicable): NA
8c. ADDRESS (City, State, and ZIP Code): Bldg. 410, Bolling AFB, DC 20332-6448	7b. ADDRESS (City, State, and ZIP Code): Bldg. 410, Bolling AFB, DC 20332-6448
	9. PROCUREMENT INSTRUMENT IDENTIFICATION NUMBER: AFOSR-84-0090
	10. SOURCE OF FUNDING NUMBERS: PROGRAM ELEMENT NO. 6.1102F; PROJECT NO. 2302; TASK NO C1; WORK UNIT ACCESSION NO.

11. TITLE (Include Security Classification) (U)
Micromechanics Models for Unsaturated, Saturated, and Dry Sands

12. PERSONAL AUTHOR(S)
J. K. Jeyapalan, M. Thiyagaram, and W. E. Saleira

13a. TYPE OF REPORT	13b. TIME COVERED	14. DATE OF REPORT (Year, Month, Day)	15. PAGE COUNT
Final-	FROM 4-1-84 TO 9-30-87	25 Jan 88	217

16. SUPPLEMENTARY NOTATION

17. COSATI CODES		
FIELD	GROUP	SUB-GROUP

18. SUBJECT TERMS (Continue on reverse if necessary and identify by block number)

19. ABSTRACT (Continue on reverse if necessary and identify by block number)

In this report, models for saturated and unsaturated soils are reviewed. In addition, the applicability of micromechanics modelling for unsaturated, saturated, and dry sands are explored. The expressions for effective moduli and poisson's ratio are developed for all levels of saturation of sands. The potential of these models for providing a better understanding of partly saturated soil behavior is also discussed on this report.

20. DISTRIBUTION/AVAILABILITY OF ABSTRACT	21. ABSTRACT SECURITY CLASSIFICATION
☒ UNCLASSIFIED/UNLIMITED ☐ SAME AS RPT ☐ DTIC USERS	UNCLASSIFIED
22a. NAME OF RESPONSIBLE INDIVIDUAL: Major Steven C. Boyce	22b. TELEPHONE (Include Area Code): (202) 767-6963 / 22c. OFFICE SYMBOL: AFOSR/NA

DD Form 1473, JUN 86 — Previous editions are obsolete. — SECURITY CLASSIFICATION OF THIS PAGE

UNCLASSIFIED

TABLE OF CONTENTS

Acknowledgements

It is a pleasure to thank Messers Rollie Boehm, Ernie Hanna, and Hassan Ben Hamida for their help with this research investigation. The financial support of the AFOSR and the technical assistance from the program managers, Major Steven C. Boyce, and Dr. Spencer Wu are gratefully acknowledged.

MICROMECHANICS MODELS FOR UNSATURATED, SATURATED, AND DRY SANDS

By

Jey K. Jeyapalan
M. Thiyagaram
W. E. Saleira

2304 Engineering Building
University of Wisconsin
Madison, Wisconsin, 53706.

Report to the

Air Force Office of Scientific Research
Bolling Air Force Base
Washington, DC

25 January 1988

CHAPTER 1

INTRODUCTION

1.1 Background

Recently much work has been directed towards developing constitutive models to represent the complex load-deformation behavior of soils. The models developed to date have primarily been for the special cases of dry and completely saturated soils. The use of these constitutive models in representing the behavior of partly saturated soils has resulted in inaccurate predictions of soil response. It is the intent of this research to formulate a constitutive model describing the behavior of partly saturated soils.

There are essentially two approaches which have been used by those attempting to develop constitutive laws for soils. The first approach is termed phenomenological modeling. Phenomenological models may be defined as those concerned with describing material behavior on the size scale of the experiment. For soils, thousands to millions of soil grains and pores would be included in a model representation of this type. Phenomenological methods or theories include emprical curve fitting, elastic theories, elastic-plastic theories, and visco-elastic theories. These methods and continuum theories are concerned with describing the overall observable behavior of the soil mass. They are not concerned with describing the actual mechanisms causing deformation, which act on the level of the grains and pores which comprise the soil mass. The second type of approach is termed micromechanical modeling. This approach attempts to derive constitutive laws by considering the deformation mechanisms acting on

a very small but representative sample of the material. For soils, a micromechanical model description might include one to hundreds of grains and pores in the model description.

The primary problem with constitutive models representing soils, is a failure to describe all aspects of their load-deformation behavior. While a model may give reasonable predictions under one set of input, it may fail to predict the soil response under another set of input. With the present knowledge it appears that a constitutive model representing all aspects of soil behavior may not be obtainable. This is due partly to a lack of understanding of the mechanisms causing soil deformation and partly due to the mathematical complexities one may encounter when modeling soils. A micromechanical approach to the constitutive modeling of soils may provide a better means to understand the soil load-deformation mechanisms.

1.2 Scope of Work

The purpose of the research studies contained in this report is to develop a constitutive model representing the load-deformation behavior of soils. The following types of investigations are contained in this report:

a) Review of the available literature on previously developed constitutive models describing the load-deformation behavior of soils.

b) Development of a constitutive model to represent the response of partly saturated soils using micromechanics, under idealized conditions.

1.3 Method of Approach and Organization

The studies undertaken to achieve this objective are described in

the subsequent chapters.

Chapter 2 contains a brief description of experimentally observed load-response behavior of soils and review of previously developed constitutive models describing this behavior.

Chapter 3 contains the solution to the problem of an elastic sphere in contact with a number of neighboring elastic spheres.

Chapter 4 contains the development of the effective moduli to describe the elastic behavior of a number of spheres in contact while surrounded by a liquid matrix phase.

Chapter 5 contains the extension of the work described in the previous chapter to three-phase systems.

Chapter 6 presents conclusions and recommendations.

CHAPTER 2

PREVIOUS WORK

2.1 Load-Deformation Behavior of Soils

When a soil mass is subjected to any arbitrary set of surface tractions, the result is a volume and shear deformation of the soil mass. The resulting displacement and stress fields within the soil mass depend on a number of variables. These variables include the type of loads applied to the soil mass, the stress history of the soil mass and the chemical, and the physical properties of the soil mass.

Experimental observations of the response of a soil mass to various applied loads have provided a great deal of information concerning the load-deformation behavior of soils. This information provided by experimental work will be briefly discussed in the next four subsections.

2.1.1 Soil Behavior During Initial or First Loading

The term initial or first loading will be understood to refer to a state of stress, occurring within the soil mass, which the soil is experiencing for the first time. In Fig. 2.1, the initial loading curves correspond to those lying beteeen points 1 and 2, and points 3 and 4. The arrows shown in Fig. 2.1 indicate the load path taken.

The amount of volume deformation resulting from an increase in stress will depend on the relative density of the soil mass. The relative density relates the actual void ratio of the soil to the maximum and minimum void ratios possible within the soil mass.

2.1.2 Soil Behavior During Unloading and Reloading

When an applied load is removed from a soil mass, rebound will normally

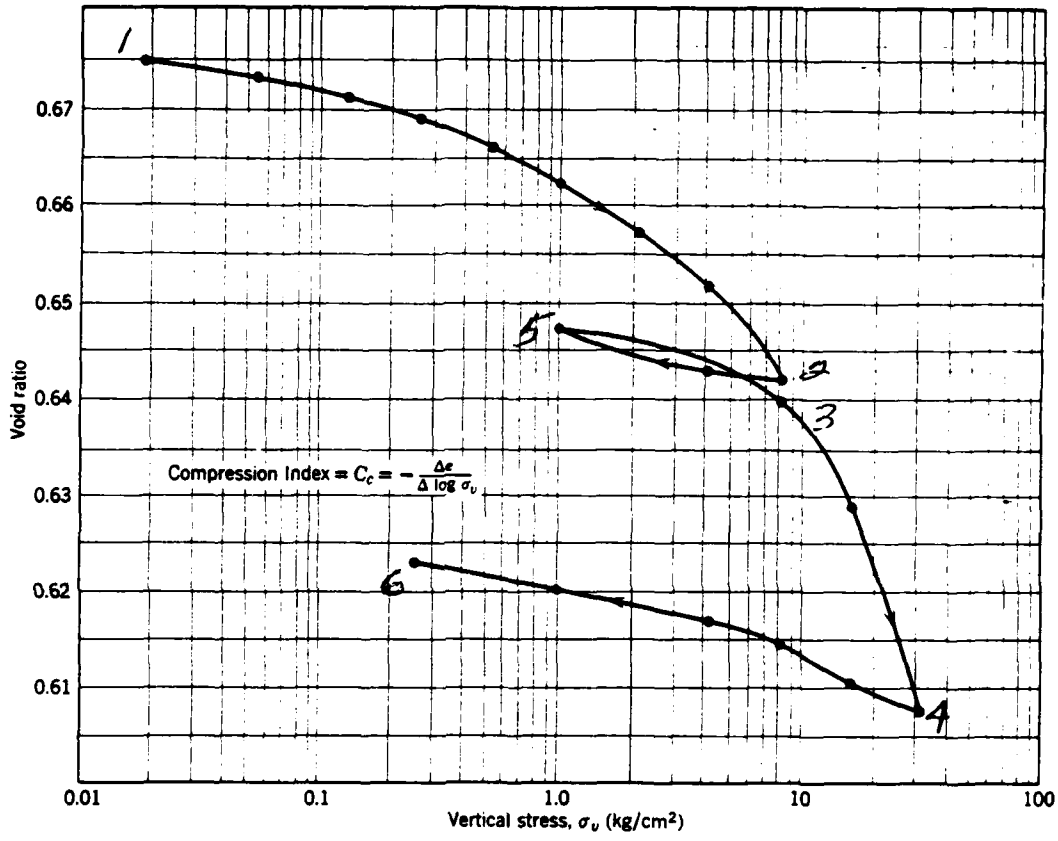

Results of confined compression test plotted as void ratio versus stress on logarithmic scale.

FIG. 2.1

occur resulting in an increase in soil volume. The stress path taken by the soil mass during unloading will typically be different from that taken during initial loading. A typical unloading curve is shown in Fig. 2.1 as that portion of the curve lying between points 2 and 5. An important fact in Fig. 2.1 is that the stress occurring within the soil mass is not a single-valued function of strain. Instead, the stress at a particular value of strain may be multi-valued.

The term reloading refers to the addition of a load to the soil mass which results in a stress state previously experienced by the soil. A typical reload curve is shown in Fig. 2.1 as that portion of the curve connecting points 5 and 3. When a soil experiences an unload-reload cycle, there will, in general, be a volume change associated with this cycle. As shown in Fig. 2.1, the unload-reload cycle begins at point 2 and ends at point 3. The volume change which occurs during this cycle is proportional to the difference in the volumetric strains corresponding to points 5 and 3 When the reload path reaches point 3 of Fig. 2.1, continued loading will follow a path similar to that for initial loading.

There will be an energy loss associated with the unload-reload cycle as apparent from the hystersis loop shown in Fig. 2.1. This demonstrates the effect of damping present within a soil mass.

2.1.3 Behavior of Soils in Simple Shear

The term simple shear means that the soil is loaded in pure shear. The behavior of soils when loaded in simple shear will depend on the initial relative density of the soil. When a soil of an initially low relative density is loaded in simple shear, a densification of the soil will result. This decrease in volume is due to particle rearrangement, yielding and fracture. Densification continues with increased loading until a minimum void

ratio is reached. Continued loading will cause the soil to fail. A dilation of the soil mass is usually associated with this failure. The dilation of the soil mass occurs because, in order for the soil to fail, grains must ride over one another. Soils which exhibit such behavior are loose granular materials and normally consolidated clays. For soils of initially high relative density, little densification occurs from the application of a simple shear loading. Rather, a dilation of the soil mass will occur since the void ratio of the soil mass is already near its minimum value. Soils which show this type of behavior are dense sands and overconsolidated clays. Typical stress-strain curves for different soils loaded in pure shear are shown in Fig. 2.2.

2.1.4 Soil Deformation in Time

For some soils, the total deformation resulting from the application of a load will not occur instantaneously, but over a period of time. This type of deformation is referred to as consolidation and occurs in silts and clays. Theories which predict the amount and rate of consolidation usually consider the soil to be saturated. The load is initially transferred to the liquid phase present in the pores of the soil mass. This results in an increase in the pore pressure so that steady-state conditions in the pores no longer exist. Over a period of time, liquid will flow from the pores, thus causing a dissipation of the pore pressures. This continues until hydrostatic pressure is achieved. As the pressure is dissipated from the pores, the load will be transferred to the soil grains resulting in consolidation of the soil mass. The permeability of the soil controls the rate at which consolidation takes place. This behavior is termed primary consolidation and is shown in Fig. 2.3.

Secondary consolidation or creep is also shown in Fig. 2.3. Secondary consolidation is defined as the deformation which takes place after the pore

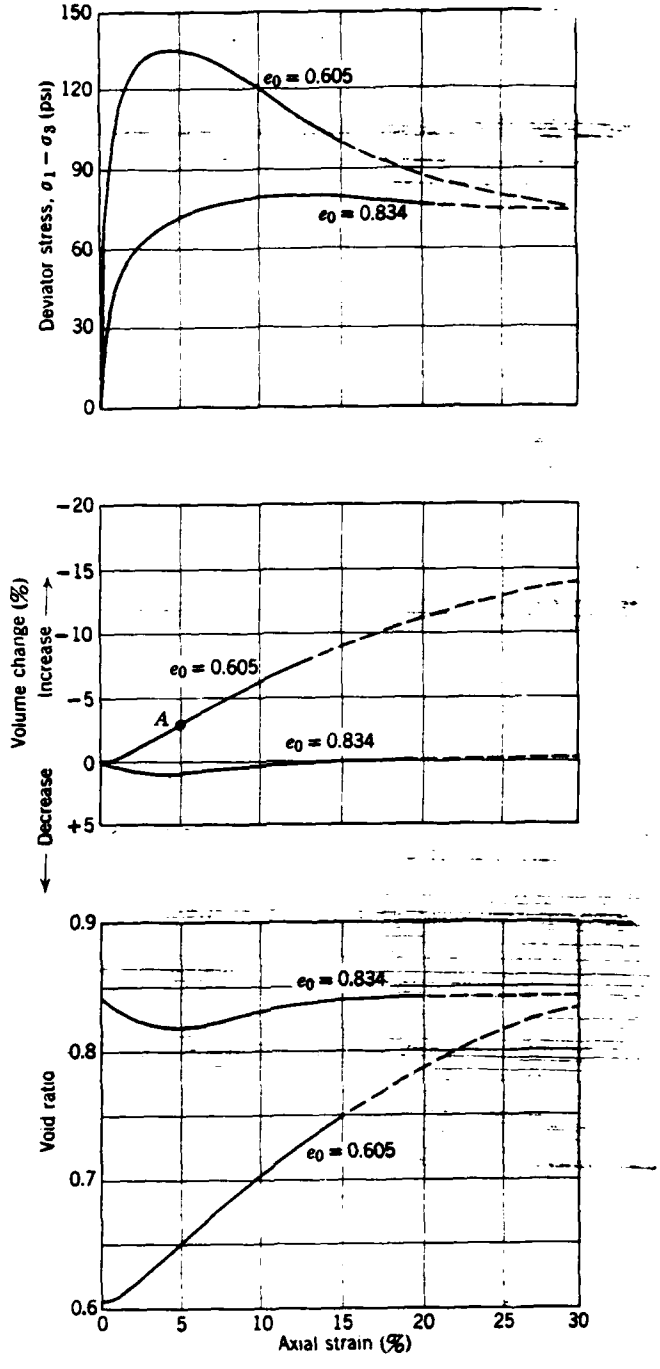

Stress-strain curves for loose and dense specimens. Medium-fine sand. $\sigma_3 = 30$ lb/in.^{2}: $e_0 = 0.605 \approx 100\%\ D_r$; $e_0 = 0.834 \approx 20\%\ D_r$. Solid line, actual test data; dashed li..., extrapolations based on results of other tests. (After Taylor, 1948.)

FIG. 2.2

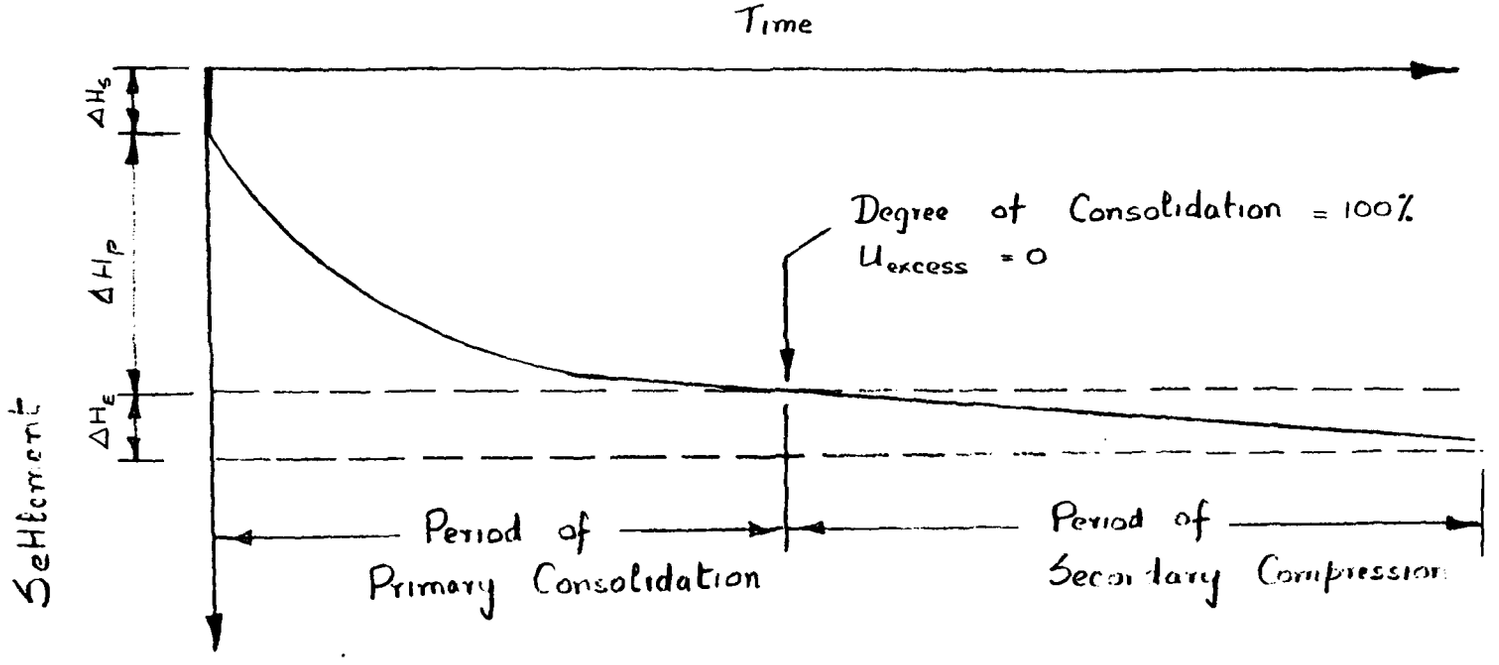
Time
ΔH_s
ΔH_p
ΔH_e
Settlement
Degree of Consolidation = 100%
U_{excess} = 0
Period of
Primary Consolidation
Period of
Secondary Compression

FIG. 2.3

pressures have reached steady state conditions. Although theories exist for the prediction of secondary consolidation, none have yet found general acceptance.

2.2 Constitutive Models Representing Soil Behavior

Over the last two decades much work has been done to develop constitutive models to represent the load-deformation behavior of soils. Thus far, most of these models have been used to represent the behavior of dry or completely saturated soils. When these models have been used to predict the behavior of partly saturated soils, they have yielded poor results for the soil response. However, these models are worthy of some attention, since they provide insight to the approaches which have been taken to develop constitutive laws describing soil behavior.

The procedure of developing a constitutive model for soils has followed two approaches. These two approaches are termed phenomenological and micromechanical modeling. The following sections of this report will discuss the soil models obtained from these two approaches.

2.2.1 Phenomenological Models

Phenomenological models are those concerned with describing behavior on the scale of the experiment. These models treat soil as a continuum including thousands to millions of soil grains and pores in the model representation. Phenomenological methods or theories include mathematical curve fitting, elasticity theory, plasticity theory and visco-elasticity theory. The soil constitutive models developed from these methods or theories are discussed below in detail.

2.2.1.1 Empirical Models

A number of models representing soil behavior have been developed using empirical curve fitting methods. This approach entails making a mathematical

fit to experimental data. In this manner, the response of the soil due to some specific input may be predicted. Herein, the input and the response are those measured experimentally.

Many researchers have taken the empirical approach to modeling the pressure-volume behavior of soils. Herrmann (1971) took such an approach in introducing the "P-α" description. In his model, the pressure was assumed to be a function of the specific volume, internal energy and the porosity of the soil. The relationship Herrmann proposed is

$$P = f\left(\frac{v_s}{\alpha},\ u_s\right) \tag{2.1a}$$

$$\alpha = \frac{v_s}{v_m} \tag{2.1b}$$

where v_s = specific volume

u_s = specific internal energy

v_m = specific volume of the matrix material

In Eqs. (2.1), the function f was assumed to be identical to that which relates pressure and volume for a mass composed entirely of matrix material. Carrol and Holt (1972) proposed that it was more reasonable to represent the pressure-volume relationship for soils by

$$P = \frac{1}{\alpha} f\left(\frac{v_s}{\alpha},\ u_s\right) \tag{2.2}$$

If the pressure volume relationship for the matrix material is known, the problem reduces to determining the function

$$\alpha = q\ (P) \tag{2.3}$$

The determination of the porosity provides the pressure-volume relationship

for the complete material. This model used the Mie-Gruneisen equation of state (see Carrol and Holt, 1972) to describe the function f. This equation is

$$P = P_r + (u_s - u_r) \frac{T_g}{v_s} \tag{2.4}$$

where P = pressure

P_r = a reference pressure

u_s = specific internal energy

u_r = a reference specific energy

v_s = specific volume

T_g = Gruneisen ratio

The Gruneisen ratio is given by

$$T_g = v_s \left(\frac{\partial P}{\partial T}\right) C_v \tag{2.5}$$

where T = temperature

C_v = specific heat at constant volume

A polynominal fit was then used to describe the function g. For situations where the variation in internal energy is less important, Butkovich (1973) developed a model relating the porosity to the applied pressure. The expression he obtained is

$$\frac{1}{\alpha} = \frac{1 - (1 - \frac{1}{\alpha_o}) \ln(\frac{P}{P_c})}{\ln(\frac{P_e}{P_c})} \tag{2.6}$$

where α_o = initial value of

P_e = the pressure required for the onset of pore closure

P_c = the pressure required for pressures within the range

The Eq. (2.4) is applicable for pressures within the range between P_e and P_c. For pressures less than P_e, the pressure-volume relationship for the matrix material is used. In Butkovich's work, the pressure-volume relationship for the matrix material was assumed to be given by soil unloading data. A polynomial fit to initial loading data was used to determine the pressure volume relationship for pressures lying between P_e and P_c. Other empirical models describing the pressure-volume relationship of soils have been developed, but the models cited above are representative of this work.

Other models have been developed which made mathematical fits to deviator stress-strain data. The simplest model of this type is obtained by approximating deviator stress versus strain data by a series of piecewise linear curves. This type of approximation is shown in Fig. 2.4. More sophisticated mathematical fits such as hyperbolas and cubic splices have been used to relate the deviator stress to the strain data. The most popular of these methods is the hyperbolic stress-strain model developed by Duncan and Chang (1970). This model is based on the finding that the deviator stress versus strain curves for a number of soils can be approximated by hyperbolas like the one shown in Fig. 2.5. This hyperbola may be represented by

$$(\sigma_1 - \sigma_3) = \frac{\varepsilon}{\frac{1}{E_i} + \frac{\varepsilon}{(\sigma_1 - \sigma_3)_{ULT}}} \qquad (2.7)$$

where $\sigma_1 - \sigma_3$ = deviator stress

ε = strain

E_1 = initial tangent modulus

The Eq. (2.7) may be transformed so that it will plot as a straight line. This transformed equation is

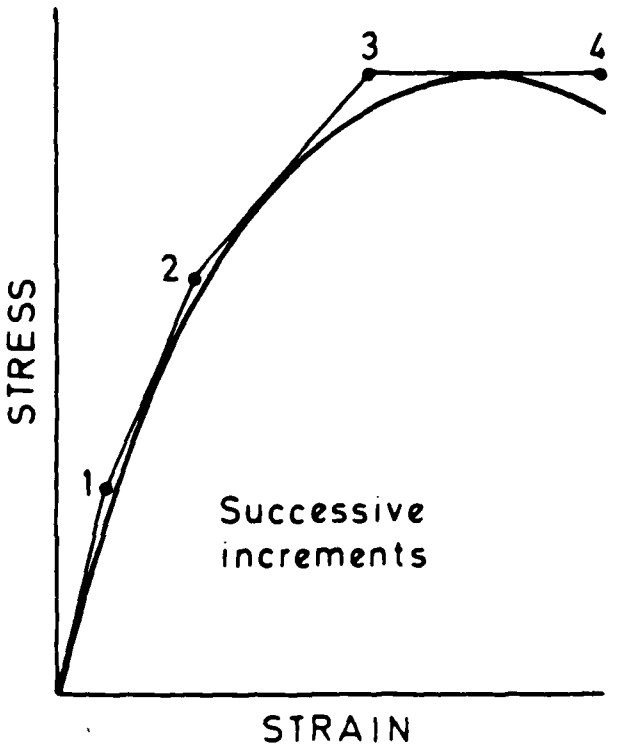

FIG. 2.4

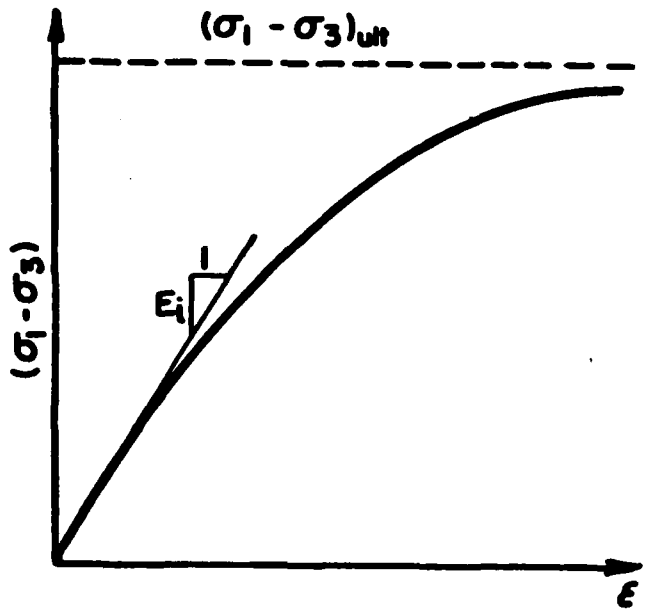

REAL

$$(\sigma_1-\sigma_3) = \frac{\varepsilon}{\frac{1}{E_i} + \frac{\varepsilon}{(\sigma_1-\sigma_3)_{ult}}}$$

FIG. 2.5

$$\frac{\varepsilon}{(\sigma_1 - \sigma_3)} = \frac{1}{E_1} + \frac{\varepsilon}{(\sigma_1 - \sigma_3)_{ULT}} \qquad (2.8)$$

A plot of Eq. (2.8) is shown in Fig. 2.6. Other empirical relations are used to account for the variation in soil strength with confining pressure and modulus values for loading and unloading. Because of these relationships, the hyperbolic model requires a number of parameters for its use. The hypobolic model also fails to realistically model actual soil behavior at or near failure.

In general, there are some basic problems associated with soil models developed from empirical models. First, an empirical model cannot be expected to provide reasonable predictions of soil behavior when the soil and site conditions being modeled deviate greatly from those used to calibrate the model. Second, this type of model cannot be expected to provide any insight to the actual physical deformation mechanisms acting within the soil mass. Despite these shortcomings empirical models are frequently used due to their simplicity.

2.2.1.2 Nonlinear Elastic Models

Some models representing soil behavior have been developed using nonlinear elasticity theories. However, these theories have not found widespread use since their predictions of unload behavior do not represent actual soil behavior. For cases where initial loading is of interest, nonlinear elasticity theories may provide reasonable predictions of soil response.

Hyperelastic constitutive laws have been used to represent soil behavior. These models use constitutive laws obtained by the differentiation of a strain energy function. Different orders of hyperelastic models are obtained by retaining the higher order derivatives obtained from the strain energy function. Hyperelastic soil models may be used to represent initial loading.

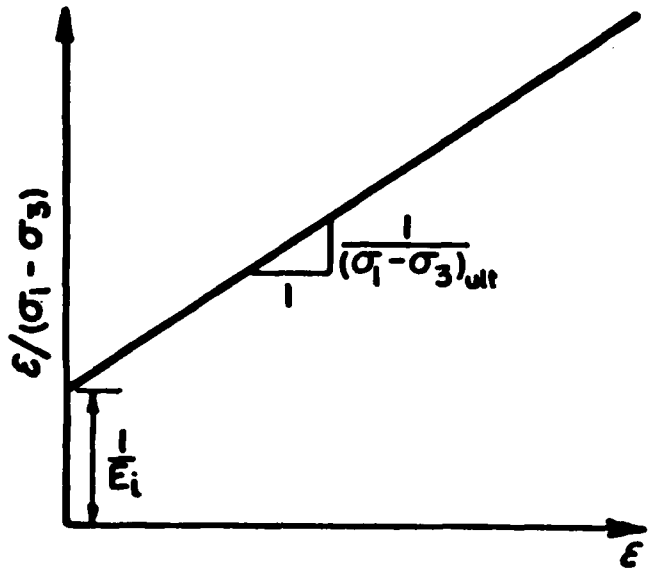

TRANSFORMED

$$\frac{\varepsilon}{(\sigma_1-\sigma_3)} = \frac{1}{E_i} + \frac{\varepsilon}{(\sigma_1-\sigma_3)_{ult}}$$

FIG. 2.6

Truesdale has proposed a rate theory which states that the rate of change of stress is a function of the rate of change of strain. This is known as the hypoelastic formulation. At present, this formulation has not been used in representing the load-deformation behavior of soils.

2.2.1.3 Elastic-Plastic Models

Elastic-plastic theory had been widely used in soil modeling. Recently, many constitutive models for soils have been presented which use this theory.

In general, this type of model assumed a yield criterion of the form

$$F(\tau_{ij}, e_{ij}^{p}, \chi) = 0 \qquad (2.9)$$

where τ_{ij} = stress tensor

e_{ij} = plastic strain tensor

χ = work hardening parameter

When the above equation is not satisfied ($F(\tau_{ij}, e_{ij}^{p}, \chi) < 0$) the material is said to behave elastically. When Eq. (2.9) is satisfied, the behavior is said to be elastic-plastic. Further deformation beyond the point where Eq. (2.9) is satisfied occurs at a combination of elastic and plastic strains, prescribed by an assumed flow rule. The yield surface is typically described in stress space as shown in Fig. 2.7. For a known stress point inside this region, the strains are found using elastic constitutive laws. When the stress point lies on the yield surface, the total strain is a combination of elastic and plastic strains. For a stress point lying on the yield surface, further loading may cause the surface to expand, translate or both, according to the work-hardening rule assumed. Unloading may be elastic or elastic-plastic. An example of the movement of the yield surface in the principal stress space is shown in Fig. 2.8. The material is initially unstressed at

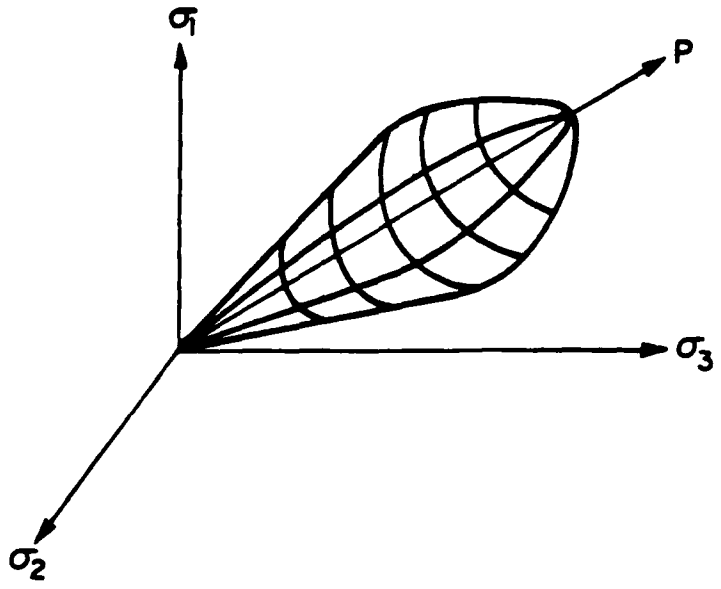

CAP MODEL IN PRINCIPAL STRESS SPACE

FIG. 2.7

point 0 and is then loaded to point 1. The behavior of the material when following this load path is elastic, since it lies within the initial yield surface. At point 1, the stress point lies on the yield surface such that further loading will result in behavior that may be elastic-plastic or elastic, depending on the stress path taken. As the material is loaded along the stress path connecting points 1 and 2 in Fig. 2.8, the material will exhibit elastic-plastic behavior. The stress point along this path remains on the yield surface, with the yield surface expanding, translating or both. In Fig. 2.8, the tensor α_{ij} would be non-zero and no expansion of the yield surface would occur. Combined hardening, in which the yield surface may translate as well as expand, is shown in Fig. 2.8. Further loading of the material from point 2 to point 3 of Fig. 2.8 will result in elastic behavior because the load path taken lies within the new yield surface. Continued loading from point 3 will result in elastic or elastic-plastic behavior, depending on the load path taken.

Schofield and Wroth (1968) developed an elastic-plastic soil model, known as the "cam-clay" model which accounts for the volume deformation and strain-hardening of soils. The basis of their model is an incremental flow rule which balances the irreversible work occurring during deformation against a mechanism for the frictional loss. Their flow rule is given by

$$Q = (\Delta t_s)^P - P\,(\frac{\Delta V}{V})^P = \mu P\,(\Delta t_s)^P \qquad (2.10)$$

where V = volume

P = pressure

Q = measure of shear stress

t_s = measure of shear strain

μ = friction parameter

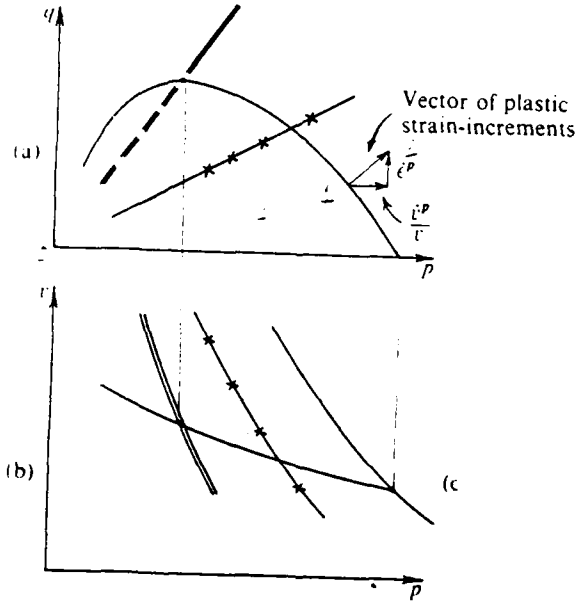

FIG 2.8

Here the superscript denotes plastic or elastic portions of the quantities indicated. The elastic volume deformation during hydrostatic deformation is given by

$$\Delta\left(\frac{V}{V_m}\right) = -A\,\frac{\Delta P}{P} \qquad \Delta\left(\frac{V}{V_m}\right)^e = -A\,\frac{\Delta P}{P} \tag{2.11}$$

where V_m = volume of matrix material

A = a constant

As yielding is occurring, the total volume change is given by

$$\Delta\left(\frac{V}{V_m}\right) = -B\,\frac{\Delta P}{P} \qquad \Delta\left(\frac{V}{V_m}\right) = B\,\frac{\Delta P}{P} \tag{2.12}$$

where B = a constant

The assumption of an associated flow rule gives the following equation for the yield surface:

$$\frac{Q}{\mu P} = \ln\frac{P^*}{P} \tag{2.13}$$

In Eq. (2.13) P^* is the intercept of the yield surface with the P axis as shown in Fig. 2.9. An important assumption of the "cam-clay" model is that the plastic volume deformation for non-hydrostatic stress states is the same as for hydrostatic states but with the P replaced by P^*. Thus, the plastic volume deformation is given by

$$\Delta\left(\frac{V}{V_m}\right)^P = -(B - A)\,\frac{\Delta P^*}{P^*} \tag{2.14}$$

The Eqs. (2.10), (2.11), and (2.12) form a system of equations from which strain increments may be determined from stress increments, or vice-versa. The constants B and A are determined experimentally. Hydrostatic loading

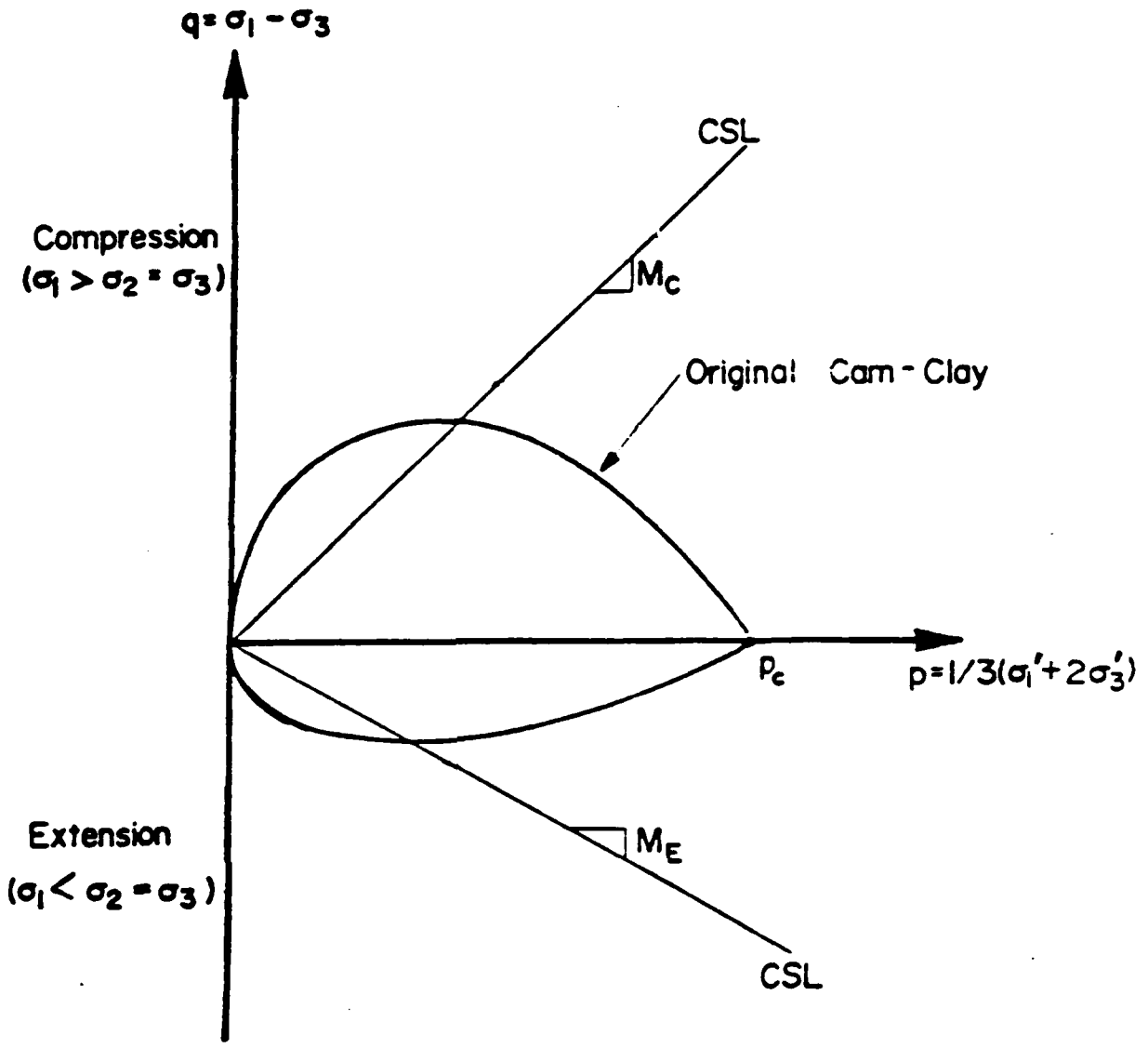

YIELD SURFACE AND CRITICAL STATE LINES FOR CAM - CLAY MODEL

FIG. 2.9

corresponds to a movement along the P axis shown in Fig. 2.9. When yielding occurs, a non-hydroelastic loading will cause the yield surface to change in accordance with Eq. (2.10). Movement of the yield surface is shown in Fig. 2.9. The critical state line is shown in Fig. 2.9 as the line connecting points of zero slope for all possible yield surfaces. This separates yielding into densification and dilation. Densification with strain-hardening occurs to the right of the critical state line, while dilation with strain softening occurs to the left.

The "cam-clay" model has proved useful in representing soil behavior. In this model, however, elastic shear stresses and soil cohesion are completely neglected. The assumption of an associated flow rule is also made. This assumption gives a plastic strain vector normal to the yield surface. Contributions such as those by Mandl and Luque (1970) and Frydman et al. (1973) have shown that normality of plastic flow is neither a mathematical necessity nor supported by experimental evidence. The "cam-clay" model predicts no non-recoverable deformations under hydrostatic loadings. This is not representative of soils. Unloading is elastic, which is not descriptive of actual soil behavior.

Sandler and Baron have introduced the "cap" model to describe the behavior of soils. This model is based on the classical plasticity model, defined by a yield surface and a strain rate vector. Inspection of this yield surface shows that three modes of soil behavior are possible. These being elastic, failure, and cap behavior. Elastic behavior occurs when the stress point lies in the region contained by the stress coordinate axes, the failure envelope, and the cap surface. The behavior in this region is considered to be linearly elastic. The failure model of behavior occurs when the stress point lies on the failure envelope. This failure envelope is assumed to be fixed and is

given by

$$J_2' = A - Ce^{-3BP} \qquad (2,14)$$

where J_2' = second invariant of the deviatoric stress tensor

A,B,C = material constants

The model assumes an associated flow rule, thus, the plastic strain during the failure mode of behavior is composed of a shear component and a dilatant component. The cap mode of behavior occurs when the stress point lies on the cap surface and continued loading results in an outward movement of the cap. The motion of the cap is related to the plastic strain by a hardening rule. The equation for the cap surface is

$$(P - P_a) + \frac{1}{9} D^2 I_1 J_2' = (P_b - P_a)^2 \qquad (2.15)$$

where P_a, P_b = pressures corresponding to points a and b as on the Yield surface

P = mean hydrostatic stress

I_1 = trace of the stress tensor

J_2' = second invarient of the deviatoric stress tensor

D = a constant

The position of the cap is defined by specifying one of the quantities, P_a or P_b. The cap is related to the strain history of the material through a strain hardening rule given by

$$\frac{-P}{e_y} = N\,(1 - e^{-3NP_B}) \qquad (2.16)$$

where M,N = material constants

when the stress point lies on either the failure envelope or the cap surface, the value of $\bar{e}_v^p$ changes exactly as the plastic volumetric strain for a stress point on the cap surface, the plastic strain rate vector will be directed as shown in Fig. (2.8). The position of the plastic strain rate vector implies that it consists of an irreversible decrease in volume in conjunction with an irreversible shear strain. This decrease in volume represents volumetric hysteresis observed in soil during compaction, As the cap moves forward, the compaction resulting from the associated flow will lead to an increase in the cap parameter $\bar{e}_v^p$. By Eq. (2.10) this leads to an increase in P_b, resulting in a movement of the cap to the right. When the stress point lies on the failure surface, the plastic strain rate vector will be directed upwards and to the left as shown in Fig. 2.8. The plastic strain rate vector indicates an increase in volume associated with the movement along the failure surface. The dilatancy will lead to a decrease in the cap parameter, $\bar{e}_y^p$ resulting in a leftward movement of the cap by Eq. (2.16). The backward movement of the cap is limited by the point where it intersects the stress point lying on the failure surface.

The basic cap model described has been modified to include viscous damping and strain hardening. The viscous cap model is used to represent materials which exhibit hysteresis during cyclic loading. This model was formulated by introducing linear viscous damping into the elastic portion of the cap model. The parameters which define the non-plastic portion of the model are an instantaneous modulus G_p, a long term modulus G_s, and a relaxation rate τ. The

three parameters are related through the equation

$$G_s = \frac{G_F G_V}{G_F + G_V} \tag{2.17}$$

$$\tau = \frac{G_d (G_F - G_S)}{G_V^2} \tag{2.18}$$

where G_V, G_F = spring moduli

G_S = long term modulus

G_d = damping constant

τ = relaxation rate

The deviatoric stress-strain relation for the viscous cap model is given by

$$\frac{dS_{ij}}{dt} = 2\,G_F \frac{d(d_{ij}^{v})}{dt} + \frac{2\,G_s\,d_{ij}^{v} - S_{ij}}{\tau} \tag{2.19}$$

where S_{ij} = deviatoric stress tensor

d_{ij}^{v} = viscoelastic deviatoric strain tensor

To determine the parameters G_F, G_S, and τ, cyclic triaxial data are used. A kinematically hardening failure envelope has been added to the general cap model by replacing the stress tensor τ_{ij} by $(\tau_{ij} - \alpha_{ij})$. Here is a tensor whose components are memory parameters defining the translation of the failure surface in stress space. In the model, it is assumed that kinematic hardening occurs only in shear, yielding the relation

$$G_{KK} = 0 \tag{2.20}$$

The kinematic hardening rule which governs the memory parameters G_{ij} is of the form

$$\alpha_{ij} = f_{ijk\ell}\ (\tau_{ij}, \alpha_{ij}, \chi, e_{ij})\ d(d^{P}_{k\ell} \qquad (2.21)$$

where α_{ij} = tensor defining the translation of the failure surface

τ_{ij} = stress tensor

χ = a work hardening parameter

e_{ij} = strain tensor

$d^{P}_{k\ell}$ = deviatoric plastic strain tensor

In order to represent the nonlinear behavior of soils at or near failure, it is necessary to assume a nonlinear hardening rule. A simple rule of this type which gives reasonable behavior at all stress levels is given as

$$\alpha_{ij} = C_{\alpha} F_{\alpha} e^{P}_{ij} \qquad (2.22)$$

where C_{α} = a constant

$$F_{\alpha} = \text{maximum}\ [0, \frac{1 - (\tau_{ij} - \alpha_{ij})\ \alpha_{ij}}{2N_{y}\ (\sqrt{J'_{2F}} - N)}]$$

$$\sqrt{J'_{2F}} = A - Ce^{-3BP}$$

N_{y} = a constant defining the size of the yield surface

Here F_{α} is related to the proximity of the yield surface to the failure surface, and the location of the stress point on the yield surface. For α_{ij} = 0, F will be equal to 1.0. Therefore, from Eq. (2.22), it is found that C_{α} is the inelastic slope for the initial yielding of the material in shear. F_{α} will decrease for continued yield, and is equal to zero when the stress point reaches the failure surface. Upon unloading from the failure surface, the

value of F will increase, reaching a value of 2 upon reyielding. Finally, the cap model has been modified to represent the behavior of saturated soils using the effective stress approach. This modification is straightforward and is achieved by replacing the stress tensor by

$$\tau'_{ij} = \tau_{ij} - u\delta_{ij} \tag{2.23}$$

where τ'_{ij} = effective stress tensor

τ_{ij} = total stress tensor

u = pore pressure

δ_{ij} = Kronecker = $\begin{cases} 1, & i = j \\ 0, & i \neq j \end{cases}$

The cap model has been used successfully to model several soils. However, there are some difficulties associated with it. A major problem is that a large number of parameters must be determined from experimental data and their determination may require special tests. Another problem is the assumption of an associated flow rule. This assumption is not necessarily correct for soils.

Other elastic-plastic constitutive models for soils have been developed. These models use different yield surfaces as a non-associated flow rule. However, the methodology used to formulate these models is the same as for those already described. The problem with classical plasticity theory is that the predicted response of a system is rate independent. It has been established that the response of a soil is rate dependent.

2.2.1.4 Viscoelastic Models

Viscoelastic models describing soil behavior have not appeared in the literature as much as those formulated using elastic-plastic theory. However, elastic-plastic theory is, in fact, a special case of viscoelastic theory. Using the more general material model provided from viscoelastic theory, soil damping and rate dependence may be accounted for. As seen for the "cap model", results improved when viscous damping was introduced into the model.

2.2.2 Micromechanical Models

Mechanistic modeling of soils has been approached from two different viewpoints. One approach has been to treat the soil as an assemblage of particles in contact. The particles within a soil mass may be random in shape and size; therefore, to use this approach some assumptions as to size and shape must usually be made. Once a model representing the soil mass has been chosen, the solution consists of representing the deformed geometry of the particles in contact. The other approach to mechanistic modeling has been to consider the soil as composed of a matrix material containing voids. A solution to this problem consists of modeling the deformation of the voids contained in the matrix material.

Mechanistic models have been formulated on two scales. One scale has been intermediate to that of the experiment and the grains and the pores within the soil mass. While this scale may be very small compared to the scale of the experiment, it may be quite large in comparison to the size scale of the grains and pores. On this scale, the behavior observed may be that of many grains and pores and may best be described by the use of a phenomonological theory. The other scale which is used in mechanistic modeling is termed the micro-scale. On this level, models are formulated at the scale of the grains and pores and are concerned with describing the actual deformation mechanisms

present on this scale.

The void deformation models have been formulated on both the intermediate scale and micro-scale. Modeling of objects in contact has usually been done on the micro-scale.

2.2.2.1 Contact Models

When a mass composed of a number of particles in contact is subject to an externally applied load, the deformation resulting from the load is due to grain movement and grain deformation. The movement of the grains will be controlled by interparticle friction, cohesion between adjacent particles, and the initial porosity of the mass. The grain deformation will be greatest at areas of contact between adjacent grains, and may be elastic or elastic-plastic, depending on the stress level present in the grains. In addition, the grains may fracture, thus changing the number and the shape of the grains and increasing the number of contacts.

Models used to describe this behavior usually consider the soil grains to be spherical in shape. The load-deformation behavior of the spheres themselves is considered to be that of an elastic material. Further simplifications are obtained by neglecting friction, cohesion, and tangential forces acting on the contacts between grains. With these simplifications, a logical step is to use Hertzian contact theory, by which the movement of adjacent spheres relative to one another may be determined. Two spheres in contact are shown in Fig. 2.10. The z axis is positioned at the centerline of the contact. The solid lines represent the deformed configuration of the spheres, while the dashed lines represent the undeformed spheres. From Hertzian contact theory, the deformation along the centerline of contact for each sphere is given by

$$u_z^1 = \frac{3\pi\,(1 - \nu_1^2)\,F}{8a\,E_1} \qquad (2.24a)$$

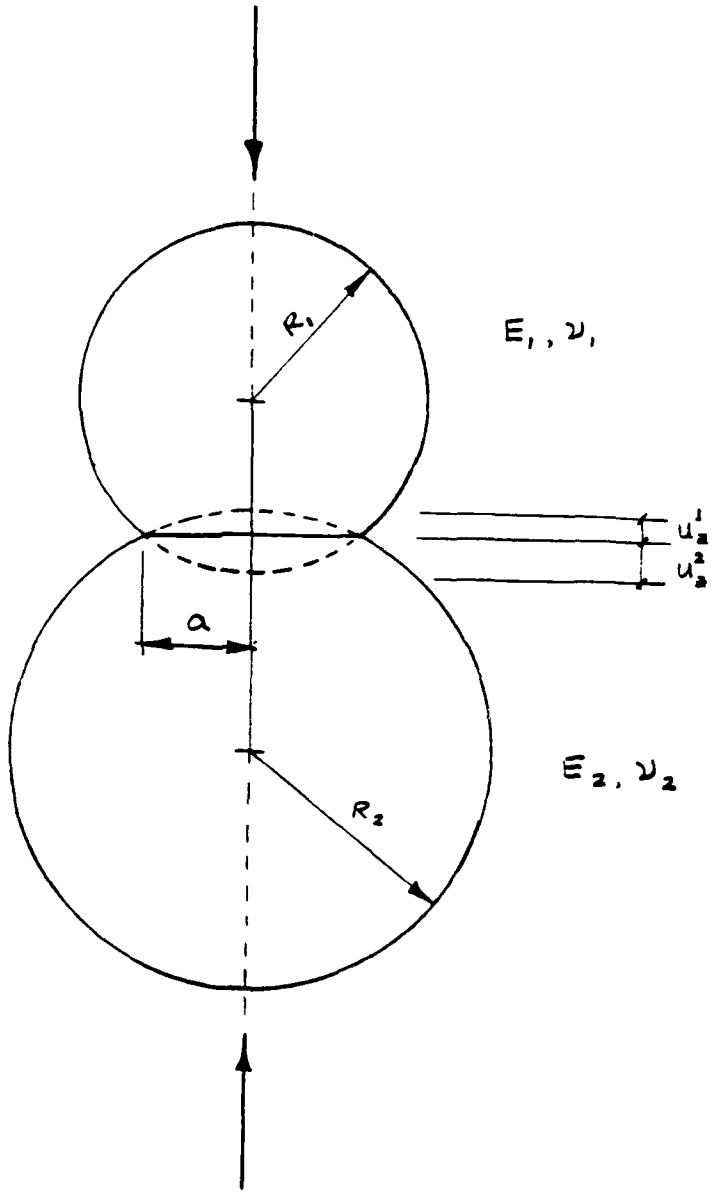

FIG. 2.10

$$u_z^2 = \frac{3\pi\ (1 - \nu_2^2)\ F}{8a\ E_2} \qquad (2.24b)$$

where

u_z^1, u_z^2 = deformation along the contact centerline for spheres 1 and 2 respectively

ν_1, ν_2 = Poisson's ratio for spheres 1 and 2 respectively

E_1, E_2 = elastic modulus for spheres 1 and 2 respectively

a = radius of the contact surface

F = force transmitted across the contact

The deformations u_1 and u_2 are shown in Fig. 2.10. The radius of the contact area between the spheres is given by

$$a = \frac{3\pi}{4} \frac{P\ R_1 R_2}{R_1 + R_2} \left[\frac{(1 - \nu_1^2)}{E_1} + \frac{(1 - \nu_2^2)}{E_2} \right]^{1/3} \qquad (2.25)$$

where R_1, R_2 = the radii of spheres 1 and 2 respectively.

Using Eqs. (2.24) and (2.25), the deformation of an assemblage of spheres may be determined when the force transmitted across each contact is known. Ko and Scott (1967) have solved this problem for the case of an assmebly of spheres in ideal packing configurations, under conditions of hydrostatic loading. All the spheres were considered to be of equal radii and of the same material properties. The solution is given by

$$\frac{\Delta V}{\Delta} = 3 \left[\frac{3C\ (1 - \nu^2)\ P}{E} \right]^{2/3} \qquad (2.26)$$

where V = volume of soil mass

C = 1, for sc (simple cubic) packing

$\sqrt{2/4}$, for fcc (face centered cubic)

P = hydrostatic pressure

E = elastic modulus

ν = Poisson's ratio

As seen from Eq. (2.26), the term C accounts for the initial density of the mass, giving smaller volumetric strains for the denser packing configurations. However, this model predicts larger than actual deformations for the simple cubic (sc) configuration, while predicting smaller than actual deformations for the face centered cubic (fcc) packing configuration. To correct this, Ko and Scott used a combination of sc and fcc blocks to represent the initial porosity of the soil. By assuming a distribution of grain contact pressures and an effective contact radius, pressure-volume relationships for sands of three initial porosities were generated. The results obtained are shown in Figs. 2.11 and 2.12 along with the limiting cases of sc and fcc packing configurations. A major shortcoming of Ko and Scott's model is that the path the soil takes during unloading is the same as that for loading, which is not representative of actual soil behavior. Warren and Anderson (1973) have formulated a contact model in which initially some of the spheres are not in contact. The pressure-volume relationship obtained is given by

$$\frac{\Delta V}{V} = 3\left[\left(\frac{N_g}{N_c}\right)\ 3\,\frac{(1-\nu^2)}{E}\,P\right]^{2/3} \qquad (2.27)$$

where N_g = number of grains in a typical cross-section

N_c = The number of contacts transmitting force across the typical cross-section

As loading progresses, more grains come into contact, until at some critical pressure, all grains make contact. It is apparent from Eq. (2.27) that as the

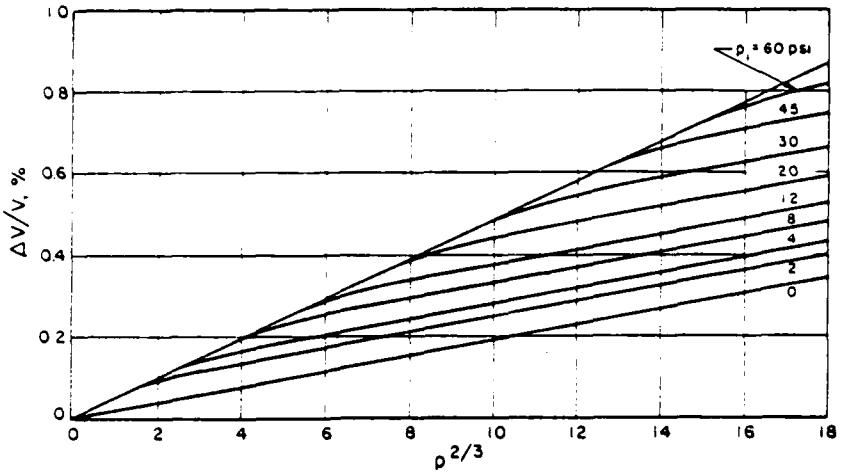

COMPRESSIBILITY OF SIMPLE CUBIC HOLEY MODEL

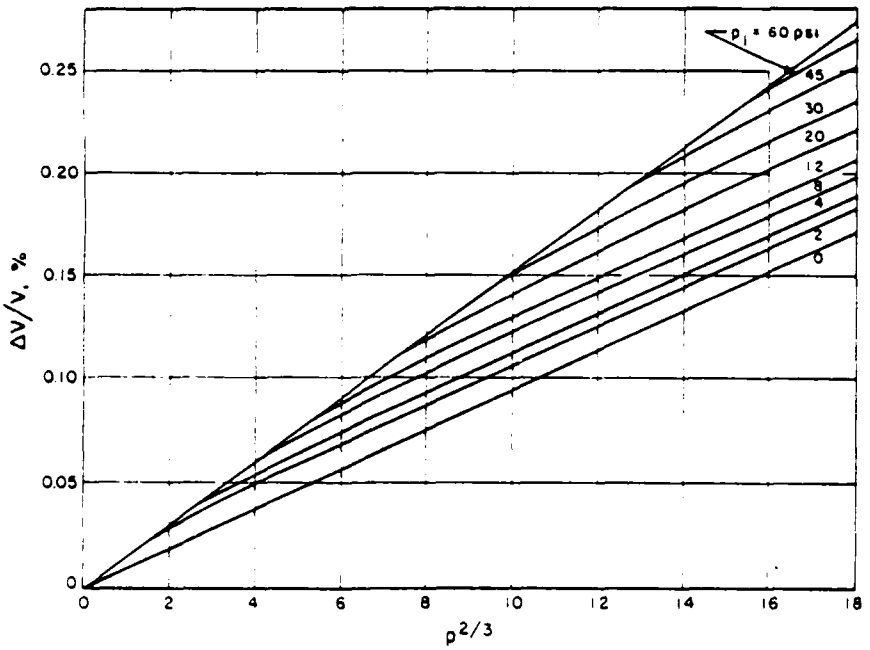

COMPRESSIBILITY OF FACE-CENTERED CUBIC HOLEY MODEL

FIG. 2.11

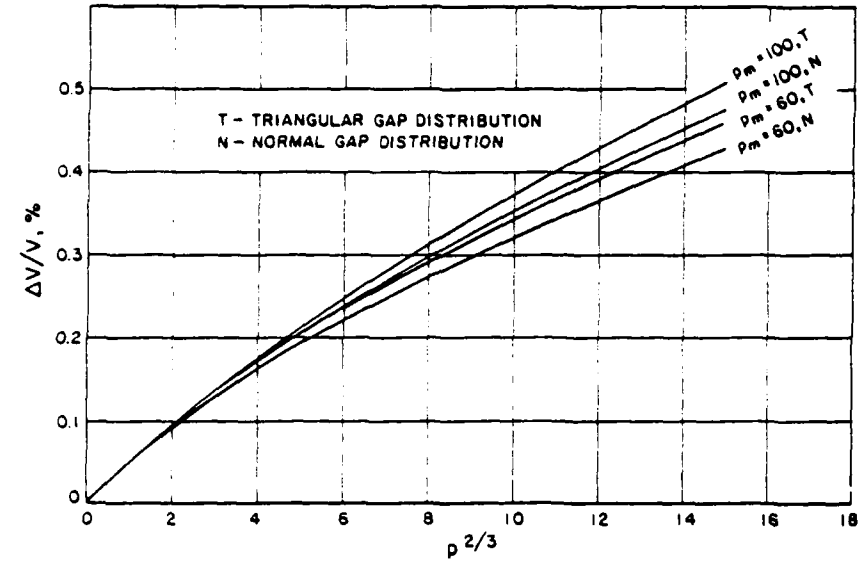

COMPRESSIBILITY OF SIMPLE CUBIC HOLEY MODEL FOR DIFFERENT p_m AND GAP DISTRIBUTIONS

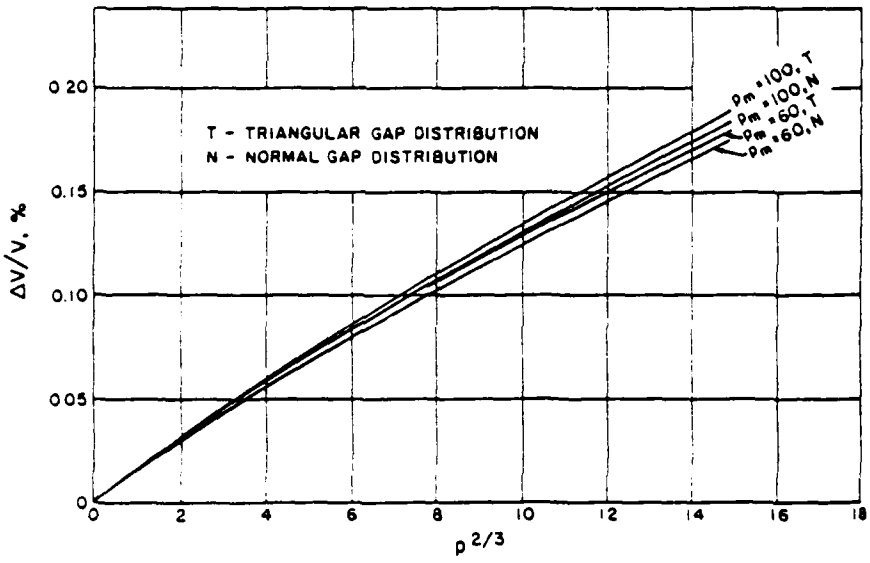

COMPRESSIBILITY OF FACE-CENTERED CUBIC HOLEY MODEL FOR DIFFERENT p_m AND GAP DISTRIBUTIONS

FIG. 2.12

number of contacts is increased, the amount of volume deformation resulting from an increase in pressure will decrease. The model will predict unloading along a path different from that of loading, as long as the grains were not all initially in contact. The difficulty with this model is the determination of the value of N_c. The variation in the value of N_c which occurs during loading corresponds to the rigid body motion of the particles within the soil mass. This model does not attempt to describe the actual grain motion within the soil mass, but rather the parameter N_c is chosen to fit experimental data.

Some models of granular media include friction of the contact between grains.. Rowe (1962) has considered the shearing of various assemblages of spheres. Using a minimum energy criterion, he arrived at the stress-dilatancy equation

$$\frac{\sigma_1}{\sigma_3} = \tan^2\left(45° + \frac{\varphi_u}{2}\right)\left[\frac{1 + \frac{\Delta V}{V}}{\Delta \varepsilon_1}\right] \qquad (2.28)$$

where σ_1 = maximum principal stress

σ_3 = least principal stress

φ_u = undrained angle of shearing resistance

$\Delta\varepsilon_1$ = the axial strain increment

This equation holds only for the case when the intermediate principal stress is equal to the least principal stress. Rowe states that the angle φ_u, must be replaced by an effective angle of shearing resistance φ_u', in order to match experimental data. Test conditions may be created so that many values of the undrained angle of shearing resistance, φ_u, may be obtained for the same soil sample. However, with pure pressure measurements during the test, the value of the effective angle of shearing resistance may be determined and this value has been found not to vary with test conditions. The Eq. (2.28) does not

account for compaction during non-hydrostatic loading. Barden et. al. (1969) used Eq. (2.28) to formulate a plastic flow rule and a set of yield surfaces. They tested the behavior of sand in plane strain and found that the yield criterion and plastic potential did not coincide. This implies non-normality of flow. However, it was found that the volumetric strain was suitably predicted by this model. Nemat-Naser formulated a model to represent the behavior of granular material undergoing shear loading. This model represents dilation and densification which occurs during shear. This is done by defining the dilatancy angle $\bar{\nu}$, which defines the position of a microscopic shear plane with respect to the observable macroscopic shear plane. In this model, it is assumed that the actual shearing takes place on many microscopic shear planes rather than on one macroscopic shear plane. To formulate the model, Nemat-Naser considered a sample of soil for which failure takes place along one microscopic shear plane S'-S'. Summing forces on the plane S'-S' gives the following equations

$$F^* = \frac{T \tan \varphi_\mu \cos (\bar{\varphi} - \bar{\nu})}{\sin \varphi} \qquad (2.29)$$

$$\tan \varphi_\mu = (\bar{\varphi} - \bar{\nu})$$

where T = total shear force on macroscopic sample

$\bar{\nu}$ = dilatancy angle

F^* = frictional force along microscopic shear plane

The angles φ_μ and $\bar{\varphi}$ are defined by the equations

$$\tau = \sigma \tan \bar{\varphi} \qquad (2.30a)$$

$$\tau^* = \sigma^* \tan \varphi_\mu \qquad (2.30b)$$

where τ = shear stress acting on macroscopic shear plane

σ = normal stress acting on macroscopic shear plane

τ^* = shear stress acting on microscopic shear plane

σ^* = normal stress acting on microscopic shear plane

The Eq. (2.29) was derived by considering all stresses in Eqs. (2.30) to be acting on the same element of area along the microscopic shear plane. By considering the rate of energy dissipation which occurs as the block slides along the plane S'-S', Nemat-Naser obtained the equations

$$\dot{w} = \frac{\tau \tan \phi_u \cos (\bar{\phi} - \bar{\nu})}{\sin \bar{\phi} \sin \bar{\nu}} \frac{\dot{V}}{V} \tag{2.31}$$

where $\dot{w}$ = rate of energy dissipation
V = the volume of the macroscopic sample.

The dot denotes the time derivatives. The following approximations are made concerning w:

$$\dot{w} = \dot{w}' + \dot{w}'' \tag{2.32a}$$

$$\dot{w}' = \tau\dot{\gamma} \tag{2.32b}$$

$$\dot{w} = \frac{\tau}{\sin \bar{\phi} \cos \bar{\phi}} \frac{\dot{V}}{V} \tag{2.32c}$$

where $\dot{\gamma}$ = the rate of shear deformation on the macroscopic sample.

Use of these approximations in Eq. (3.31) gives the equation

$$\frac{1}{V_i} \frac{\dot{V}_i}{\dot{\gamma}} = \frac{\cos (\phi_u + \bar{\nu}_i) \sin \bar{\nu}_i}{\cos \phi_u} \tag{2.33}$$

The Eq. (2.33) applies to one microscopic failure plane. If one microscopic shear plane is denoted by i, Eq. (2.33) is written as

$$\frac{1}{V_i} \frac{\dot{V}_i}{\dot{\gamma}} = \frac{\cos (\phi_u + \bar{\nu}_i) \sin \bar{\nu}_i}{\cos \phi_u} \tag{2.34}$$

the volume fraction, V_i, of the family of particles having a dilatancy angle, is defined by,

$$P_i(\bar{\nu}) = \frac{V_i}{V} \tag{2.35}$$

where P_i = volume fraction of family of particles having dilatancy angle $\bar{\nu}_i$.

The restriction if P_i is the following

$$\int_{\bar{\nu}_o^-}^{\bar{\nu}_o^+} p_i(\bar{\nu})\, d\bar{\nu} = 1 \tag{3.36}$$

In Eq. (3.36) $\bar{\nu}_o^+$ and $\bar{\nu}_i^-$ form the range of variation of the dilatancy angle, $\bar{\nu}$. Using Eqs. (2.35) and 2.36) in Eq. (2.34), Nemat-Naser arrived at the final result given by

$$\frac{1}{V}\frac{\dot{V}}{\dot{\gamma}} = \frac{1}{\cos \phi_u} \int_{\bar{\nu}_o^-}^{\bar{\nu}_o^+} p(\bar{\nu}) \cos(\phi_u + \bar{\nu}) \sin \bar{\nu}\, d\bar{\nu}. \tag{3.37}$$

The Eq. 3.37 contains all experimentally observed behavior of granular material in simple shear. However, the accuracy of the predictions made by Eq. (3.37) will depend on the chosen form of the distribution function $P(\bar{V})$. This distribution function may be very difficult to determine for an actual soil sample. Anotner shortcoming of this model is that the individual particles within the sample mass are considered to be rigid. Wilkins (1970) took a different approach to develop a theory for the shear strength of a granular media. He used an empirical curve fitting method and Rowe's Eq.

(2.28) to predict the number of unstable contacts in a granular assemblage as a function of the stress ratio. According to this approach, when all the contacts on a grain become unstable, the grain is no longer considered to contribute to the system and it effectively becomes a void. When the number of voids not supporting any stresses is equal to the number of particles which continue to carry loads, the medium is assumed to fail. Although this attempt is interesting, it becomes unattractive due to its empirical nature. Volume changes and stress-strain relations are neglected in Wilkins' formulation.

Other contact models have been developed for which the plastic flow of the bodies in contact are considered to be important. Kakar and Chakladar (1967) have solved this problem for spheres in a variety of packing configurations. In this model, it is assumed that the particle surfaces which are not in contact remain spherical. They solved this for a simple cubic packing. Assumptions were that the volume of the spheres remain constant, that the contacts transmit the load applied to the assembly, and that the material near the contact is in a state of uniaxial stress. The material of the contacts was allowed to yield until the stress developed at the contacts was balanced by the applied pressure. The relationship that Kakar and Chakladar obtained is given by

$$\frac{\Delta V}{V} = 3\left(\frac{6P}{\pi Y} - 1\right) - 2\left(\frac{4P}{\pi Y} + 1\right)^{3/2} \qquad (2.38)$$

where P = applied pressure

Y = yield strength

V = volume of the assembly

The Eq. (3.38) is valid until the contact areas touch, thus forming a new geometry. The results shown are for a simple cubic packing configuration and these show that the yielding model predicts larger strains for a given load

than those contained from the elastic Hertzian contact model. The actual stress-strain curve will likely fall in between those by the Hertzian and Kakar and Chaklader theories. Not all points within a sphere will yield at once; thus, the actual behavior is stiffer than that predicted by the complete yielding model as formulated by Kakar and Chaklader.

2.2.2.2 Void Deformation Models

One approach to modeling soils has been to consider the soil as a mass composed of a matrix material and voids. The deformation resulting from the application of loads to a material of this type will depend on the materials making up the matrix and voids, the size and the shape of the voids, and the column fraction of the voids. A common assumption in using this approach to model soils is that the voids are either spherical or flat in shape. O'Connell and Budiansky (1974) have considered the effect that flat cracks would have on the moduli of a material containing such voids. The equation they obtained for the bulk modulus of such a material is

$$\frac{K}{K_m} = 1 - \frac{16}{9}\left[\frac{1-\nu^2}{1-2\nu}\right] d \qquad (2.39a)$$

$$\nu = \nu_m \left[1 - \frac{16}{9}\, d\right] \qquad (2.39b)$$

$$d = \frac{1}{V} \Sigma\, a_c^3 \qquad (2.39c)$$

where K = bulk modulus of material

K_m = bulk modulus of matrix material

ν = Poisson's ratio of material

ν_m = Poisson's ratio of matrix material

d = crack density

a_c = crack length

V = volume of material

The Eqs. (2.39) were developed by considering the cracks to contain only air. The Eqs. (2.39) indicate that a sufficiently large crack density would have a considerable effect on the material properties, while the cracks themselves may be of negligible volume. As the pressure is increased on such a material, the cracks would close and their effect would disappear.

Other researchers have considered the effects of spherical voids on material behavior. MacKenzie (1950) determined the effective bulk modulus for a material represented by a matrix containing spherical voids. The term effective refers to material properties which are descriptive of the entire mass being considered. The porous material is modeled as a collection of spheres of matrix material, each containing a spherical void. Under this assumption, the problem reduces to that of determining the solution for one of these composite spheres with a uniform radial pressure acting on its boundary. The term composite refers to the material composed of both matrix and voids. The expression MacKenzie obtained for the effective bulk modulus of such a material is

$$\frac{1}{K} = \frac{V}{V_m K_m} = \frac{3}{4G_m \left(\frac{V}{V_m} - 1\right)} \qquad (2.40)$$

where K = effective bulk modulus

K_m = bulk modulus of matrix material

G_m = shear modulus of matrix material

V_m = volume of matrix material

V = volume of composite material

The Eq. (2.40) was developed under the assumption that air is contained in the voids. Hashin(1970) has determined upper and lower bounds for the effective bulk and shear moduli of an elastic matrix material which contains spherical

inclusions of another elastic material. The upper and lower bounds were determined from the theorems of potential energy and complementary energy. The bounds determined for the effective bulk modulus coincided and this result is given by

$$K = K_m + \frac{(K_p - K_m)(4G_m + 3K_m)c}{4G_m + 3K_p + 3(K_m - K_p)c} \tag{2.41}$$

where K = effective bulk modulus

K_m = bulk modulus of the matrix material

K_p = bulk modulus of the inclusions

G_m = shear modulus of the matrix material

c = the column fraction of the inclusions

The bounds Hashin obtained for the effective shear modulus did not coincide. These bounds are given by

$$G_l = \frac{G_m}{1 + (1 - \frac{G_p}{G_m})y_1^{(\sigma)}c} \tag{2.42a}$$

$$G_u = G_m[1 + \frac{G_p}{G_m} - 1)y_1^{(\varepsilon)}c] \tag{2.42b}$$

where G_l = lower bound on effective shear modulus

G_u = upper bound on effective shear mobulus

G_p = shear modulus of the inclusion

The coefficients $y_1^{(\sigma)}$ and $y_1^{(\varepsilon)}$ are determined from the equations

$$y_1^{(\sigma)} = \frac{2G_m}{\tau}[B_1^{(\sigma)} + \frac{21\,B_3^{(\sigma)}}{5(7 - 4\nu_p)} \tag{2.43a}$$

$$y_2^{(\sigma)} = \frac{2G_m B_3^{(\sigma)}}{5\tau} \tag{2.43b}$$

$$y_1^{(\sigma)} \left[\frac{2(1 - \frac{G_p}{G_m})(\rho_o^7 - \rho_o^5)}{5\ (1 - \nu_m)}\right] +$$

$$y_2^{(\sigma)} \left|1[7-10\nu_p) - (7-10\nu_m)\ \nu]\ 4\rho_o^7 - (7+7\nu_m)\Omega\right| = 0 \tag{2.43c}$$

$$y_1^{(\sigma)} \left|\frac{G_p}{G_m} + \frac{(7-5\nu_m)(1 - \frac{G_p}{G_m})(1 - \rho_o^3)}{15\ (1 - \nu_m)}\right| + 21 y_2^{(\sigma)} \Omega \left|\frac{1}{\rho_o^2} - 1\right| = 1 \tag{2.43d}$$

$$y_1^{(\varepsilon)} = \frac{2}{\gamma}\left[B_1^{(\varepsilon)} + \frac{21\ B_3^{(\varepsilon)}}{3(7-4\nu_p)}\right. \tag{2.44a}$$

$$y_2^{(\varepsilon)} = \frac{2\ B_3^{(\varepsilon)}}{5\ \gamma} \tag{2.44b}$$

$$y_1^{(\varepsilon)} \left[\frac{2(1 - \frac{G_p}{G_m})(\rho_o^7\ p\ \rho_o^5}{5(1 - \nu_m)}\right] + y_2^{(\varepsilon)} \left|[(7-10\nu_p) -\right.$$

$$\left.(7-10\nu_m)\Omega\right|\ 4\rho_o - 4(7-10\nu_m)\Big| = 0 \tag{2.44c}$$

$$y_1^{(\varepsilon)} \left[\frac{G_p}{G_m} = \frac{(7-5\nu_m)(1 - \frac{G_p}{B_m})}{15(1-\nu_m)} + \frac{2(4-5\nu_m)(1 - \frac{G_p}{G_m})\ \rho_o^3}{15(1-\nu_m)}\right]$$

$$+ 21\ y_2^{(\varepsilon)} \nu \left[\frac{1}{\rho_o^2} - 1\right] = 1 \tag{2.44d}$$

$$\Omega = \frac{4(7-10\nu_p) + \frac{G_p}{G_m}(7+5\nu_p)}{35(1-\nu_m)} \tag{2.45a}$$

$$\rho_o^3 = C_s \tag{2.45b}$$

where ν_m = Poisson's ratio of the matrix material

ν_p = Poisson's ratio of the inclusions

τ = shear stress on macroscopic sample

γ = shear strain on macroscopic sample

C_s = volume concentration of spheres

The terms τ and γ appearing in Eqs. (2.43) and (2.44) are known from the boundary conditions used to determine the limits on the effective shear modulus. These boundary conditions correspond to the cases when the surface tractions and surface displacements are known on a sample of the composite material. The boundary conditions for the case when surface tractions are known are given by

$$\sigma_{xy} = (x = \pm a,\ y = \pm b) \tag{2.46}$$

The boundary conditions for the case when the surface displacements are known are given by

$$u_x(x, y) = \frac{\gamma}{2} y \tag{2.47a}$$

$$u_y(x, y) = \frac{\gamma}{2} x \tag{2.47b}$$

The bounds determined by Hashin have been successfully used to approximate the effective elastic moduli of composite materials.

Some spherical void models have been developed which account for the plastic yielding of the matrix material. Torre (1948) developed such a model and the result he obtained is given by

$$P = Y_m \ln\left(\frac{a}{a - r}\right) \tag{2.48a}$$

$$\alpha = \frac{V}{V_m} \tag{2.48b}$$

where P = pressure

Y_m = yield stress of matrix material

V_m = volume of matrix material

V = volume of composite material

A problem with Eq. (2.48a) is that the matrix material is considered to be fully plastic. A model should be able to describe elastic as well as plastic phases, which occur for both loading and unloading. A step toward including both elastic and plastic phases is to prescribe a work-hardening rule for the matrix material. Chadwick (1963) developed such a model. Although this model is rigorously derived, certain essential parts remain in integral form making it difficult to use. Carrol and Holt (1972) as well as Chu and Hashin (1971) took an approach which simplified the results. Considering the same spherical pore geometry, they derived the pressure-volume relationship for the composite material by temporarily assuming that the matrix material is incompressible. Carrol and Holt then used an empirical relationship to describe the pressure-volume relationship for the matrix material. The empirical relationship used is given by

$$P = \frac{1}{\alpha} f\left(\frac{v_s}{\alpha}, u_s\right) \tag{2.49a}$$

$$\alpha = \frac{v_s}{v_m} \tag{2.49b}$$

where v_s = specific volume of composite material

v_m = specific volume of matrix material

u_s = specific internal energy

Using the method outlined above, Carrol and Holt obtained the pressure-volume

relationship of a mass composed of an ideally elastic-plastic matrix material containing voids. This is given by

$$P = \frac{4\, G_m\, (\alpha_o - \alpha)}{3\alpha\, (\alpha - 1)}, \quad (\alpha_o \geq \alpha \geq \alpha_1) \tag{2.50a}$$

$$P = \frac{2G_m}{3} + Y_m - \frac{2G_m\alpha_o}{\alpha} + Y_m \ln\left[\frac{2G_m(\alpha_o - \alpha)}{Y_m(\alpha - 1)}\right], \quad (\alpha_1 \geq \alpha \geq \alpha_2) \tag{2.50b}$$

$$P = \frac{2Y_m}{3} \ln\left[\frac{\alpha}{\alpha - 1}\right], \quad (\alpha_2 \geq \alpha > 1) \tag{2.50c}$$

$$\alpha_1 = \frac{2\, G_m\alpha_o + Y_m}{2G + Y_m} \tag{2.50d}$$

$$\alpha_2 = \frac{2\, G_m\alpha_o}{2\, G + Y_m} \tag{2.50e}$$

$$\alpha = \frac{V}{V_m} \tag{2.50f}$$

$$\alpha_o = \frac{V_o}{V_m} \tag{2.50g}$$

where P = pressure

G_m = shear modulus of matrix material

V_o = initial volume of composite material

V = volume of composite material

Y_m = yield stress of matrix material

There are two problems associated with using Eqs. (2.50) to represent soil behavior. First, the parameters obtained by using Eqs. (2.49) to describe the pressure-volume relationship of the matrix material are not fundamentally related to the actual behavior of the soil grains. Second, soils exhibit a pronounced reverse yielding during unloading which is not predicted by Eqs. (2.50). Bhatt et al. (1975) attempted to remove these difficulties by making

the matrix a Monr-Coulomb material. The yield criterion for the matrix material is given by

$$(1 + D)\,\sigma_1 - \sigma_3 = Y = 0 \tag{2.51}$$

where σ_1 = greatest principal stress

σ_3 = least principal stress

D = a constant

Y_m = yield stress for the matrix material

The results obtained by Bhatt et al, using the yield criterion given by Eq. (2.51), are given by

$$P = \frac{4\,G_m\,(\alpha_o - \alpha)}{3\alpha\,(\alpha - 1)}\,, \quad (\alpha_o \le \alpha \le \alpha_1) \tag{2.52a}$$

$$P = \frac{4\,G_m\,(\alpha_o - \alpha)}{3\alpha\,(\alpha - 1)}\left\{\alpha\left[\frac{2\,G_m\,(\alpha_o - \alpha)}{Y_m\,(\alpha - 1)}\right]^{\frac{3}{2D+3}} - \alpha + 1\right\}$$

$$= \frac{Y_m}{D}\left[\frac{2G_m\,(\alpha_o - \alpha)}{Y\,(\alpha - 1)}\right]^{\frac{2D}{2D+3}} - 1\Big]\,, \quad (\alpha_1 \le \alpha \le \alpha_2) \tag{2.52b}$$

$$\frac{Y_m}{D}\left\{\left[\frac{\alpha}{\alpha - 1}\right]^{\frac{2D}{3}} - 1\right\} \tag{2.52c}$$

$$\alpha_1 = \frac{2\,G\,\alpha_o + Y_m}{2\,G + Y_m} \tag{2.52d}$$

In Eqs. (2.52) all terms have the same meaning as those appearing in Eqs.(2.50). The parameter α_2 is determined from the equation given by

$$\frac{2\,G_m\,(\alpha_o - \alpha_2)}{Y_m\,(\alpha_2 - 1)} = \left[\frac{\alpha^2}{\alpha_2 - 1}\right]^{1 + \frac{2D}{3}} \tag{2.53}$$

when the soil is unloaded in the fully plastic state, the following relationships hold

$$P = \frac{Y_m}{D}\left[\left(\frac{\alpha}{\alpha-1}\right)^{\frac{2D}{3}} - 1\right] - \frac{Y_m(2+D)}{D}\left(\frac{c}{a}\right)^{2D} + \frac{2\,G_m\,(\alpha-\alpha^*)}{3}\left[\frac{3+D}{D(\alpha-1}\left(\frac{a}{c}\right)^3 + \frac{2}{\alpha}\right] \tag{2.54a}$$

$$\alpha = \frac{2\,G_m\,\alpha^* - Y'}{2\,G - Y_m} \tag{2.54b}$$

$$Y' = Y_m\left[\left(\frac{c}{a}\right)^{2D+3} + \frac{1}{(1+D)}\left(\frac{c}{a}\right)^{\frac{3+D}{1+D}}\right] \tag{2.54c}$$

where α^* = the value of α when unloading is initiated.

The Eqs. (2.54) must be solved numerically to obtain the pressure-volume relationship during unloading. This is done by choosing values of $c/a > 1$, and calculating α from Eq. (2.54b) and P from Eq. (2.54a). Some problems with the model just described have been recognized. First, the predicted high-pressure compressibility is often too low. Second, low pressure behavior is not adequately represented. Schatz et al. (1974), modified Bhatt's model to allow for the curvature of the Mohr-Coloumb failure surface. The failure criterion which Schatz, et al. incorporated into Bhatt's model is given by

$$\sigma_1 - \sigma_3 - Y_1 + (Y_1 - Y_0)\, e^{\sigma_1/\sigma_0} = 0 \tag{2.55}$$

where Y_0 = yield stress for $_{max}$ = 0 condition

Y_1 = ultimate strength

The term σ_1/σ_0 which appears in Eqs. (2.55) is descriptive of the rate of transition from low to high yield strengths. Another modification which

Schatz et al. incorporated into Bhatt's model included the effects of flat cracks on the bulk modulus of the matrix material. This modification of the bulk modulus is given by

$$\frac{K}{K_m} = 1 - \gamma \left[1 - \frac{P}{P_{c1}}\right], \quad (P < P_{c1}) \tag{2.56a}$$

$$K = K_m, \quad (P \geq P_{c1}) \tag{2.56b}$$

where γ = a constant

P_{c1} = pressure required for complete crack closure

K = effective bulk modulus of matrix material

K_m = bulk modulus of composite material

P = Pressure

The modification given in Eqs. (2.56) has the effect of dividing the voids into two populations, spherical voids which deform according to Eq. (2.55) and flat cracks which deform according to Eqs. (2.56). These modifications improve the predictins made by Bhatt's model. One problem with Bhatt's and Schatz's models is that neither allows for a distribution of pore sizes. An approach to account for the pore size variation in actual material is to start with the ideally plastic spherical pore model and then allow for each sphere to have a different porosity with the requirement that the total porosity is equal to that of the material being modeled. Krener and Schopt (1973) have developed such a model which considers an ideally plastic matrix material. Their result for the pressure-volume relationship of one pore is given by

$$P = \frac{4 G_m}{3} \left[\alpha\left(1 - \frac{V_p}{V_p^0}\right) - \bar{\alpha}\left(1 - \frac{\bar{V}_p}{\bar{V}_p^0}\right)\right] + \frac{2Y_m}{3} \ln\left[1 + \left(\frac{1-\alpha}{\alpha}\right)\frac{V_p^0}{V_p}\right] \tag{2.57a}$$

$$\alpha = \frac{V}{V_m} \quad \ldots\ldots\ldots\ldots\ldots\ldots\ldots\ldots \quad (2.57b)$$

where P = pressure

Y_m = yield stress of matrix material

V = total volume

V_m = volume of matrix maerial

V_p = current volume of pores

V_p = initial volume of pores.

The overbars in Eqns. (2.57) denote averages taken over the entire volume of material being considered. The pressure-volume relationship for the entire material is determined by evaluating Eqns (2.27) for all pores present in the material under consideration. An apparent problem for this model is the determination of the pore size distribution.

Other spherical void deformation models have been developed, but the models described in this section are representative of work which has been done to date in this area.

2.3 Conclusions

The soil models reviewed in the previous sections, with few exceptions, have only considered the pores within the soil mass to contain air. The modification of many of these models to represent saturated soil conditions is straightforward through the effective stress principle. However, many situations exist when the soil is partly saturated. The degree of saturation is a soil parameter used to describe the amount of liquid present within the pores of the soil mass. By definition the degree of saturation is given by

$$S = \frac{V_F}{V_p}, \quad (0 \leq S \leq 1) \quad \ldots\ldots\ldots\ldots\ldots\ldots\ldots\ldots (2.58)$$

where S = degree of saturation

V_F = volume of fluid contained in the soil mass

V_p = volume of the pores contained in the soil mass.

Using the definition given by Eqn. (2.58), the three conditions which a constitutive model should be able to represent are

1. $S = 0$ (voids completely filled with air),
2. $0 < S < 1.0$ (voids filled with an air-fluid mixture), and
3. $S = 1.0$ (voids completely filled with fluid).

The second condition presents problems, due to the complexity of having an air-water mixture present in the pores. One problem is that, as the pressure is increased some of the air will be driven into solution. Because of this and the compressibility of the air phase, it is difficult to predict the pore pressure resulting from the application of a load. If the pore pressures could be predicted, the principle of effective stress could be used to model the partly saturated system.

Phenomenological models have been used a great deal to model soil behavior. It would seem that empirical models obtained from curve-fitting methods are undesirable for use as a constitutive model representing soil behavior. These models should not be expected to yield reasonable results when used to represent conditions which deviate greatly from those by which the model was calibrated. They also provide no understanding as to the actual deformation mechanisms acting within the soil mass. Elastic models are poor representations of soil behavior primarily due to their inability to predict unloading behavior. Elastic-plastic models have been used a great deal and provide reason-

able results for many situations. While these models may work well, they often require a great many parameters and may be difficult to use in practice. Little work has been done using viscoelastic models for soils.

Micromechanical models attempt to derive constitutive laws from observing the actual mechanisms causing deformation of the microstructure. Thus, as these deformation mechanisms are more fully understood, a better understand of the complex behavior of soils can be achieved.

CHAPTER 3

ASSEMBLAGE OF SPHERES IN CONTACT

1.1 Contact Forces

In an assemblage of spheres which are in contact, there are three types of forces which may act on the area of contact. Two of these are forces which act in directions normal and tangential to the contact area. The third force is a torsional couple acting on the contact area. The forces are shown acting on an area of contact in Fig. 3.1. The area of contact results from the compression of one sphere upon another. The remainder of this chapter will be concerned with the normal forces which act on the area of contact.

1.2 Hertz Solution for the Pressure Between Two Spherical Bodies in Contact

The solution for the pressure between two spherical bodies in contact was first determined by Hertz. Discussion of this solution is given by Timoshenko and Goodier (1951). The Hertz solution will be reviewed in the remainder of this section.

Two spherical bodies in contact are shown in Fig. 3.2. Here R_1 and R_2 are the radii of spheres 1 and 2, respectively. Sphere 1 has material constants E_1 and V_1. while sphere 2 has material constants E_2 and V_2. The x, y plane is tangent to the point of contact. The z_1 and z_2 coordinate directions are considered positive when directed from the origin of the x, y plane to the centers of spheres 1 and 2, respectively. When there is no pressure between the bodies the coordinate directions ε_1 amd ε_2 are given by

$$z_1 = R_1-[R_1^2- r^2]^{1/2} \tag{3.1a}$$

$$z_2 = R_2-[R_2^2- r^2]^{1/2} \tag{3.1b}$$

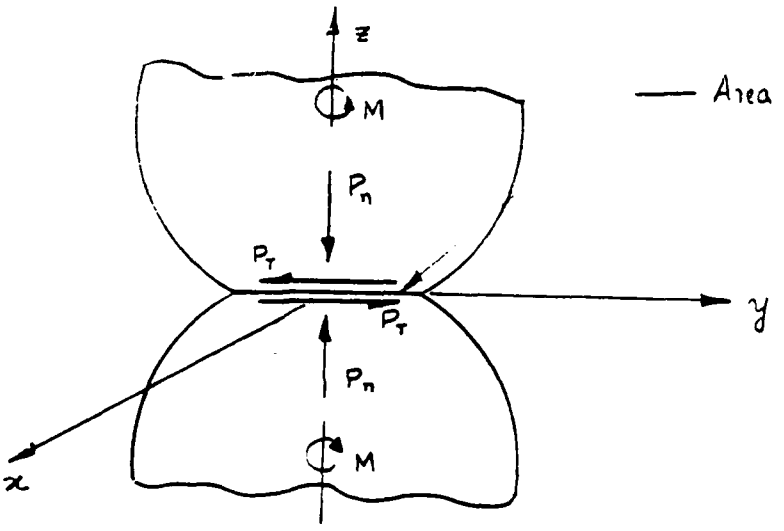

P_n = Normal force on contac

P_T = Tangential force on con

M = Torsional couple

FIG. 3.1

where $r^2 = x^2 + y^2$

Approximations of z_1 and z_2 may be obtained by performing Taylor series expansions of Eqs. (3.1) about r = 0. These approximations are given by

$$z_1 = \frac{r^2}{2 R_1} \tag{3.2a}$$

$$z_2 = \frac{r^2}{2 R_2} \tag{3.2b}$$

The use of Eqs. (3.2) is limited to cases in which the distance r is small in comparison to R_1 and R_2. Addition of Eqs. (3.2) yields the following equation

$$z_1 + z_2 = \frac{r^2 (R_1 + R_2)}{2 R_1 R_2} \tag{3.3}$$

As shown in Fig. 3.1, Eqs. (3.3) represents the distance between points on the surface of spheres 1 and 2 for a particular value of r.

If the two spherical bodies shown in Fig. 3.2 are subjected to a compressive force F directed along the z_1 and z_2 axes such that there is force equilibrium, the bodies will make contact over a small circular surface. The projection of this surface on the x, y plane is termed the region of contact.

The displacements in a direction normal to the x, y plane, of points lying on the surfaces of spheres 1 and 2 will be denoted by w_1 and w_2, respectively. As the spheres are pressed together, the distance between two such points on the region of contact will diminish by

$$\alpha = w_1 - w_2 \tag{3.4}$$

where $\alpha = [w_1 + w_2]|_{r=0}$

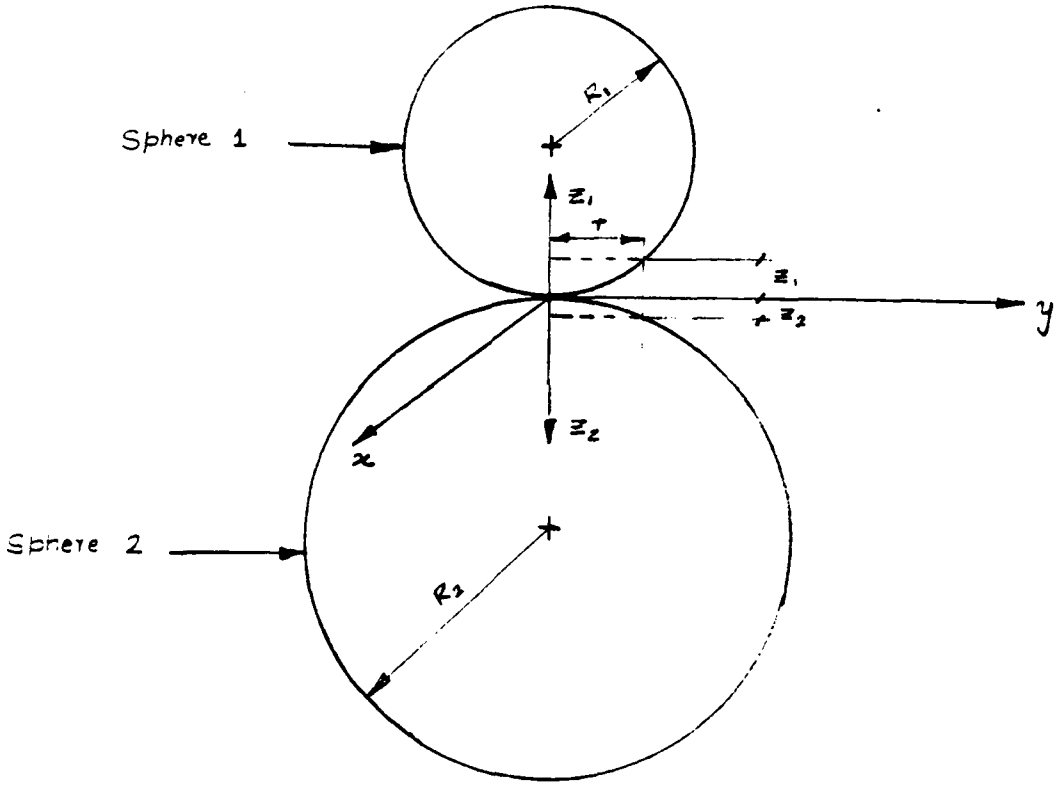

FIG. 3.2

From Eqs. (3.3) and (3.4) the following relationship is obtained for all points lying on the region of contact.

$$\alpha - (w_1 + w_2) = z_1 + z_2 = \frac{r^2(R_1 + R_2)}{2 R_1 R_2} \tag{3.5}$$

It is assumed that the radius of the region of contact is very small in comparison to the radii R_1 and R_2. Then when considering the local deformation within the region of contact, the spnere may be considered to be represented by a half-space. This enables one to see the solution for a point load acting on an elastic half-space to determine the displacements, w_1 and w_2, within the region of contact. The geometry for the problem of a point load acting on an elastic half-space is shown in Fig. 3.3. The solution for the displacement at z = 0, in the z-coordinate direction, is given by

$$w_{z=0} = \frac{F(1-\nu^2)}{\pi E r} \tag{3.6}$$

where F = the magnitude of the point load

E = modulus of elasticity

ν = Poisson's ratio

The Eq. (3.6) may be used to determine the displacement, w, on the plane z = 0, when a pressure P(r) is applied over a circular area on this plane. For a point A lying within a circular area, as shown in Fig. 3.4, the deflection, w, at point A may be determined from Eqs. (3.6) by making the following substitution

$$F = \iint_B P(s)\, s\, d\Phi ds \tag{3.7}$$

In Eq. (3.7), the integration is taken over the load area, B. The displacement of point A, shown in Fig. 3.4, is given by

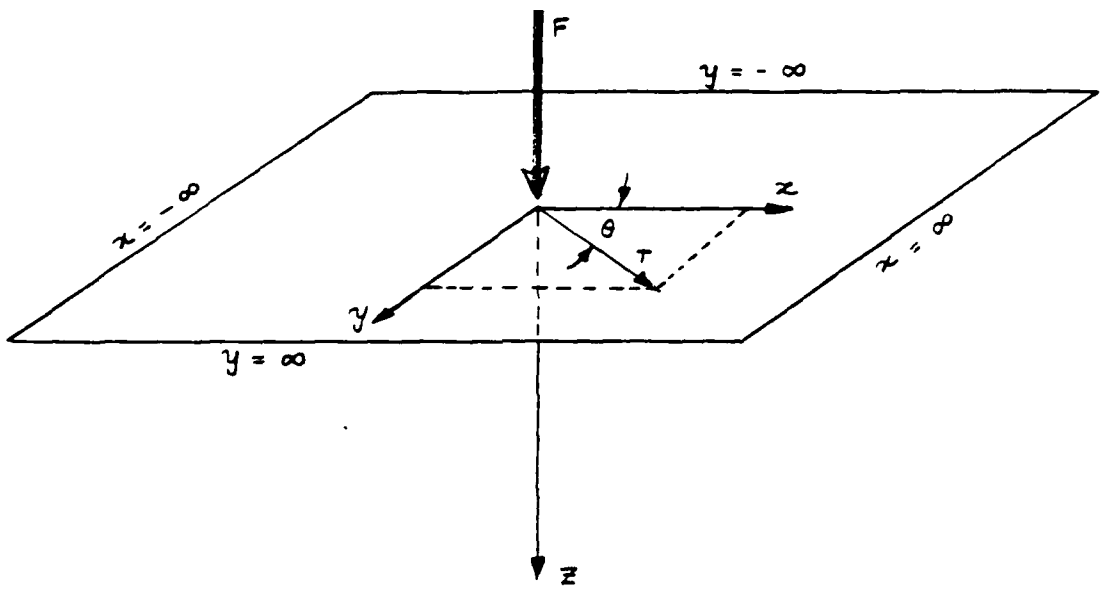

FIG. 33

$$w|_{z=0} = \frac{(1-\nu^2)}{\pi E} \iint_B P(s,\phi)\, ds d\phi \qquad (3.8)$$

In Eq. (3.8), the angle ϕ ranges from $\frac{\pi}{2}$ to $\frac{\pi}{2}$.
By substituting Eq. (3.8)

into Eq. (3.5), the following equation is obtained.

$$\frac{K_1 + K_2}{\pi} \iint_{R_c} P(s,\phi)\, ds d\phi = \alpha - \left(\frac{(R_1 + R_2)}{2 R_1 R_2} \right) r^2 \qquad (3.9)$$

where $K_1 = \dfrac{(1-\nu_1^2)}{E_1}$

$K_2 = \dfrac{(1-\nu_2^2)}{E_2}$

R_c = the area contained within the region of contact

The pressure distribution, P(s), is chosen such that Eq. (3.9) is satisfied. The pressure distribution which satisfies Eq. (3.9) is an elliptical cap over the region of contact. A cross-section of this pressure distribution along the chord BC shown in Fig. 3.4 is shown in Fig. 3.5. The maximum pressure, $P_o(\phi)$, along the chord BC is given by

$$P_o(\phi) = \frac{P_o}{a} \left(a^2 - r^2 \sin^2 \phi \right)^{1/2}, \quad \left(-\frac{\pi}{2} \le \phi \le \frac{\pi}{2} \right) \qquad (3.10)$$

where P_o = the pressure acting on the center of the contact region

a = the radius of the region of contact

The distribution of the pressure along the chord BC in Fig. 3.5 is given by

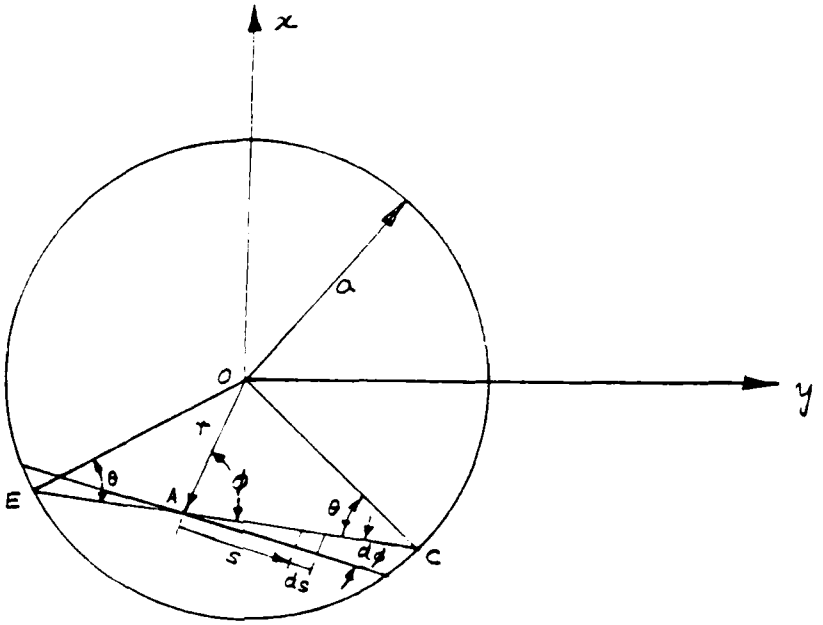

FIG 3.4

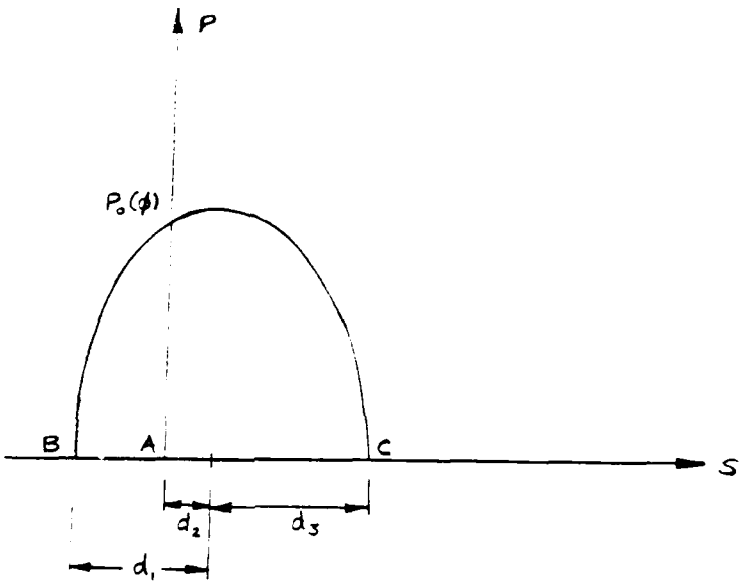

$$d_1 = d_3 = a \cos\theta \qquad -\pi/2 \le \theta \le \pi/2$$

$$d_2 = r \cos\phi \qquad -\pi/2 \le \phi \le \pi/2$$

FIG. 3.5

$$P(s,\varphi) = \frac{P_o(\varphi)}{a\cos\theta}\left[a^2\cos^2\theta - (s - r\cos\varphi)^2\right]^{1/2}, \quad \left(-\frac{\pi}{2} \leq \theta \leq \pi/2\right) \tag{3.11}$$

the relationship between the angles θ and φ is given by

$$a\sin\theta = r\sin\varphi \tag{3.12}$$

It is useful to express the variable s in terms of an angle β. This relationship is given by

$$S = r\cos\varphi + a\cos\theta\cos\beta, \quad (0 \leq \beta \leq \pi) \tag{3.13}$$

Substition of Eqs. (3.10), (3.11), (3,12), and (3.13) into Eq. (9) results in the following equation.

$$-\frac{(K_1 + K_2)}{\pi a}\int_{-\frac{\pi}{2}}^{\frac{\pi}{2}}\int_{0}^{\pi} P_o\,(a^2 - r^2\sin^2\Phi)\sin^2\beta\,d\beta d\phi = \alpha - \frac{(R_1 + R_2)}{2R_1R_2}r^2 \tag{3.14}$$

The expression obtained by performing the integration indicated in Eq. (3.14) is given by

$$\frac{(K_1 + K_2)}{9}P_o\left[\frac{a^2\pi}{2} - \frac{r^2\pi}{4}\right] = \alpha - \left[\frac{(R_1 + R_2)}{2R_1R_2}\right]r^2 \tag{3.15}$$

The Eq. (3.15) shows that Eq. (3.9) is satisfied by an elliptical pressure distribution acting on the region of contact, provided that the radius of the

contact region, a, and the displacement, α, are given by

$$a = \frac{\pi R_1 R_2 (K_1 + K_2) P_o}{2 (R_1 + R_2)} \tag{3.16a}$$

$$\alpha = \frac{\pi a (K_1 + K_2) P_o}{2} \tag{3.16b}$$

The constant, P_o, is determined from the static equilibrium of one sphere. For equilibrium of one sphere, the integral of the pressure, P(s), over the region of contact must equal the force, P, pressing the spheres together. The pressure distribution, P(s), symmetric with respect to the center of the contact region and is given by

$$P(r) = \frac{P_o}{a} \left\{ a^2 - r^2 \right\}^{1/2}, \quad (r \leq a) \tag{3.18}$$

The condition for the equilibrium of one of the spheres shown in Fig. 3.2 is given by

$$\iint_{R_c} P(r)\, dA = 2\pi \int_o^a \frac{P_o}{a} [a^2 - r^2]^{1/2} r dr = F \tag{3.19}$$

Integration of Eq. (3.19) yields the following value for P_o

$$P_o = \frac{3F}{2\pi a^2} \tag{3.20}$$

The displacements, w_1 and w_2, normal to the region of contact and lying within the region of contact are determined from Eqs. (3.8). These displacements are given by

$$w_1 = \frac{\pi K_1 P_o}{4a} [2a^2 - r^2], \qquad (r \leq a) \tag{3.21a}$$

$$w_2 = \frac{\pi K_2 P_o}{4a} [2a^2 - r^2], \qquad (r \leq a) \tag{3.21b}$$

The solution obtained for the two spheres in contact provides information about the displacements and stresses occurring on the surface of the sphere, within the region of contact. It does not provide a solution describing the stress and displacement fields in the interior of the sphere.

3.3 General Solution to the Axisymmetric Field Problem of Elasticity for a Region Bounded by a Sphere

In this section the solution of the elastic field equations for a sphere subject to either axisymmetric surface displacements or surface tractions is obtained. A sphere is shown in Fig. 3.6 relative to both the rectangular coordinates, (x,y,z) and the spherical coordinates (ρ,φ,θ).

The following restrictions are imposed on the sphere

1. Surface displacements or tractions are axisymmetric with respect to the z-axis.
2. The sphere is in static equilibrium.
3. Body forces are negligible.

The approach taken to obtain a solution to this problem is to use Boussinesq's solution in the harmonic function.

The general solution for a region with torsion-free rotational symmetry, in the absence of body forces, may be obtained as the sum of the two displacements fields given by

$$2G\,\vec{u}_1 = \vec{\nabla}\,\Phi\,(r,z) \tag{3.22}$$

$$2G\,\vec{u}_2 = \vec{\nabla}\,[z\,\Psi\,(r,z)] - 4\,(1-\nu)\,\Psi\,(r,z)\hat{e}_z \tag{3.23}$$

where $\vec{u}_1, \vec{u}_2$ = displacement vectors in rectangular coordinates

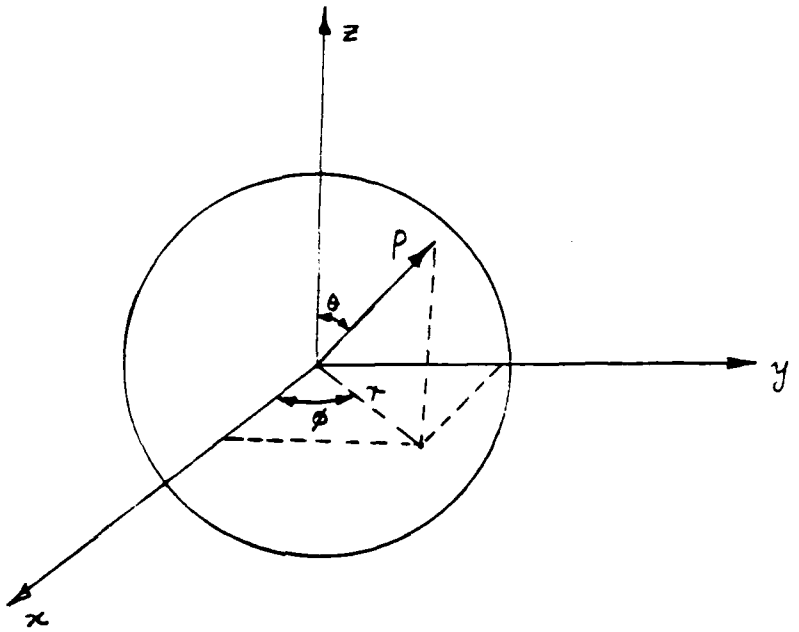

FIG 3.6

$\vec{\nabla}$ = gradient operator

$\hat{e}_x, \hat{e}_y, \hat{e}_z$ = unit vector in the x,y, and z coordinates directions respectively

$r^2 = x^2 + y^2 + z^2$

G = shear modulus

ν = Poisson's ratio

In Eqs. (3.22) and (3.23) $\phi(r,z)$ and $\psi(r,z)$ are arbitrary harmonic functions. Henceforth, the solutions given by Eqs. (3.22) and (3.23) will be referred to as the first and second Boussinesq solutions, respectively.

The region of interest is bounded by a sphere; therefore, it will be useful to employ spherical coordinates. Spherical coordinates are related to rectangular coordinates through the mapping

$$x = \rho \sin\phi \cos\theta \tag{3.24a}$$

$$y = \rho \sin\phi \sin\theta \tag{3.24b}$$

$$z = \rho \cos\phi \tag{3.24c}$$

The relationship between the displacement components in spherical coordinates and in rectangular coordinates is given by

$$u_\rho = \sin\phi \cos\theta \, u_x + \sin\phi \sin\theta \, u_y + \cos\phi \, u_z \tag{3.25a}$$

$$u_\phi = \cos\phi \cos\theta \, u_x + \cos\phi \sin\theta \, u_y - \sin\phi \, u_z \tag{3.25b}$$

$$u_\theta = \sin\theta \, u_x + \cos\theta \, u_y \tag{3.25c}$$

where u_ρ, u_ϕ, u_θ = components of the displacement vector in the ρ, ϕ, and θ coordinate directions respectively.

u_x, u_y, u_z = components of the displacement vector in the x, y, and z coordinate directions respectively.

From Eqs. (3.22) and (3.25), the displacement components in spherical coordinates for the first Boussinesq solution are given by

$$2G\ u_\rho = \sin\phi\cos\theta\frac{\partial\Phi}{\partial x} + \sin\phi\sin\theta\frac{\partial\Phi}{\partial y} + \cos\phi\frac{\partial\Phi}{\partial z} \tag{3.26a}$$

$$2G\ u_\phi = \cos\phi\cos\theta\frac{\partial\Phi}{\partial x} + \cos\phi\sin\theta\frac{\partial\Phi}{\partial y} - \sin\phi\frac{\partial\Phi}{\partial z} \tag{3.26b}$$

$$2G\ u_\theta = 0 \tag{3.26c}$$

The combination of Eqs. (3.23) and (3.25) gives the following displacement components for the second Boussinesq solution.

$$2G\ u_\rho = \sin\phi\cos\theta\frac{\partial\Phi}{\partial x} + \sin\phi\sin\theta\frac{\partial\Phi}{\partial y} + \cos\phi\left[\frac{\partial\Psi}{\partial z} - (3-4\nu)\Psi\right] \tag{3.27a}$$

$$2G\ u_\phi = \cos\phi\cos\theta\frac{\partial\Psi}{\partial x} + \cos\phi\sin\theta\frac{\partial\Psi}{\partial y} - \sin\theta\left[\frac{\partial\Psi}{\partial z} - (3-4\nu)\Psi\right] \tag{327.b}$$

$$2G\ u_\theta = 0 \tag{3.27c}$$

$$\Phi = \Phi(\rho,\phi) \tag{3.28a}$$

$$\Psi = \Psi(\rho,\phi) \tag{3.28b}$$

From Eq. (3.28a) the partial derivatives of the harmonic function ϕ appearing in Eqs. (3.26) are given by

$$\frac{\partial \Phi}{\partial x} = \frac{\partial \Phi}{\partial \rho}\frac{\partial \rho}{\partial x} + \frac{\partial \Phi}{\partial \phi}\frac{\partial \phi}{\partial x} \tag{3.29a}$$

$$\frac{\partial \Phi}{\partial y} = \frac{\partial \Phi}{\partial \rho}\frac{\partial \rho}{\partial y} + \frac{\partial \Phi}{\partial \phi}\frac{\partial \phi}{\partial y} \tag{3.29b}$$

$$\frac{\partial \Phi}{\partial z} = \frac{\partial \Phi}{\partial \rho}\frac{\partial \rho}{\partial z} + \frac{\partial \Phi}{\partial \phi}\frac{\partial \phi}{\partial z} \tag{3.29c}$$

From Eqs. (3.28b) the partial derivatives of the harmonic function appearing in Eqs. (3.27) are given by

$$\frac{\partial \Psi}{\partial x} = \frac{\partial \Psi}{\partial \rho}\frac{\partial \rho}{\partial x} + \frac{\partial \Psi}{\partial \phi}\frac{\partial \phi}{\partial x} \tag{3.30a}$$

$$\frac{\partial \Psi}{\partial y} = \frac{\partial \Psi}{\partial \rho}\frac{\partial \rho}{\partial y} + \frac{\partial \Psi}{\partial \phi}\frac{\partial \Phi}{\partial y} \tag{3.30b}$$

$$\frac{\partial \Psi}{\partial z} = \frac{\partial \Psi}{\partial \rho}\frac{\partial \rho}{\partial z} + \frac{\partial \Psi}{\partial \varphi}\frac{\partial \varphi}{\partial z} \tag{3.30c}$$

The gradients of ρ and ϕ are obtainable from Eqs. (3.24). These gradients are

$$\vec{\nabla}\rho = \frac{\partial \rho}{\partial x}\hat{e}_x + \frac{\partial \rho}{\partial y}\hat{e}_y + \frac{\partial \rho}{\partial z}\hat{e}_z$$

$$= \sin\varphi\cos\theta\,\hat{e}_x + \sin\varphi\sin\theta\,\hat{e}_y + \cos\varphi\,\hat{e}_z \tag{3.31a}$$

$$\vec{\nabla}\phi = \frac{\partial \phi}{\partial x}\hat{e}_x + \frac{\partial \phi}{\partial y}\hat{e}_y + \frac{\partial \phi}{\partial z}\hat{e}_z = \frac{\cos\varphi\cos\theta}{\rho}\hat{e}_x + \frac{\cos\varphi\sin\theta}{\rho}\hat{e}_y - \frac{\sin\varphi}{\rho}\hat{e}_z \tag{3.31b}$$

Combining Eqs. (3.26), (3.29), and (3.31) gives the following displacement components for the first Boussinesq solution

$$2G\,u_\rho = \frac{\partial \Phi}{\partial \rho} \tag{3.32a}$$

$$2G\,u_\phi = \frac{\sin\varphi}{\rho}\frac{\partial \Phi}{\partial(\cos\Phi)} \tag{3.32b}$$

Combining Eqs. (3.27), (3.30) and (3.31) gives the following displacement components for the second Boussinesq solution

$$2G\ u_\rho = \cos\Phi \left[\rho \frac{\partial \Psi}{\partial \rho} - (3-4\nu)\Psi \right] \tag{3.33a}$$

$$2G\ u_\phi = -\sin\Phi \left[\cos\Phi \frac{\partial \Psi}{\partial(\cos\phi)} - (3-4\nu)\Psi \right] \tag{3.33b}$$

In Eqs. (3.32) and (3.33), $\cos\varphi$ has been chosen as an independent variable. The harmonic functions, ϕ and ψ, will be represented, in part, by spherical harmonics which are functions of $\cos\varphi$.

The strain-displacement relationships referred to the spherical coordinate system, for the case of rotational symmetry about the z-axis are given by

$$\varepsilon_{\rho\rho} = \frac{\partial u_\rho}{\partial \rho} \tag{3.34a}$$

$$\varepsilon_{\rho\rho} = \frac{1}{\rho}\frac{\partial u_\phi}{\partial \phi} + \frac{u_\rho}{\rho} \tag{3.34b}$$

$$\varepsilon_{\theta\theta} = \frac{u_\rho}{\rho} + \frac{\cot\phi}{\rho} u_\phi \tag{3.34c}$$

$$\varepsilon_{\rho\phi} = \frac{1}{2}\left[\frac{1}{\rho}\frac{\partial u_\rho}{\partial \phi} + \frac{\partial u_\phi}{\partial \rho} - \frac{u_\phi}{\rho} \right] \tag{3.34d}$$

$$\varepsilon_{\phi\theta} = 0 \tag{3.34e}$$

$$\varepsilon_{\theta\rho} = 0 \tag{3.34f}$$

From these strain-displacement relations and the displacement components given by Eqs. (3.32) and the strain field for the first Boussinesq solution is

$$2G\ \varepsilon_{\rho\rho} = \frac{\partial^2 \phi}{\partial \rho^2} \tag{3.35a}$$

$$2G\ \varepsilon_{\phi\phi} = \frac{\sin^2\phi}{\rho^2}\frac{\partial^2 \phi}{\partial(\cos\phi)^2} - \frac{\cos\phi}{\rho^2}\frac{\partial \phi}{\partial(\cos\phi)} + \frac{1}{\rho}\frac{\partial \phi}{\partial \rho} \tag{3.35b}$$

$$2G\,\varepsilon_{\theta\theta} = \frac{1}{\rho}\frac{\partial\phi}{\partial\rho} - \frac{\cos\phi}{\rho^2}\frac{\partial\phi}{\partial(\cos\phi)} \tag{3.35c}$$

$$2G\,\varepsilon_{\rho\phi} = \frac{\sin\phi}{\rho^2}\frac{\partial\phi}{\partial(\cos\phi)} - \frac{\sin\phi}{\rho}\frac{\partial^2\phi}{\partial\rho\partial(\cos\phi)} \tag{3.35d}$$

$$\varepsilon_{\phi\theta} = 0 \tag{3.35e}$$

$$\varepsilon_{\phi\rho} = 0 \tag{3.35f}$$

Substituting the displacement components given by Eqs. (3.33) into the strain-displacement relations given by Eqs. (3.34) yields the following strain field for the second Boussinesq solution

$$2G\,\varepsilon_{\rho\rho} = \cos\phi\left[\rho\frac{\partial^2\psi}{\partial\rho^2} - 2(1-2\nu)\frac{\partial\psi}{\partial\rho}\right] \tag{3.36a}$$

$$2G\,\varepsilon_{\phi\phi} = \cos\phi\frac{\partial\psi}{\partial\rho} - \frac{\cos^2\phi}{\rho}\frac{\phi\psi}{\partial(\cos\phi)} + \frac{\sin^2\phi\cos\phi}{\rho}\frac{\partial^2\psi}{\partial(\cos\phi)^2} - 2(1-2\nu)\frac{\sin^2\phi}{\rho}\frac{\partial\psi}{\partial(\cos\phi)} \tag{3.36b}$$

$$2G\,\varepsilon_{\theta\theta} = \cos\phi\frac{\partial\psi}{\partial\rho} - \frac{\cos^2\phi}{\rho}\frac{\partial\psi}{\partial(\cos\phi)} \tag{3.36c}$$

$$2G\,\varepsilon_{\rho\phi} = 2(1-\nu)\frac{\sin\phi\cos\phi}{\rho}\frac{\partial\psi}{\partial(\cos\phi)} + (1-2\nu)\sin\phi\frac{\partial\psi}{\partial\rho} - \sin\phi\cos\phi\frac{\partial^2\phi}{\partial\rho\partial(\cos\phi)} \tag{3.36d}$$

$$\varepsilon_{\phi\theta} = 0 \tag{3.36e}$$

$$\varepsilon_{\theta\rho} = 0 \tag{3.36f}$$

The stress fields corresponding to the two solutions are determined from the

constitutive equations for an isotropic, linearly elastic material. These constitutive equations are

$$\sigma_{\rho\rho} = 2G\,\varepsilon_{\rho\rho} + \lambda e \tag{3.37a}$$

$$\sigma_{\varphi\varphi} = 2G\,\varepsilon_{\varphi\varphi} + \lambda e \tag{3.37b}$$

$$\sigma_{\theta\theta} = 2G\,\varepsilon_{\theta\theta} + \lambda e \tag{3.37c}$$

$$\sigma_{\rho\varphi} = 2G\,\varepsilon_{\rho\varphi} \tag{3.37d}$$

$$\sigma_{\theta\rho} = 2G\,\varepsilon_{\theta\rho} \tag{3.37e}$$

$$\sigma_{\varphi\theta} = 2G\,\varepsilon_{\varphi\theta} \tag{3.37f}$$

where e = volumetric strain $= \varepsilon_{\rho\rho} + \varepsilon_{\varphi\varphi} + \varepsilon_{\theta\theta}$

$$\lambda = \frac{2\nu G}{(1-2\nu)}$$

Substitution of the strain field given by Eqs. (3.35) into the constitutive relations given by Eqs. (3.37) gives the following stress field for the first Boussinesq solution

$$\sigma_{\rho\rho} = \frac{\partial^2 \Phi}{\partial \rho^2} \tag{3.38a}$$

$$\sigma_{\rho\varphi} = \frac{\sin^2\varphi}{\rho^2}\,\frac{\partial^2 \Phi}{\partial(\cos\varphi)^2} - \frac{\cos\varphi}{\rho^2}\,\frac{\partial \Phi}{\partial(\cos\varphi)} + \frac{1}{\rho}\,\frac{\partial \Phi}{\partial \rho} \tag{3.38b}$$

$$\sigma_{\theta\theta} = \frac{1}{\rho}\,\frac{\partial \Phi}{\partial \rho} - \frac{\cos\varphi}{\rho^2}\,\frac{\partial \Phi}{\partial(\cos\varphi)} \tag{3.38c}$$

$$\sigma_{\rho\varphi} = \frac{\sin\varphi}{\rho}\left[\frac{1}{\rho}\frac{\partial\dot{\varphi}}{\partial(\cos\varphi)} - \frac{\partial^2\dot{\varphi}}{\partial\rho\partial(\cos\varphi)}\right] \tag{3.38d}$$

$$\sigma_{\varphi\theta} = 0 \tag{3.38e}$$

$$\sigma_{\theta\rho} = 0 \tag{3.38f}$$

Substitution of the displacement components given by Eqs. (3.36) into the constitutive relations given by Eqs. (3.37) yields the following stress field for the second Boussinesq solution.

$$\sigma_{\rho\rho} = \rho\cos\varphi\frac{\partial^2\psi}{\partial\rho^2} - 2(1-\nu)\cos\varphi\frac{\partial\psi}{\partial\rho} - 2\nu\frac{\sin^2\varphi}{\rho}\frac{\partial\psi}{\partial(\cos\varphi)} \tag{3.39a}$$

$$\sigma_{\varphi\varphi} = \frac{\sin^2\varphi\cos\varphi}{\rho}\frac{\partial^2\psi}{\partial(\cos\varphi)^2} + (1-2\nu)\cos\varphi\frac{\partial\psi}{\partial\rho} \tag{3.39b}$$

$$\sigma_{\theta\theta} = (1-2\nu)\cos\varphi\frac{\partial\psi}{\partial\rho} - \frac{1}{\rho}\left[\cos^2\varphi + 2\nu\sin^2\varphi\right]\frac{\partial\psi}{\partial(\cos\varphi)} \tag{3.39c}$$

$$\sigma_{\rho\varphi} = \sin\varphi\left[(1-2\nu)\frac{\partial\psi}{\partial\rho} + 2(1-\nu)\frac{\cos\varphi}{\rho}\frac{\partial\psi}{\partial(\cos\varphi)} - \cos\varphi\frac{\partial^2\psi}{\partial\rho\partial(\cos\varphi)}\right] \tag{3.39d}$$

$$\sigma_{\varphi\theta} = 0 \tag{3.39e}$$

$$\sigma_{\theta\rho} = 0 \tag{3.39f}$$

The term of the harmonic functions, ϕ and ψ, will be determined. These functions satisfy Laplace's equation. When written in spherical coordinates,

this equation is

$$\frac{\partial^2\Theta}{\partial\rho^2} + \frac{2}{\rho}\frac{\partial\Theta}{\partial\rho} + \frac{\cot\phi}{\rho^2}\frac{\partial\Theta}{\partial\phi} + \frac{1}{\rho^2}\frac{\partial^2\Theta}{\partial\phi^2} + \frac{1}{\rho^2\sin^2\phi}\frac{\partial^2\Theta}{\partial\theta^2} = 0 \qquad (3.40)$$

A particular solution to Eq. (3.40) is of the form

$$\Theta_n = \rho^n \Psi_n \qquad (3.41)$$

where $\Psi_n = \Psi_n(\cos\phi)$

Substituting the solution given by Eq. (3.41) into Eq. (3.40) yields the following

$$\sin^2\phi \frac{\partial^2\Psi_n}{\partial(\cos\phi)^2} - 2\cos\phi \frac{\partial\Psi_n}{\partial(\cos\phi)} + n(n+1)\Psi_n = 0 \qquad (3.42)$$

The Eq. (3.42) is Legendre's equation, for which there are two solutions. These solutions are given by

$$\Psi_n = P_n(\cos\phi) \quad , (-\infty \leq n < \infty) \qquad (3.42a)$$

$$\Psi_n = Q_n(\cos\phi) \quad , (-\infty < n < \infty) \qquad (3.42b)$$

The solution P_n is called the Legendre polynominal of degree n. The solution Q_n is called the Legendre function of the second kind of degree n. The solution Q_n contains a logarithmic singularity $\cos\phi = \pm$ to the problem under consideration. The solution to be employed is P_n. An equation defining P_n is

$$P_n \cos\phi) = \frac{1}{2^n n!} \frac{d^n}{d(\cos\phi)^n} \left[(\cos^2\phi - 1)^n \right] \qquad (3.43)$$

Henceforth, the argument of P_n is $\cos\phi$. Recurrence relations for the Legendre polynomials, applicable for all values of n are.

$$P_n = P_{n-1} \qquad (3.44a)$$

$$(2n+1) \cos\phi \; P_n = (n+1) \; P_{n+1} + n \; P_{n-1} \qquad (3.44b)$$

$$\sin^2\phi \; P_n' = n \; P_{n-1} - n \cos\phi \; P_n \qquad (3.44c)$$

where $$P_n' = \frac{d \; P_n}{d(\cos\phi)}$$

The harmonic functions, ϕ and ψ, will be of the form given by Eq. (3.41), where V_n is given by Eqs. (3.42a). By virtue of the first recurrence relation given by Eqs. (3.44), the functions, ϕ and ψ are given by

$$\phi_n = \rho^{-n-1} \; P_n \; , \; (-\infty < n < \infty) \qquad (3.45a)$$

$$\psi_n = \rho^{-n-1} \; P_n \; , \; (-\infty < n < \infty) \qquad (3.45b)$$

In the Eqs. (3.45), the functions ϕ_n and ψ_n represent component solutions. A solution to a particular problem characterized by specific boundary conditions, will be determined by superposition of the component solutions ϕ_n and ψ_n. The component solutions to the first and second Boussinesq solutions will henceforth be denoted as $[A_n]$ and $[B_n]$, respectively. Using Eq. (3.45a), the displacement strain, and stress fields for solution $[A_n]$ are given by

$$2G\, u_\rho = -\frac{(n+1)}{\rho^{n+2}} P_n \tag{3.46a}$$

$$2G\, u_\phi = -\frac{\sin\phi}{\rho^{n+2}} P'_n \tag{3.46b}$$

$$u_\theta = 0 \tag{3.46c}$$

$$2G\, \varepsilon_{\rho\rho} = \frac{(n+1)(n+2)}{\rho^{n+3}} P_n \tag{3.46d}$$

$$2G\, \varepsilon_{\rho\phi} = \frac{1}{\rho^{n+3}} \left[P'_{n-1} - (n+1)(n+2) P_n \right] \tag{3.46e}$$

$$2G\, \varepsilon_{\theta\theta} = -\frac{P'_{n+1}}{\rho^{n+3}} \tag{3.46f}$$

$$2G\, \varepsilon_{\rho\phi} = \frac{\sin\phi}{\rho^{n+3}} (n+2) P'_n \tag{3.46g}$$

$$\varepsilon_{\phi\theta} = 0 \tag{3.46h}$$

$$\varepsilon_{\theta\rho} = 0 \tag{3.46i}$$

$$\sigma_{\rho\rho} = \frac{(n+1)(n+3)}{\rho^{n+3}} P_n \tag{3.46j}$$

$$\sigma_{\rho\phi} = \frac{1}{\rho^{n+3}} \left[P'_{n+1} - (n+1)(n+3) P_n \right] \tag{3.46k}$$

$$\sigma_{\theta\theta} = \frac{P'_{n+1}}{\rho^{n+3}} \tag{3.46l}$$

$$\sigma_{\rho\phi} = \frac{\sin\phi}{\rho^{n+3}} (n+2) P'_n \tag{3.46m}$$

$$\sigma_{\rho\theta} = 0 \tag{3.46n}$$

$$\sigma_{\theta\rho} = 0 \tag{3.46o}$$

Using the expression for ψ shown in Eq. (3.45b), the displacement strain, and stress fields for solution $[C_n]$ are given by

$$2G\, u_\rho = \frac{-(n+4-4\nu)}{(2n+1)\rho^{n+1}} \left[(n+1)\, P_{n+1} + n\, P_{n-1} \right] \tag{3.47a}$$

$$2G\, u_\varphi = \frac{-\sin\varphi}{(2n+1)\rho^{n+1}} \left[(n-3+4\nu)\, P'_{n+1} + (n+4-4\nu)\, P'_{n-1} \right] \tag{3.47b}$$

$$u_\theta = 0 \tag{3.47c}$$

$$2G\, \varepsilon_{\rho\rho} = \frac{(n+1)}{(2n+1)\rho^{n+2}} \left[(n+1)(n+4-4\nu) P_{n+1} + n(n+4-4\nu) P_{n-1} \right] \tag{3.47d}$$

$$2G\, \varepsilon_{\varphi\varphi} = \frac{1}{(2n+1)\rho^{n+2}} \left[(2n+1)\, P'_n - (n+1)(n^2-n+1+4n\nu)\, P_{n+1} \right.$$
$$\left. -n(n+1)(n+4-4\nu)\, P \right]_{n-1} \tag{3.47e}$$

$$2G\, \varepsilon_{\theta\theta} = \frac{1}{\rho^{n+2}} \left[(n+1)\, P_{n+1} + P'_n \right] \tag{3.47f}$$

$$2G\, \varepsilon_{\rho\varphi} = \frac{\sin\varphi}{(2n+1)\rho^{n+2}} \left[(n^2+2n-1+2\nu)\, p'_{n+1} \right.$$
$$\left. + (n+1)(n+4-4\nu)\, P'_{n-1} \right] \tag{3.47g}$$

$$\varepsilon_{\varphi\theta} = 0 \tag{3.47h}$$

$$\varepsilon_{\theta\rho} = 0 \tag{3.47i}$$

$$\sigma_{\rho\rho} = \frac{(n+1)}{(2n+1)\rho^{n+2}} \left[(n^2+5n+4-2\nu)\, P_{n+1} + n(n+4-4\nu)\, P_{n-1} \right] \tag{3.47j}$$

$$\sigma_{\varphi\varphi} = \frac{-1}{(2n+1)\rho^{n+2}} \left[(n+1)(n^2-n+1-2\nu)\, P_{n+1} + n(n+1)(n+4-4\nu)\, P_{n+1} \right.$$
$$\left. - (2n+1)\, P'_n \right] \tag{3.47k}$$

$$\sigma_{\theta\theta} = \frac{\pi 1}{\rho^{n+2}} \left[(n+1)(1-2\nu) P_{n+1} + P'_n \right] \quad (3.47l)$$

$$\tau_{r\theta} = \frac{\sin\varphi}{(2n+1)\rho^{n+2}} \left[(n+1)(n+4\neg 4\nu) P^{*}_{n=1} + (n^2+2n\neg +2\nu) P'_{n+1} \right] \quad (3.47m)$$

$$\sigma_{\varphi\theta} = 0 \quad (3.47n)$$

$$\sigma_{\theta\rho} = 0 \quad (3.47o)$$

The boundary conditions to be considered correspond to the two cases when either the surface displacements or surface tractions are specified on the sphere. For the case when axisymmetric surface displacements are specified, the known displacements components will be u_ρ and u_ϕ. These quantities may be represented by

$$u_\rho = u_\rho (R, \cos\varphi) \qquad \text{on } S \quad (3,48a)$$

$$u_\varphi = u_\varphi (R, \cos\varphi) \qquad \text{on } S \quad (3.48b)$$

where S = the surface of the sphere

R = the radius of the sphere

For the case when axisymmetric surface tractions are specified, the known stress components will be $\sigma_{\rho\rho}$ and $\sigma_{\rho\phi}$. These quantities may be represented by

$$\sigma_{\rho\rho} = \sigma_{\rho\rho}\,(R, \cos\phi) \qquad \text{on } S \tag{3.49a}$$

$$\sigma_{\rho\phi} = \sigma_{\rho\phi}\,(R, \cos\phi) \qquad \text{on } S \tag{3.49b}$$

To apply the boundary conditions given by Eqns. (3.48) or Eqns. (3.49), these boundary conditions must be represented as series expansions. For the displacement boundary conditions given by Eqns. (3.48), these series have the form

$$u_\rho\,(R, \cos\phi) = \sum_{n=0}^{\infty} \xi_u^u P_n \tag{3.50a}$$

$$u_\phi\,(R, \cos\phi) = \sin\phi \sum_{n=1}^{\infty} \eta_n^u P_n' \tag{3.50b}$$

The Eqn. (3.50a) is a series expansion for a Legendre polynominal. Eqn. (3.50b) is the series equation for an associated Legendre function of the first kind, of degree n. The significance of Eqn. (3.50b) is that the $\cos\phi = \pm 1$, the series expansion is equal to zero, which is required by the condition of symmetry. The coefficients in the series are given by

$$\xi_n^u = \frac{(3n+1)}{2} \int_{-1}^{1} u_\rho(R, \cos\varphi)\, P_n\,(\cos\phi)\, d\,(\cos\phi)$$

$$(n = 0, 1, 2, 3, \ldots) \tag{3.51a}$$

$$\eta_n^u = \frac{(2n+1)(n-1)!}{2(1+n)!} \int_{-1}^{1} u_\phi\,(R, \cos\phi)\, \sin\varphi\, P_n\,(\cos\phi)$$

$$d\,(\cos\phi),\ (n = 1, 2, 3, \ldots) \tag{3.51b}$$

In Eqns. (3.51), the superscript u is used to denote that surface displacements are the specified boundary conditions. Expansion of the surface tractions given by Eqns. (3.49) is done in the same way as the surface displacements, except that the coefficients appearing in Eqns. (3.50) and (3.51) are denoted by ξ_n^σ and R_n^σ. The superscript σ is used to denote that the surface tractions are the specified boundary conditions.

The Eqns. (3.50) show that the expansions of the boundary conditions are in terms of Legendre polynominals, or their derivatives, of one degree n. In order to meet these boundary conditions, the quantities being specified for solutions $[A_n]$ and $[C_n]$ should also be in terms of Legendre polynominals, or their derivatives, of one degree n. Solution $[A_n]$ satisfies this requirement, but solution $[C_n]$ does not. Therefore, the solution $[B_n]$ is formed from a linear combination of solutions $[A_n]$ and $[C_n]$. The component solution $[B_n]$ is given by

$$[B_n] = (2n+1)[C_n] - (n+4-4\nu)\,[A_{n-1}] \tag{3.52}$$

From Eqn. (3.52), the displacement, strain, and stress fields for solution $[B_n]$ are

$$2G\,u_\rho = -\frac{(n+1)(n+4-4\nu)}{\rho^{n+1}}\,P_{n+1} \tag{3.53a}$$

$$2G\,u_\varphi = -\frac{\sin\varphi}{\rho^{n+1}}\,(n-3+4\nu)\,P'_{n+1} \tag{3.53b}$$

$$u_\theta = 0 \tag{3.53c}$$

$$2G\,\varepsilon_{\rho\rho} = \frac{(n+1)^2(n+4-4\nu)}{\rho^{n+1}} P_{n+1} \tag{3.53a}$$

$$2G\,\varepsilon_{\varphi\varphi} = \frac{1}{\rho^{n+2}} \left[(n-3+4\nu) P'_n - (n+1) \right.$$

$$\left. (n^2-n+1+3n\nu) P_{n+1} \right] \tag{3.53e}$$

$$2G\,\varepsilon_{\theta\theta} = \frac{1}{\rho^{n+2}} \left[(2n+1)(n+1) P_{n+1} + (n-3+4\nu) \right] P'_n \tag{3.53f}$$

$$2G\,\varepsilon_{\rho\varphi} = \frac{\sin}{\rho^{n+2}} (n^2+2n-1+2\nu) P'_{n+1} \tag{3.53g}$$

$$\varepsilon_{\varphi\theta} = 0 \tag{3.53n}$$

$$\varepsilon_{\theta\rho} = 0 \tag{3.53i}$$

$$\sigma_{\rho\rho} = \frac{(n+1)(n^2+5n+4-2\nu)}{\rho^{n+2}} P_{n+1} \tag{3.53j}$$

$$\sigma_{\varphi\varphi} = \frac{-1}{\rho^{n+2}} \left[(n+1)(n^2-n+1-2\nu) P_{n+1} - (n-3+4\nu) P'_n \right] \tag{3.53k}$$

$$\sigma_{\theta\theta} = \frac{-1}{\rho^{n+2}} \left[(n+1)(2n+1)(1-2\nu) P_{n+1} + (n-3+4\nu) P'_n \right] \tag{3.53l}$$

$$\sigma_{\rho\varphi} = \frac{\sin\varphi}{\rho^{n+2}} (n^2+2n-1+2\nu) P'_{n+1} \tag{3.53m}$$

$$\sigma_{\varphi\theta} = 0 \tag{3.53n}$$

$$\sigma_{\theta\rho} = 0 \tag{3.53o}$$

The solution to the problem under consideration will be determined as a suitable combination of the component solutions $[A_n]$ and $[B_n]$. The form of the solution is taken to be

$$[S] = \sum_{n=-\infty}^{\infty} \left[a_n [A_n] + b_n [B_n] \right] \tag{3.54}$$

In Eqn. (3.54), [S] represents the solution to the displacement, strain and stress fields. The coefficients a_n and b_n are constants of superposition which are chosen such that the specified boundary conditions are satisfied.

Some values of the constants a_n and b_n may be determined by evaluating the component solutions $[A_n]$ and $[B_n]$ at $\rho = 0$. These solutions become singular at the origin ($\rho = 0$) for $n \geq 0$. The solution should not contain these singularities, as the condition that [S] be finite at the origin is imposed. This condition requires that

$$a_n = b_n = 0, \quad (n \geq 0) \tag{3.55}$$

Therefore, the solution [S] is given by

$$[S] = \sum_{n=1}^{\infty} \left[a_{-n} [A_{-n}] + b_{-n} [B_{-n}] \right] \tag{3.56}$$

3.3.1 Solution when the Displacements are Specified on the Surface of the Spnere

The boundary conditions which will be considered are the displacement components, u_ρ and u_ϕ, specified on the surface at the sphere. Due to the restriction of axisymmetry, these boundary conditions can be represented as

$$u_\rho = u_\rho (R, \cos\phi) \qquad \text{on S} \tag{3.57a}$$

$$u_\phi = u_\phi (R, \cos\phi) \qquad \text{on S} \tag{3.57b}$$

where S = the surface of the sphere

R = the radius of the sphere

Provided the functions u_ρ (4, cosφ) and u_ϕ (R, cosφ) are sufficiently smooth, they may be represented by

$$u_\rho (R, \cos\phi) = \sum_{n=0}^{\infty} \xi_n^u P_n \qquad (3.58a)$$

$$u_\phi (R, \cos\phi) = \sin\phi \sum_{n=1}^{\infty} \eta_n^u P_n \qquad (3.58b)$$

The coefficients ξ_n^u amd η_n^u are given by

$$\xi_n^u = \frac{(2n+1)}{2} \int_{-1}^{1} u_\rho (R, \cos\phi) P_n (\cos\phi) \, d(\cos\phi) \qquad (3.59a)$$

$$\eta_n^u = \frac{(2n+1)(n-1)!}{2(n+1)!} \int_{-1}^{1} u_\phi (R, \cos\phi) \sin\phi \, P_n' (\cos\phi) \, d(\cos\phi) \qquad (3.59b)$$

The solution to the interior displacement, strain and stress fields is assumed to be given by Eqn. (3.56). Using the displacement components u_ρ and u_ϕ of [S], in conjunction with Eqns. (3.58) yields the following set of equations from which to evaluate a_n and b_n.

$$(1-2\nu) R b_{-2}^u = G \xi_o^u \qquad (3.60a)$$

$$n a_{-n-1}^u - (n+1)(n-2+4\nu) R^2 b_{-n-2}^u = 2G \xi_n^u R^{1-n}, \quad (n = 1, 2, 3, \ldots) \qquad (3.60b)$$

$$-a^{u}_{n-1} + (n+5-4\nu)\, R^{2} b^{u}_{-n-2} = 2G\, \eta^{u}_{n}\, R^{1-n}$$

$$(n = 1, 2, 3, \ldots) \qquad (3.60c)$$

Solution of Eqns. (3.60) gives the following constants of superposition.

$$a_{-n-1} = \frac{G\,[(n+5-4\nu)\,\xi^{u}_{n} + (n^{2} + 3n-2+4n\nu)\,\eta^{u}_{n}\,]}{[3n+1-2\nu(2n+1)]\, R^{n+1}},$$

$$(n = 1, 2, 3, \ldots) \qquad (3.61a)$$

$$b^{u}_{-n-2} = \frac{G\,[\xi^{u}_{n} + n\, N^{u}_{n}]}{[3n+1-2(2n+1)\nu]\, R^{n+1}}, \quad (n = 0, 1, 2, \ldots.) \qquad (3.61b)$$

The displacement fields for the component solution $[A_n]$ and $[B_n]$ vanish for n = 1. Therefore, the values of a^{u}_{-1} and b^{u}_{-1} remain undetermined. The solution to the problem characterized by the boundary conditions in Eqns. (3.57) is given by

$$[S] = \sum_{n=1}^{\infty} a^{u}_{-n-1}\, [A_{-n-1}] + \sum_{n=0}^{\infty} b^{u}_{-n-2}\, [B_{-n-2}] \qquad (3.62)$$

In Eqn. (3.62), the constants of superposition a^{u}_{-n-1} and b^{u}_{-n-2} are given by Eqns. (3.61). The coefficients ξ^{u}_{n} and η^{u}_{n} appearing in Eqns. (3.61) are evaluated by Eqns. (3.59) for arbitrary surface displacements of the form given by Eqns. (3.57). The component solutions $[A_{-n-1}]$ and $[B_{-n-2}]$ may be determined from Eqns. (3.46) and Eqns. (3.53), respectively.

3.3.2 Solution when the Tractions are Specified on the Surface of the Spnere

The boundary conditions to be considered are the stresses, $\sigma_{\rho\rho}$ and $\sigma_{\sigma\phi}$ specified on the surface of the sphere. Because of the restriction that the surface tractions be axisymmetric, these stresses may be represented by

$$\sigma_{\rho\rho} = \sigma_{\rho\rho}\ (R,\ \cos\phi) \qquad \text{on } S \tag{3.63a}$$

$$\sigma_{\rho\phi} = \sigma_{\rho\phi}\ (R,\ \cos\phi) \qquad \text{on } S \tag{3.63b}$$

Provided that the functions $\sigma_{\rho\rho}\ (R,\ \cos\phi)$ and $\sigma_{\rho\phi}\ (R,\ \cos\phi)$ are sufficently smooth, they may be represented by

$$\sigma_{\rho\rho}\ (R,\ \cos\phi) = \sum_{n=0}^{\infty} \xi_n^{\sigma} P_n \tag{3.64a}$$

$$\sigma_{\rho\phi}\ (R,\ \cos\phi) = \sin\phi \sum_{n=1}^{\infty} \eta_n^{\sigma} P_n' \tag{3.64b}$$

The coefficients ξ_n^{σ} and μ_n^{σ} are given by

$$\xi_n^{\sigma} = \frac{(2n+1)}{2} \int_{-1}^{1} \sigma_{\rho\rho}\ (R,\ \cos\phi)\ P_n\ (\cos\phi)\ d\ (\cos\phi) \tag{3.65a}$$

$$\eta_n^{\sigma} = \frac{(2n+1)(n-1)!}{2(n+1)!} \int_{-1}^{1} \sigma_{\rho\phi}(R,\ \cos\phi)\ \sin\phi\ P_n'\ (\cos\phi)\ d\ (\cos\phi) \tag{3.65b}$$

The solution to the interior displacement, strain, and stress fields are assumed to be given by [S] in Eqn. (3.56). Using the stresses $\sigma_{\rho\rho}$ and $\sigma_{\rho\phi}$ of [S] in conjunction with Eqns. (3.64) yields the following set of equations from which to evaluate the constants a_n^{σ} and b_n^{σ}.

$$2\ (1+\nu)\ b_{-2} = \xi_o^{\sigma} \tag{3.66a}$$

$$n(n-1)\ a_{-n-1} = (n+1)\ [(n+1)(n-2)-2\nu]\ R^2\ b_{-n-2} = R^2\ \xi_n^{\sigma}\ , \qquad (n = 1,\ 2,\ 3,\ldots) \tag{3.66b}$$

$$-(n-1)\, a_{-n-1} + (n^2+2n-1+2\nu)\, R^2\, b_{-n-2} = R^2\, \sigma_n^c\,,$$

$$(n = 1, 2, 3, \ldots) \qquad (3.66c)$$

The Eqns. (3.66) are not compatible for n = 1, this value of n results in two equations with one unknown. By the consideration of static equilibrium, another condition may be obtained which will render Eqns. (3.66) compatible. A sphere with symmetric surface tractions about the z-axis is shown in Fig. 3.6. Under symmetric loading, equilibrium is automatically satisfied in the z and y coordinate directions. Equilibrium of the sphere will require the following

$$\int_S \vec{T} \cdot \hat{e}_z \, ds = 0 \qquad (3.67)$$

where $\vec{T}$ = stress vector

$\hat{e}_z$ = the unit vector in the z coordinate direction

In Eqn. (3.67), the integral is taken over the surface of the sphere S. The stresses which will be known on the surface of the sphere are $\sigma_{\rho\rho}$ and $\sigma_{\rho\phi}$. Therefore, the stress vector T is given by

$$\vec{T} = \sigma_{\rho\rho}\, \hat{e}_\rho + \sigma_{\rho\phi}\, \hat{e}_\phi \qquad (3.68)$$

where $\hat{e}_\rho$, $\hat{e}_\phi$ = the unit vectors in the ρ and ϕ coordinate directions respectively.

The unit vectors $\hat{\sigma}_\rho$ and $\hat{\sigma}_\phi$ are given by

$$\hat{e}_\rho = \sin\phi \cos\theta\, \hat{e}_x + \sin\phi \sin\theta\, \hat{e}_y + \cos\phi\, \hat{e}_z \qquad (3.69a)$$

$$\hat{e}_\phi = \cos\phi \cos\theta\, \hat{e}_x + \cos\phi \sin\theta\, \hat{e}_y - \sin\phi\, \hat{e}_z \qquad (3.69b)$$

Substitution of Eqns. (3.68) and (3.69) into Eqns. (3.67) gives the following

condition for equilibrium.

$$\int_0 \left[\sigma_{\rho\rho} \cos\phi - \sigma_{\rho\phi} \sin\phi \right] ds = 0 \tag{3.70}$$

The stresses $\sigma_{\rho\rho}$ and $\sigma_{\rho\phi}$ may be expressed in the form given by Eqns. (3.64). The surface element ds is given by

$$ds = R^2 \, d\theta d(\cos\phi) \tag{3.71}$$

Using Eqns. (3.64) and (3.71) in Eqn. (3.70) yields the following condition of equilibrium.

$$R^2 \int_0^{2\pi} \int_{-1}^{1} \left[\cos\phi \sum_{n=0}^{\infty} \xi_n^u \, P_n'(\cos\phi) - \sin^2\phi \sum_{n=1}^{\infty} \eta_n^u \, P'(\cos\phi) \right] d\theta d(\cos\phi) \tag{3.72}$$

Using the recurrence relation given by Eqns. (3.44c) in Eqn. (3.70) gives

$$R^2 \int_0^{2\pi} \int_{-1}^{1} \left[\cos\phi \sum_{n=0}^{\infty} \xi_n^\sigma \, P_n(\cos\phi) - \sum_{n=1}^{\infty} \eta_n^\sigma \, n \, P_{n-1}(\cos\phi) \right.$$

$$\left. + \cos\phi \sum_{n=1}^{\infty} \eta^\sigma \, n \, P_n(\cos\phi) \right] d\theta d(\cos\phi) = 0 \tag{3.73}$$

The ortnogonality relationship applicable to Legendre's polynominals is

$$\int_{-1}^{1} P_n(\cos\phi) \, P_m(\cos\phi) \, d(\cos\phi) = \begin{cases} 0 \, , & m \neq n \\ \dfrac{2}{2n+1} , & m = n \end{cases} \tag{3.74}$$

Noting that $P_0(\cos\phi) = 1$ and $P_1(\cos\phi) = \cos\phi$, and evaluating Eqn. (3.73) in accordance with Eqn. (3.73) gives the following equilibrium condition.

$$\frac{4\pi R^2}{3}\left(\xi_1^{\sigma} - 2\,\eta_1^{\sigma}\right) = 0 \tag{3.75}$$

The Eqns. (3.66) are compatible due to Eqn. (3.74). Solution of Eqns. (3.66) yields the following constants of superposition.

$$a_{-n-1}^{\sigma} = \frac{(n^2+2n-1+2\nu)\;\xi_n^{\sigma} + (n+1)(n^2-n-2-2\nu)\;\eta_n^{\sigma}}{2(n-1)[n^2+n+1+(2n+1)\nu]\;R^{n-2}}\,,$$

$$(n = 2,3,4,\ldots) \tag{3.76a}$$

$$b_{-n-2}^{\sigma} = \frac{\xi_n^{\sigma} + n\,\eta_n^{\sigma}}{2\,[n^2+n+1+(2n+1)\nu]\;R^{n}}, (n = 0,\ 1,\ 2,\ldots) \tag{3.76b}$$

The coefficients of superposition a_{-1}, a_{-2}, and b_{-1} remain undetermined because the stress fields vanish for the component solutions $[A_{-1}]$, $[A_{-2}]$, and $[B_{-1}]$. The solution to the problem characterized by the boundary conditions given in Eqns. (3.63) is

$$[S] = \sum_{n=2}^{\infty} a_{-n-1}^{\sigma}\,[A_{-n-1}] + \sum_{n=0}^{\infty} b_{-n-2}^{\sigma}\,[B_{-n-2}] \tag{3.77}$$

In Eqn. (3.77) the constants of superpositions are given by Eqn. (3.76). The coefficients ξ_n^{σ} and η_n^{σ} appearing in Eqns. (3.76) are determined from Eqns. (5.65). The component solutions $[A_{-n-1}]$ and $[B_{-n-1}]$ may be determined from Eqns. (3.46) and Eqs. (3.53). The solution given by Eqns. (3.77) is the same as that determined by Sternberg, Eubank, and Badowski).

3.4 Solution to Specific Elasticity Problems for a Sphere Subject to Axisymmetric Surface Displacements or Surface Tensions

The results of Sections 3.2 and 3.3 will be used to determine elastic solutions for a sphere, subjected to a number of particular boundary

conditions. The boundary conditions which will be considered for the sphere are as follows:

1. The surface displacements resulting from the contacts with two adjacent spheres along an axis of symmetry.
2. The surface tractions resulting from the contacts with two adjacent spheres along an axis of symmetry.
3. A uniform radial pressure applied over the entire surface of the sphere.

The boundary conditions listed above satisfy the restrictions imposed on the general solution given in Section 3.3. Therefore, the results of Section 3.3 may be used to determine solutions to the problems characterized by the boundary conditions listed above.

3.4.1 Solution when the Surface Displacements, Resulting from Three Sphere in Contact Along an Axis of Symmetry, are Known

The surface displacements on the region of contact resulting from pressing two spheres together are provided by Hertz contact theory. It is assumed that the surface displacements on the region of contact, parallel to the region of contact, are negligible. The surface displacements perpendicular to the region of contact, for the case of two spheres in contact, are given by Eqns. (3.21).

Three spheres in contact along the axis of symmetry are shown in Fig. 3.7. The displacement, u_z, for the region of contact is assumed to be given by Hertz contact theory. Therefore, Eqns. (3.21) are used to obtain the following displacement boundary conditions for the center sphere shown in Fig. 3.7.

$$u_z\,(R,\ \cos\phi) = \frac{3\,(1-\nu^2)F}{8\,a^3\,E}\,[2a^2-R^2\sin^2\phi],$$

$$(0 \leq \phi \leq \phi') \quad \ldots\ldots \quad (3.77a)$$

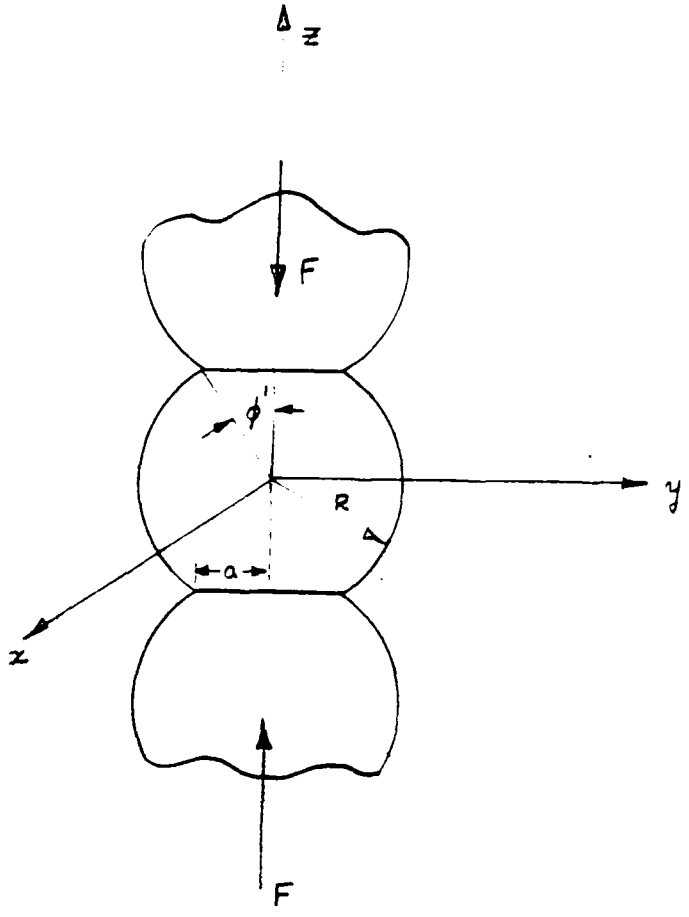

FIG 3.7

AD-A189 727 MICROMECHANICS MODELS FOR UNSATURATED SATURATED AND DRY SANDS(U) WISCONSIN UNIV-MADISON J K JEYAPALAN ET AL 25 JAN 88 AFOSR-TR-88-0154 AFOSR-84-0090 2/3

UNCLASSIFIED F/G 8/10 NL

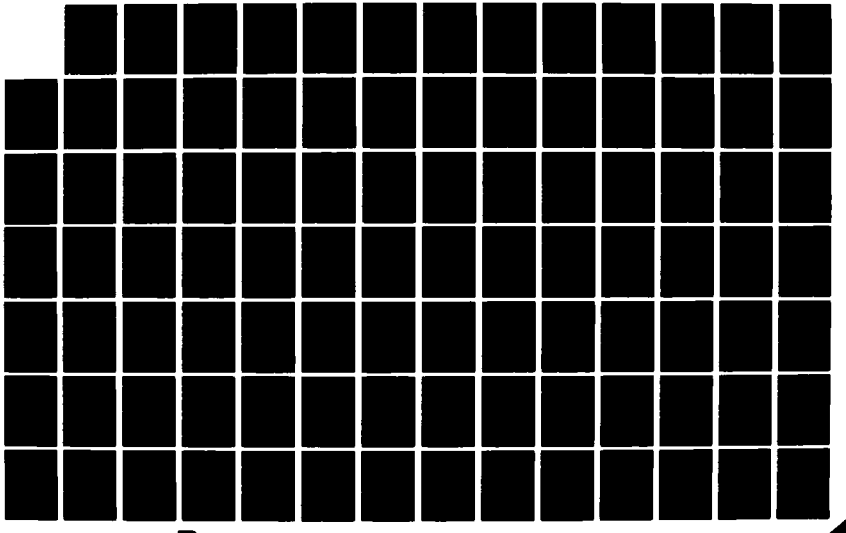

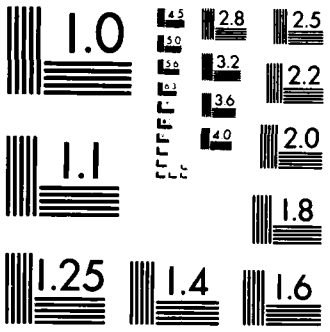

$$u_z\,(R,\,\cos\phi) = \frac{3(1-\nu^2)F}{8\,a^3\,E}\,[2a^2 - R^2\sin^2\phi],$$

$$(\pi - \phi' \leq \phi \leq \pi) \quad \ldots\ldots\ldots \quad (3.77b)$$

where F = total force transmitted through the contact

a = radius of the region of contact

ϕ' = angle defining the region of contact

R = radius of sphere

E = elastic modulus

Using Eqns. (3.25), the spherical displacement components, u_ρ and u_ϕ. are

$$u_\rho = u_z \cos\phi \qquad (3.78a)$$

$$u_\phi = u_z \sin\phi \qquad (3.78b)$$

The boundary conditions given by Eqns. (3.77) and the development components in Eqns.(3.78) can be combined to yield the following boundary conditions in terms of the spherical displacement components, u_ρ and u_ϕ.

$$u_\rho(R,\cos\phi) = \begin{cases} \dfrac{-3(1-\nu^2)F}{8\,a^3E}\,[2a^2 - R^2\sin^2\phi]\,\cos\phi, (0 \leq \phi \leq \phi^1) \\ \dfrac{3(1-\nu^2)F}{8\,a^3\,E}\,[2a^2 - R^2\sin^2\phi]\,\cos\phi, (\pi - \phi' \leq \phi \leq \pi) \end{cases} \qquad (3.79a)$$

$$u_\phi(R,\cos\phi) = \begin{cases} \dfrac{3(1-\nu^2)F}{8\,a^3\,E}\,[2a^2 - R^2\sin\phi]\,\sin\phi, (0 \leq \phi \leq \phi') \\ \dfrac{-3(1-\nu^2)F}{8\,a^3\,E}\,[2a^2 - R^2\sin^2\phi]\,\sin\phi, (\pi - \phi' \leq \phi \leq \pi) \end{cases} \qquad (3.79b)$$

To determine the displacement, strain and stress fields for a sphere whose displacement boundary conditions are given by Eqns. (3.79), it is necessary to evaluate the constants ξ_n^u and η_n^u given by Eqns. (3.61). In this case, these constants are given by

$$\xi_n^u = \frac{3(2n+1)(1-\nu^2)}{16\, a^3\, E}\left[\int_{-1}^{\cos(\pi-\phi')} [2a^2 - R^2\sin\phi]\cos\phi\, P_n(\cos\phi)\, d(\cos\phi) - \int_{\cos\phi'}^{1} [2a^2 - R^2\sin^2\phi]\cos\phi\, P_n(\cos\phi)\, d(\cos\phi)\right] \quad \ldots\ldots\ldots\ldots\ldots \quad (3.80a)$$

$$\eta_n^u = \frac{3(2n+1)(1-\nu^2)F}{16n(n+1)a^3\, E}\left[-\int_{-1}^{\cos(\pi-\phi')} [2a^2 - R^2\sin^2\phi]\sin^2\phi\, P_n'(\cos\phi)\, d(\cos\phi) + \int_{\cos\phi'}^{1} [2a^2 - R^2\sin^2\phi]\sin^2\phi\, P_n'(\cos\phi)\, d(\cos\phi)\right] \quad \ldots\ldots\ldots\ldots\ldots \quad (3.80b)$$

The expressions for the constants given in Eqns. (3.80) may be simplified since the functions contained in the integrals are odd or even functions, depending on the value of n. These functions are odd for an odd value of n, and even for an even value of n. Therefore, the constants ξ_n^u and η_n^u, will be zero for odd values of n. In view of this the constants are given by

$$\xi_{2n}^u = \frac{-3(4n+1)(1-\nu^2)F}{8\, a^3\, E}\int_{\cos\phi'}^{1} [2a^2 - R^2\sin^2\phi]\cos\phi\, P_{2n}(\cos\phi)\, d(\cos\phi), \quad (n = 0,1,2,\ldots.) \quad \ldots \quad (3.81a)$$

$$\eta_{2n}^u = \frac{3(4n+1)(1-\nu^2)F}{16n(2n+1)a^3 E}\int_{\cos\phi'}^{1} [2a^2 - R^2\sin^2\phi]\sin^2\phi\, P_{2n}'(\cos\phi)\, d(\cos\phi), \quad (n = 1,2,3,\ldots.) \quad \ldots \quad (3.81b)$$

Evaluation of the integrals contained in Eqns. (3.81) yields the following expressions for ξ^u_{2n} and η^u_{2n}.

$$\xi^u_o = \frac{-3(1-\nu^2)F}{8\,a^3\,E}\left[\frac{(2a^2-R^2)\sin^2\phi'}{2} + \frac{R^2(1-\cos^4\phi')}{4}\right] \quad . \quad . \quad . \quad (3.82a)$$

$$\xi^u_{2n} = \frac{3(1-\nu^2\,R^2F}{8\,a^3\,E}\left\{[2\sin^2\phi' - 1]\left[\frac{(2n+1)P_{2n+2}(\cos\phi')}{(4n+3)}\right.\right.$$

$$\left. + \frac{(4n+1)P_{2n}(\cos\phi')}{(4n+3)(4n-1)} - \frac{2nP_{2n-2}(\cos\phi')}{(4n-1)}\right]$$

$$- \frac{6P_{2n+4}(\cos\phi')}{(4n+7)(4n+5)(4n+3)} + \frac{6\,\cos\phi'\,P_{2n+3}(\cos\phi')}{(4n+5)(4n+3)}$$

$$+ 3\left[\frac{8}{(4n+7)(4n-1)} - \cos^2\phi'\right]\frac{P_{2n+2}(\cos\phi')}{(4n+3)}$$

$$+ \left[\cos^3\phi' - \frac{18\,\cos\phi'}{(4n+5)(4n-1)}\right]P_{2n+1}(\cos\phi')$$

$$+ 6\left[\cos^2\phi' - \frac{6}{(4n+5)(4n-3)}\right]\frac{(4n+1)\,P_{2n}(\cos\phi')}{(4n+3)(4n-1)}$$

$$+ \left[\frac{18\cos\phi'}{(4n+3)(4n-3)} - \cos^3\phi'\right]P_{2n-1}(\cos\phi')$$

$$+ 3\left[\frac{8}{(4n+3)(4n-5)} - \cos^2\phi'\right]\frac{P_{2n-2}(\cos\phi')}{(4n-1)}$$

$$\left. - \frac{6\,\cos\phi'\,P_{2n-3}(\cos\phi')}{(4n-1)(4n-3)} - \frac{6\,P_{2n-4}(\cos\phi')}{(4n-1)(4n-3)(4n-5)}\right\},$$

$$(n = 1,2,3,....) \quad . \quad . \quad . \quad . \quad (3.82b)$$

$$\eta_{2n}^{u} = \frac{3(1-\nu^2)R^2F}{8\,a^3\,E}\,\frac{(4n+1)}{(2n+1)(4n-1)}\Bigg\{[2\sin^2\phi'-1][P_{2n-2}(\cos\phi') - P_{2n}(\cos\phi')] - \frac{2\,P_{2n+2}(\cos\phi')}{(4n+3)(4n+1)} + \frac{2\cos\phi'\,P_{2n+1}(\cos\phi')}{(4n+1}$$

$$+\left[\frac{6}{(4n+3)(4n-3)} - \cos^2\phi'\right] P_{2n}(\cos\phi') - \frac{4\,(4n-1)\cos\phi'\,P_{2n-1}(\cos\phi')}{(4n+1)(4n-3)} + \left[\cos^2\phi' - \frac{6}{(4n+1)(4n-5)}\right]$$

$$P_{2n-2}(\cos\phi') + \frac{2\cos\phi'\,P_{2n-3}(\cos\phi')}{(4n-3)} + \frac{2\,P_{2n-4}(\cos\phi')}{(4n-3)(4n-5)}\Bigg\}$$

$$+\frac{\xi_{2n}^{u}}{(2n+1)},\quad (n = 1,2,3,....) \qquad (3.82c)$$

The general solution [S] given in Section 3.3 may be modified so that it does not include the zero terms which occur for odd values of n. Then, the solution to the problem characterized by the boundary conditions given in Eqns. (3.79) is

$$[S] = \sum_{n=1}^{\infty} a_{-2n-1}^{u}\,[A_{2n-1}] + \sum_{n=o}^{\infty} b_{2n-2}^{u}\,[B_{-2n-2}] \qquad (3.83)$$

The constants of superposition, a_{-2n-1}^{u} and b_{-2n-2}^{u}, are given by

$$a_{-2n-1}^{u} = \frac{G[(2n+5-4\nu)\,\xi_{2n}^{u} + 2(2n^2+3n-1+4n\nu)\eta_{2n}^{u}]}{[6n+1 - 2(4n+1)\,\nu]} \qquad (3.84a)$$

$$b_{-2n-2}^{u} = \frac{G[\xi_{2n}^{u} + 2n\,\eta_{2n}^{u}]}{[6n+1-2(4n+1)\nu]} \qquad (3.84b)$$

The component solutions, $[A_{-2n-1}]$ and $[B_{-2n-2}]$, may be determined from Eqns. (3.46) and (3.53), respectively. The component solution $[A_{-2n-1}]$ is given by

$$2G\, u_\rho = -2n\rho^{2n-1} P_{2n} \quad \ldots\ldots\ldots\ldots\ldots\ldots \quad (3.85a)$$

$$2G\, u_\phi = -\sin\phi\rho^{2n-1} P'_{2n} \quad \ldots\ldots\ldots\ldots\ldots\ldots \quad (3.85b)$$

$$u_\theta = 0 \quad \ldots\ldots\ldots\ldots\ldots\ldots\ldots\ldots \quad (3.85c)$$

$$2G\, \varepsilon_{\rho\rho} = 2n(2n-1)\rho^{2n-2} P_{2n} \quad \ldots\ldots\ldots\ldots\ldots\ldots \quad (3.85d)$$

$$2G\, \varepsilon_{\phi\phi} = \rho^{2n-2}[P'_{2n-1} - 2n(2n-1) P_{2n}] \quad \ldots\ldots\ldots \quad (3.85e)$$

$$2G\, \varepsilon_{\theta\theta} = -\rho^{2n-2} P'_{2n-1} \quad \ldots\ldots\ldots\ldots\ldots\ldots \quad (3.85f)$$

$$2G\, \varepsilon_{\rho\phi} = -(2n-1)\sin\phi\rho^{2n-2} P'_{2n} \quad \ldots\ldots\ldots\ldots \quad (3.85g)$$

$$\varepsilon_{\phi\theta} = 0 \quad \ldots\ldots\ldots\ldots\ldots\ldots\ldots\ldots \quad (3.85h)$$

$$\varepsilon_{\theta\rho} = 0 \quad \ldots\ldots\ldots\ldots\ldots\ldots\ldots\ldots \quad (3.85i)$$

$$\sigma_{\rho\rho} = 2n(2n-1)\rho^{2n-2} P_{2n} \quad \ldots\ldots\ldots\ldots\ldots\ldots \quad (3.85j)$$

$$\sigma_{\phi\phi} = \rho^{2n-2}[P'_{2n-1} - 2n(2n-1) P_{2n}] \quad \ldots\ldots\ldots \quad (3.85k)$$

$$\sigma_{\theta\theta} = -\rho^{2n-2} P'_{2n-1} \quad \ldots\ldots\ldots\ldots\ldots\ldots \quad (3.85l)$$

$$\sigma_{\rho\phi} = -(2n-1)\rho^{2n-2} \sin\phi\, P'_{2n} \quad \ldots\ldots\ldots\ldots\ldots \quad (3.85m)$$

$$\sigma_{\phi\theta} = 0 \quad \ldots\ldots\ldots\ldots\ldots\ldots\ldots\ldots \quad (3.85n)$$

$$\sigma_{\theta\rho} = 0 \quad \ldots\ldots\ldots\ldots\ldots\ldots\ldots\ldots \quad (3.85o)$$

The component solution $[B_{-2n-2}]$ is given by

$$2G\, u_\rho = -(2n+1)(2n-2+4\nu)\rho^{2n+1} P_{2n} \quad \ldots\ldots\ldots\ldots \quad (3.86a)$$

$$2G\, u_\phi = (2n+5-4\nu)\rho^{2n+1} \sin\phi\, P'_{2n} \quad \ldots\ldots\ldots\ldots \quad (3.86b)$$

$$u_\theta = 0 \quad \ldots\ldots\ldots\ldots\ldots\ldots\ldots\ldots \quad (3.86c)$$

$$2G\, \varepsilon_{\rho\rho} = -(2n+1)^2(2n-2+4\nu)\rho^{2n} P_{2n} \quad \ldots\ldots\ldots\ldots \quad (3.86d)$$

$$2G\, \varepsilon_{\phi\phi} = -\rho^{2n}\Big[(2n+5-4\nu) P'_{2n+1} - (2n+1)[(2n+1)^2 + 2(n+1)(3-4\nu)] P_{2n}\Big] \quad \ldots \quad (3.86e)$$

$$2G\, \varepsilon_{\theta\theta} = -\rho^{2n}\Big[(4n+3)(2n+1) P_{2n} - (2n+5-4\nu) P'_{2n+1}\Big] \quad \ldots\ldots \quad (3.86f)$$

$$2G\, \varepsilon_{\rho\phi} = \Big[4n(n+1) - 1 + 2\nu\Big]\rho^{2n} \sin\phi\, P'_{2n} \quad \ldots\ldots\ldots \quad (3.86g)$$

$$\varepsilon_{\phi\theta} = 0 \quad \ldots \quad (3.86h)$$

$$\varepsilon_{\theta\rho} = 0 \quad \ldots \quad (3.86i)$$

$$\sigma_{\rho\rho} = -(2n+1)[(2n+1)(2n-2) - 2\nu]\,\rho^{2n} P_{2n} \quad \ldots \quad (3.86j)$$

$$\sigma_{\phi\phi} = \rho^{2n}[(2n+1)(4n^2+10n+7-2\nu) P_{2n} + (2n+5-4\nu) P'_{2n+1}] \quad \ldots \quad (3.86k)$$

$$\sigma_{\theta\theta} = \rho^{2n}[(2n+5-4\nu) P'_{2n+1} - (4n+3)(2n+1)(1-2\nu) P_{2n}] \quad \ldots \quad (3.86l)$$

$$\sigma_{\rho\phi} = (4n^2+4n-1+2)\,\rho^{2n} \sin\phi\, P'_{2n} \quad \ldots \quad (3.86m)$$

$$\sigma_{\phi\theta} = 0 \quad \ldots \quad (3.86n)$$

$$\sigma_{\theta\rho} = 0 \quad \ldots \quad (3.86o)$$

3.4.2 Solution when the Surface Tractions Resulting from Three Spheres in Contact Along an Axis of Symmetry are Known

The surface tractions resulting from the contact of two spheres are known from Hertz contact theory. On the contact surface, the normal stress is known from Eqn. (3.18). For the problem of three spheres in contact, as shown in Fig. 3.7, it is assumed that the normal stress on the contact surfaces are given by Eqn. (3.18). Therefore, the stress boundary condition is given by

$$\sigma_{\rho\rho}(R, \cos\phi) = -\frac{3RF}{2\pi a^3}\left[\cos^2\phi - \cos^2\phi'\right]^{1/2},$$

$$(0 \leq \phi \leq \phi';\ \pi-\phi \leq \phi \leq \pi) \quad \ldots . \quad (3.87)$$

where F = force transmitted through the contact

a = radius of contact region

ϕ' = angle defining the region of contact

R = radius of the sphere

In order to use the solution developed in Section 3.3, the stress components on the surface of the sphere, $\sigma_{\rho\rho}$ and $\sigma_{\rho\phi}$, must be determined. These stress components are given by

$$\sigma_{\rho\rho} = \sigma_{zz} \cos^2\phi \quad \ldots \quad (3.88a)$$

$$\sigma_{\rho\phi} = \sigma_{zz} \sin\phi \cos\phi \quad \ldots \quad (3.88b)$$

From Eqns. (3.87) and (3.88), the desired boundary conditions are given by

$$\sigma_{\rho\rho}(R,\cos\phi) = \frac{-3RF}{2\pi a^3}\left[\cos^2\phi - \cos^2\phi\right]^{1/2} \cos^2\varphi,$$

$$(0 \leq \phi \leq \phi';\ \pi-\phi' \leq \phi \leq \pi) \ldots . \quad (3.89a)$$

$$\sigma_{\rho\phi}(R,\cos\phi) = \frac{3RF}{2\pi a^3}\left[\cos^2\phi - \cos^2\phi'\right]^{1/2} \sin\phi \cos\phi,$$

$$(0 \leq \phi \leq \phi';\ \pi-\phi \leq \phi \leq \pi) \ldots . \quad (3.89b)$$

To determine the displacement, strain and stress fields for the interior of a sphere whose surface tractions are given by Eqns. (3.89), it is necessary to determine the constants, ξ_n^σ and η_n^σ, given by Eqns. (3.65). For the boundary conditions in Eqns. (3.89), the constants are given by

$$\xi_n^\sigma = -\frac{3(2n+1)RF}{4\pi a^3}\left[\int_{-1}^{\cos(\pi-\phi')}[\cos^2\phi - \cos^2\phi']^{1/2}\cos^2\phi\, P_n(\cos\phi)\, d(\cos\phi) + \int_{\cos\phi'}^{1}[\cos^2\phi - \cos^2\phi']^{1/2}\cos^2\phi\, P_n(\cos\phi)\, d(\cos\phi)\right]$$

$$(n = 0,1,2,\ldots.) \quad \ldots\ldots\ldots\ldots (3.90a)$$

$$\eta_n^\sigma = \frac{3(2n+1)RF}{4n(n+1)\pi a^3}\left[\int_{-1}^{\cos(-\phi')}[\cos^2\phi - \cos^2\phi']^{1/2}\sin^2\phi\cos\phi\, P_n'(\cos\phi)\, d(\cos\phi) + \int_{\cos\phi'}^{1}[\cos^2\phi - \cos^2\phi']^{1/2}\sin^2\phi\cos\phi P_n'(\cos\phi)\, d(\cos\phi)\right] \quad (n = 1,2,3,\ldots) \quad \ldots\ldots (3.90b)$$

The above integrals for ξ_n^σ and η_n^σ may be simplified since the functions contained within the integrals are odd or even functions, depending on the value of n. These functions are odd for odd values of n and otherwise even. Therefore, the constants ξ_n^σ and η_n^σ may be determined as follows

$$\xi_{2n}^{\sigma} = \frac{-3(2n+1)RF}{2\pi\, a^3} \int_{\cos\phi'}^{1} [\cos^2\phi - \cos^2\phi']^{1/2} \cos^2\phi\, P_n(\cos\phi) d(\cos\phi),$$

$$(n = 1,2,3,....) \quad . \quad . \quad . \quad (3.91a)$$

$$\eta_{2n}^{\sigma} = \frac{3(2n+1)RF}{2n(n+1)\pi\, a^3} \int_{\cos\phi'}^{1} [\cos^2\phi - \cos^2\phi']^{1/2} \sin^2\phi \cos\phi\, P'_{2n}(\cos\phi) d(\cos\phi),$$

$$(n = 1,2,3,....) \quad . \quad . \quad . \quad (3.91b)$$

Evaluation of the integrals in Eqns. (3.91) yields the following eqations for ξ_{2n}^{σ} and η_{2n}^{σ}.

$$\xi_{o}^{\sigma} = \frac{-3FR}{2\pi a^3} \left[\frac{\sin^3\phi'}{4} + \frac{\cos^7\phi'\sin\phi'}{8} - \frac{\cos^4\phi'}{8} \ln\left(\frac{1+\sin\phi'}{\cos\phi'}\right) \right] . \quad (3.92a)$$

$$\xi_{2n}^{\sigma} = \frac{(4n+1)3FR}{2\pi\, a^3} \sum_{m=o}^{n} \frac{(-1)^m (4n-2m)!}{2^{2n} m!(2n-m)!(2n-2m)!}$$

$$\left[\frac{-\sin\phi}{(2n-2m+4)} + \frac{(2n-2m+2)!\cos\phi'^{\,2(m-m+2)}}{2^{2(n-m+1)}[(n-m+1)!]^2(2n-2m+4)} \ln\left(\frac{1+\sin\phi'}{\cos\phi'}\right) \right.$$

$$\left. + \frac{\sin\phi'}{(2n-2m+4)} \sum_{k=o}^{n-m} \frac{(2m-2m+2)!(k!)^2\cos\phi'^{\,2(n-m-k+1)}}{2^{2(m-m-k+1)}[(n-m+1)!]^2(2k+1)!} \right],$$

$$(n = 1,2,3,....) \quad . \quad . \quad . \quad . \quad . \quad . \quad . \quad . \quad . \quad (3.92b$$

$$\eta_{2n}^{\sigma} = \frac{(2n-2)'3FR}{2\pi(2n-1)!a^3} \left\{ 2n \sum_{m=0}^{n} \frac{(-1)^m (4n-2m)!}{2^{2m} m!(2n-m)!(2n-2m)!} \left[\frac{\sin\phi'}{(2n-2m+1)} \right. \right.$$

$$- \frac{(2n-2m+2)!\ \cos\phi'^{\,2(n-m+1)}}{2^{2(n-m+1)}[(n-m+1)!]^2(2n-2m+1)} \ln\left(\frac{1+\sin\phi'}{\cos\phi'}\right)$$

$$- \frac{\sin\phi'}{(2n-2m+1)} \sum_{k=o}^{n-m} \frac{(2n-2m+2)!\ (k!)^2\ \cos\phi'^{\,2(n-m-k+1)}}{2^{2(n-m-k+1)}[(n-m+1)!]^2(2k+1)!} \Bigg]$$

$$+ (2n-1) \sum_{m=o}^{n} \frac{(-1)^m(4n-2m-4)!}{2^{2(n-1)}m!(2n-m-2)!(2n-2m-2)!} \Bigg[\frac{\sin\phi'}{(2n-2m-1)}$$

$$+ \frac{\sin\phi'}{(2n-2m+1)(2n-2m-1)\cos^2\phi'} - \frac{(2n-2m+2)(2n-2m+2)!\cos\phi'^{\,2(n-m)}}{2^{2(n-m+1)}[(n-m+1)!]^2(2n-2m+1)(2n-2m-1)}$$

$$\ln\left(\frac{1+\sin\phi'}{\cos\phi'}\right) - \frac{(2n-2m+2)\sin\phi'}{(2n-2m+1)(2n-2m-1)} \sum_{k=o}^{n-m}$$

$$\frac{(2n-2m+2)!(k!)^2\cos\phi'^{\,2(n-m-k+1)}}{2^{2(n-m-k+1)}[(n-m+1)!]^2(2k+1)!} \Bigg] \Bigg\} + \frac{2n(2n-1)!}{(2n+1)!}\,\xi_{2n}^{\sigma} \quad ,$$

$$(n = 1,2,3,....) \quad . \quad . \quad . \quad . \quad (3.92c)$$

The general solution [S] given in Section 3.3 may be modified so that it does not include the zero terms which occur for odd values of n. Then the solution to the problem characterized by the boundary conditions in Eqns. (3.89) is given by

$$[S] = \sum_{n=1}^{\infty} a_{-2n-1}^{\sigma}\,[A_{-2n-1}] + \sum_{n=0}^{\infty} b_{-2n-2}^{\sigma}\,[B_{-2n-2}] \quad . \quad . \quad . \quad (3.93a)$$

$$a_{-2n-2}^{\sigma} = \frac{(4n^2+4n-1+2\nu)\ \xi_{2n}^{\sigma} + 2(2n-1)(2n^2-n-1-\nu)\ \eta_{2n}^{\sigma}}{2(2n-1)\ [4n^2+2n+1+(4n+1)\nu]\ R^{2n-2}} \quad . \quad . \quad . \quad . \quad (3.93b)$$

$$b^{\sigma}_{2n-2} = \frac{\xi^{\sigma}_{2n} + 2n\,\eta^{\sigma}_{2n}}{2[4n^2+2n+1+(4n+1)\nu]R^{2n}} \quad \ldots\ldots\ldots\ldots \quad (3.93c)$$

The component solutions $[A_{-2n-1}]$ and $[B_{-2n-2}]$ are given by Eqns. (3.85) and Eqns. (3.86), respectively.

3.4.3 Solution for a Sphere Under the Action of a Uniform Radial Pressure

A sphere subjected to a uniform radial pressure is shown in Fig. 3.8 . The boundary conditions for this sphere are

$$\sigma_{\rho\rho}\,(R,\cos\phi) = -\sigma_u \quad ,(0 \leq \phi \leq \pi) \quad \ldots\ldots\ldots\ldots\ldots\ldots \quad (3.94a)$$

$$\sigma_{\rho\phi}\,(R,\cos\phi) = 0 \quad ,(0 \leq \phi \leq \pi) \quad \ldots\ldots\ldots\ldots\ldots\ldots \quad (3.94b)$$

where σ_u = the magnitude of the uniform radial pressure

To determine the displacement, strain and stress fields for the problem characterized by the boundary conditions given in Eqns. (3.94), the constants ξ^{σ}_n and η^{σ}_n must be determined from Eqns. (3.66). For these boundary conditions, the constants ξ^{σ}_n and η^{σ}_n are determined as follows.

$$\xi^{\sigma} = \frac{-(2n+1)}{2}\int_{-1}^{1} \sigma_u\, P_n(\cos\phi)\, d(\cos\phi) \ ,$$

$$(n = 0,1,2,\ldots.) \quad \ldots\ldots\ldots \quad (3.95a)$$

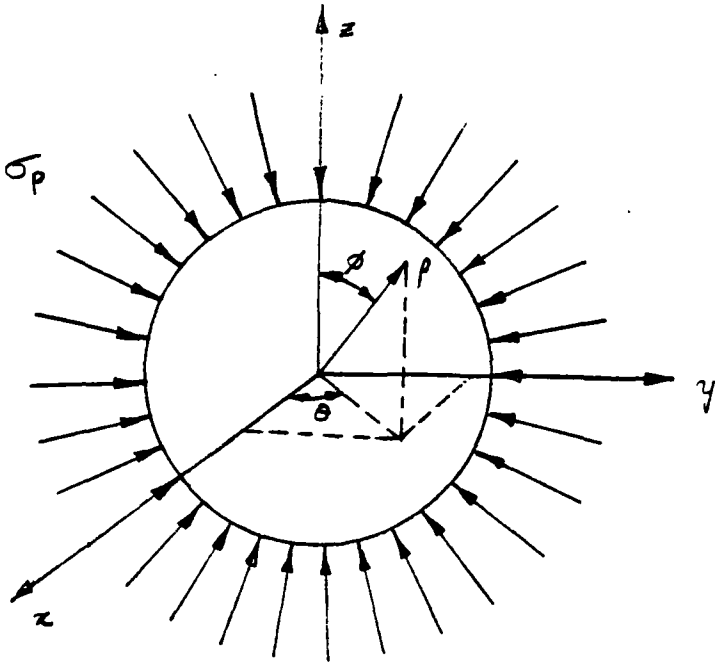

FIG. 3.8

$$\eta_n^{\sigma} = 0, \ (n = 1,2,3,....) \quad . . . . . (3.95b)$$

Evaluating the integral in Eqns. (3.95) yields the following for the constants $_n$ and $_n$.

$$\xi_o^{\sigma_u} = - \sigma_u \quad . . . . . (3.96a)$$

$$\xi_n^{\sigma_u} = 0 \ , \ (n = 1,2,3,....) \quad . . . . . (3.96b)$$

$$\eta_n^{\sigma_u} = 0 \ , \ (n = 1,2,3,....) \quad . . . . . (3.96c)$$

In Eqns. (3.96), the superscript σ_u has been used to denote that the constants were determined for the case of a uniformly applied pressure. The Eqns. (3.96) show that $\xi_n^{\sigma_u}$ and $\eta_n^{\sigma_u}$ are equal to zero for $n \geq 1$. Due to this, the solution [S] reduces to

$$[S] = b_{-2} \, [B_{-2}] \quad . . . . . (3.97)$$

where $b_{-2} = \dfrac{\sigma_u}{2(1+\nu)}$

The component solution $[B_{-2}]$ is determined from Eqns. (3.54). Substituting solution $[B_{-2}]$ into Eqn. (3.97) yields the following displacement, strain and stress fields corresponding to the solution [S].

$$u_\rho = - \frac{(1-2\nu) \ \sigma_u \rho}{2G(1+\nu)} \quad . . . . . (3.98a)$$

$$u_\phi = 0 \quad \ldots \quad (3.98b)$$

$$u_\theta = 0 \quad \ldots \quad (3.98c)$$

$$\varepsilon_{\rho\rho} = \frac{-(1-2\nu)\ \sigma_u}{2G(1+\nu)} \quad \ldots \quad (3.98d)$$

$$\varepsilon_{\phi\phi} = \frac{-(1-2\nu)\ \sigma_u}{2G(1+\nu)} \quad \ldots \quad (3.98e)$$

$$\varepsilon_{\theta\theta} = \frac{-(1-2\nu)\ \sigma_u}{2G(1+\nu)} \quad \ldots \quad (3.98f)$$

$$\varepsilon_{\rho\phi} = 0 \quad \ldots \quad (3.98g)$$

$$\varepsilon_{\phi\theta} = 0 \quad \ldots \quad (3.98h)$$

$$\varepsilon_{\theta\rho} = 0 \quad \ldots \quad (3.98i)$$

$$\sigma_{\rho\rho} = -\sigma_u \quad \ldots \quad (3.98j)$$

$$\sigma_{\phi\phi} = -\sigma_u \quad \ldots \quad (3.98k)$$

$$\sigma_{\theta\theta} = -\sigma_u \quad \ldots \quad (3.98l)$$

$$\sigma_{\rho\phi} = 0 \quad \ldots \quad (3.98m)$$

$$\sigma_{\phi\theta} = 0 \quad \ldots \quad (3.98n)$$

$$\sigma_{\theta\rho} = 0 \quad \ldots \quad (3.98o)$$

The solution given in Eqns. (3.98) may be verified by an approach other than Boussinesq's solution in two harmonic functions. For a sphere subjected to the boundary conditions given by Eqns. (3.94) there will be an infinite number of possible axes of symmetry passing through the origin. Due to this symmetry the displacement strain and stress fields will be independent of the spherical coordinate directions ϕ and θ. In view of this symmetry the displacement components are given by

$$u_\rho = u_\rho(\rho) \quad \ldots \quad (3.99a)$$

$$\phi = 0 \quad \ldots \quad (3.99b)$$

$$\theta = 0 \quad \ldots \quad (3.99c)$$

From the strain-displacement relationships given by Eqns. (3.34), the strain components are given by

$$\varepsilon_{\rho\rho} = \frac{du_\rho}{d_\rho} \quad \ldots \quad (3.100a)$$

$$\varepsilon_{\phi\phi} = \frac{u_\rho}{\rho} \quad \ldots \quad (3.100b)$$

$$\varepsilon_{\theta\theta} = \frac{u_\rho}{\rho} \quad \ldots \quad (3.100c)$$

$$\varepsilon_{\rho\phi} = 0 \quad \ldots \quad (3.100d)$$

$$\varepsilon_{\phi\theta} = 0 \quad \ldots \quad (3.100e)$$

$$\varepsilon_{\theta\rho} = 0 \quad \ldots\ldots\ldots\ldots\ldots\ldots\ldots \quad (3.100f)$$

From the constitutive relationships given by Eqns. (3.37), the stress components are given by

$$\sigma_{\rho\rho} = (\lambda+2G)\,\varepsilon_{\rho\rho} + \lambda(\varepsilon_{\rho\rho}+\varepsilon_{\theta\theta}) \quad \ldots\ldots\ldots\ldots \quad (3.101a)$$

$$\sigma_{\phi\phi} = (\lambda+2G)\,\varepsilon_{\phi\phi} + \lambda(\varepsilon_{\theta\theta}+\varepsilon_{\rho\rho}) \quad \ldots\ldots\ldots\ldots \quad (3.101b)$$

$$\sigma_{\theta\theta} = (\lambda+2G)\,\varepsilon_{\theta\theta} + \lambda(\varepsilon_{\rho\rho}+\varepsilon_{\phi\phi}) \quad \ldots\ldots\ldots\ldots \quad (3.101c)$$

$$\sigma_{\rho\phi} = 0 \quad \ldots\ldots\ldots\ldots\ldots\ldots\ldots \quad (3.101d)$$

$$\sigma_{\phi\theta} = 0 \quad \ldots\ldots\ldots\ldots\ldots\ldots\ldots \quad (3.101e)$$

$$\sigma_{\theta\rho} = 0 \quad \ldots\ldots\ldots\ldots\ldots\ldots\ldots \quad (3.101f)$$

For the case when the stress components are functions of the spherical coordinate ρ only, the differential equations of equilibrium, in the absence of inertia and body forces, reduce to the following

$$\frac{d\sigma_{\rho\rho}}{d\rho} + \frac{2\sigma_{\rho\rho} \quad \sigma_{\phi\phi} \quad \sigma_{\theta\theta}}{\rho} = 0 \quad \ldots\ldots\ldots\ldots\ldots \quad (3.102a)$$

$$\sigma_{\phi\phi} - \sigma_{\theta\theta} = 0 \quad \ldots\ldots\ldots\ldots\ldots\ldots \quad (3.102b)$$

Combining Eqns. (3.99), (3.100), (3.101) and (3.102) yields the following.

$$\frac{d^2u_\rho}{d_\rho} + \frac{2}{\rho}\frac{du_\rho}{d_\rho}\frac{2}{\rho^2}u_\rho = 0 \quad \ldots\ldots\ldots\ldots\ldots\ldots \quad (3.103)$$

The Eqn. (3.103) is a linear, second order, homogeneous differential equation which is solved for the displacement component, u_ρ. Solution of Eqn. (3.103) given the following for u_ρ.

$$u_\rho = A_1 \rho + \frac{A_2}{\rho} \quad \ldots\ldots\ldots\ldots\ldots\ldots \quad (3.104)$$

where A_1, A_2 = constants to be determined from the boundary conditions.

Combining Eqns. (3.100), (3.101a) and (3.104), the stress component, id given by

$$\sigma_{\rho\rho} = (3\lambda + 2)\, A_1 + \frac{4G}{\rho^3} A_2 \quad \ldots\ldots\ldots\ldots\ldots\ldots \quad (3.105)$$

The Eqn. (3.105) shows that in order for the stress, $\sigma_{\rho\rho}$, to remain finite at the origin of the sphere, the constant, A_2, must equal zero. Applying the boundary condition given by Eqn. (3.93a) to Eqn. (3.105), the constant A_1 is given by

$$A_1 = \frac{-\sigma_u}{(3\lambda+2G)} \quad \ldots\ldots\ldots\ldots\ldots\ldots \quad (3.106)$$

where $\lambda = \frac{2\nu G}{(1-2\nu)}$

Substitution of Eqns. (3.104) and (3.105) into Eqns. (3.100) and (3.101) yields the following displacement, strain and stress fields.

$$u_\rho = \frac{-(1-2\nu)\sigma_u}{2G(1+\nu)}\rho \quad \ldots\ldots\ldots\ldots\ldots\ldots\ldots\ldots \quad (3.107a)$$

$$u_\phi = 0 \quad \ldots\ldots\ldots\ldots\ldots\ldots\ldots\ldots\ldots\ldots \quad (3.107b)$$

$$u_\theta = 0 \quad \ldots\ldots\ldots\ldots\ldots\ldots\ldots\ldots\ldots\ldots \quad (3.107c)$$

$$\varepsilon_{\rho\rho} = \frac{-(1-2\nu)\sigma_u}{2G(1+\nu)} \quad \ldots\ldots\ldots\ldots\ldots\ldots\ldots\ldots \quad (3.107d)$$

$$\varepsilon_{\phi\phi} = \frac{-(1-2\nu)\sigma_u}{2G(1+\nu)} \quad \ldots\ldots\ldots\ldots\ldots\ldots\ldots\ldots \quad (3.107e)$$

$$\varepsilon_{\theta\theta} = \frac{-(1-2\nu)\sigma_u}{2G(1+\nu)} \quad \ldots\ldots\ldots\ldots\ldots\ldots\ldots\ldots \quad (3.107f)$$

$$\varepsilon_{\rho\phi} = 0 \quad \ldots\ldots\ldots\ldots\ldots\ldots\ldots\ldots\ldots\ldots \quad (3.107g)$$

$$\varepsilon_{\phi\theta} = 0 \quad \ldots\ldots\ldots\ldots\ldots\ldots\ldots\ldots\ldots\ldots \quad (3.107h)$$

$$\varepsilon_{\theta\rho} = 0 \quad \ldots\ldots\ldots\ldots\ldots\ldots\ldots\ldots\ldots\ldots \quad (3.107i)$$

$$\sigma_{\rho\rho} = -\sigma_u \quad \ldots\ldots\ldots\ldots\ldots\ldots\ldots\ldots\ldots\ldots \quad (3.107j)$$

$$\sigma_{\phi\phi} = -\sigma_u \quad \ldots\ldots\ldots\ldots\ldots\ldots\ldots\ldots\ldots\ldots \quad (3.107k)$$

$$\sigma_{\theta\theta} = -\sigma_u \quad \ldots\ldots\ldots\ldots\ldots\ldots\ldots\ldots\ldots\ldots \quad (3.107l)$$

$$\sigma_{\rho\phi} = 0 \quad \ldots\ldots\ldots\ldots\ldots\ldots\ldots\ldots\ldots\ldots \quad (3.107m)$$

$$\sigma_{\phi\theta} = 0 \quad \ldots\ldots\ldots\ldots\ldots\ldots\ldots\ldots \quad (3.107n)$$

$$\sigma_{\theta\rho} = 0 \quad \ldots\ldots\ldots\ldots\ldots\ldots\ldots\ldots \quad (3.107o)$$

The solution given by Eqns. (3.107) is the same as that obtained from the Boussinesq solution in two harmonic functions. The Boussinesq solution is given by Eqns. (3.98).

3.5 The Elastic Sphere in Contact with an Arbitrary Number of Adjacent Spheres

In this section, superposition will be used to obtain the displacement, strain and stress fields for a sphere in contact with an arbitrary number of adjacent spheres.

In the remainder of this Section, tensor notation will be employed since it provides a convenient way to express tensor transformations. The following rules regarding tensor notation will be followed.

1. A superscript denotes a contravariant tensor
2. A subscript denotes a covariant tensor
3. A repeated index implies summation from 1 to 3.

Superposition of an arbitrary number of contacts on a sphere will require the use of local and global coordinates systems. Local coordinate systems will be required for each contact pair, while a global coordinate system will be used to reference the total solution. Local coordinate systems set up for contact pair m are shown in Fig. 3.9. A subscript m will be used to denote the local coordinate systems for contact pair m. The global coordinate system is shown in Fig. 3.10.

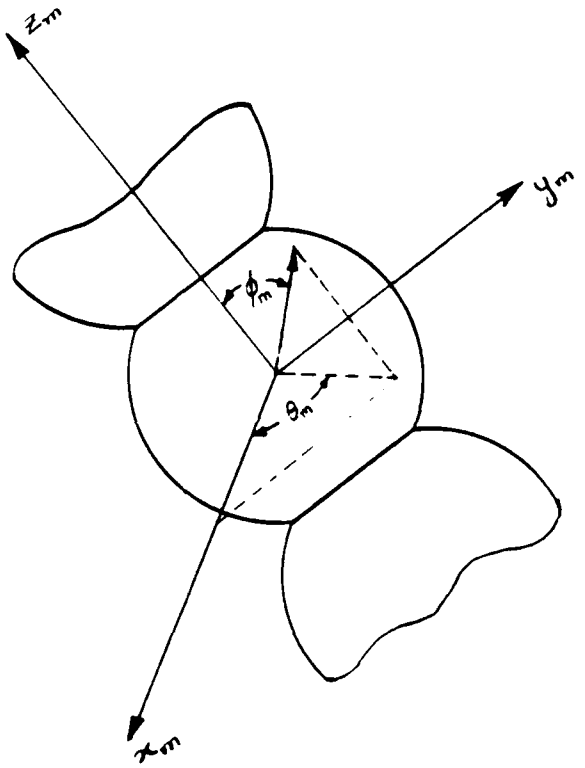

FIG. 3.9

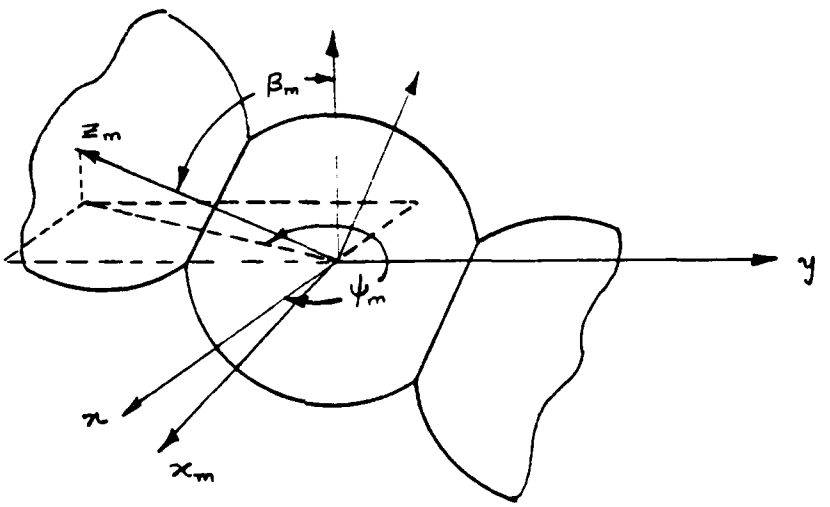

FIG. 3.10

Also shown in Fig. 3.10 are the angles ψ_m and β_m, which establish the position of the local coordinate system, (x_m, y_m, z_m), relative to the global coordinate system (x, y, z). The tensor notation which will be used in defining the local and global coordinate systems is listed in Table 3.1. Hats (^) and overbars (¯) will be used to denote quantities referenced to local spherical coordinate systems and local rectangular coordinate systems, respectively. The absence of these symbols indicate quantities referenced to the global coordinate system. The tensor components of the displacement, strain and stress fields will be denoted by v_i, e_{ij} and τ_{ij}, respectively. The physical components of these fields will be denoted by u_i, ε_{ij} and τ_{ij}.

3.5.1 Transformation of Displacement Fields

The solution obtained for the displacement field resulting from a pair of contacts is referenced to the local coordinate system, $(\hat{x}_1, \hat{x}_2, \hat{x}_3)$. To determine the displacements relative to the global coordinate system, (x_1, x_2, x_3), it is helpful to first determine the displacements relative to the coordinate system $(\bar{x}_1, \bar{x}_2, \bar{x}_3)$. The two local coordinate systems are related through the mapping.

$$\bar{x}_1 = \hat{x}_1 \sin\hat{x}_2 \cos\hat{x}_3 \quad \ldots\ldots\ldots\ldots\ldots\ldots \quad (3.108a)$$

$$\bar{x}_2 = \hat{x}_1 \sin\hat{x}_2 \sin\hat{x}_3 \quad \ldots\ldots\ldots\ldots\ldots\ldots \quad (3.108b)$$

$$\bar{x}_3 = \hat{x}_1 \cos\hat{x}_2 \quad \ldots\ldots\ldots\ldots\ldots\ldots \quad (3.108c)$$

Coordinates	Tensor Notation	Description
$(\rho_m, \phi_m, \theta_m)$	$(\hat{x}_1, \hat{x}_2, \hat{x}_3)$	Local spherical coordinate system
(x_m, y_m, z_m)	$(\bar{x}_1, \bar{x}_2, \bar{x}_3)$	Local rectangular coordinate system
(x, y, z)	(x_1, x_2, x_3)	Global coordinate system

Table 3.1

The Jacobian matrix of the set of functions in Eqns. (3.108) is given by

$$[J] = \begin{bmatrix} \frac{\partial \bar{x}_1}{\partial \hat{x}_1} & \frac{\partial \bar{x}_1}{\partial \hat{x}_2} & \frac{\partial \bar{x}_1}{\partial \hat{x}_3} \\ \frac{\partial \bar{x}_2}{\partial \hat{x}_1} & \frac{\partial \bar{x}_2}{\partial \hat{x}_2} & \frac{\partial \bar{x}_2}{\partial \hat{x}_3} \\ \frac{\partial \bar{x}_3}{\partial \hat{x}_1} & \frac{\partial \bar{x}_3}{\partial \hat{x}_2} & \frac{\partial \bar{x}_3}{\partial \hat{x}_3} \end{bmatrix} = \begin{bmatrix} \sin\hat{x}_2\cos\hat{x}_3 & x_1\cos\hat{x}_2\cos\hat{x}_3 & -x_1\sin\hat{x}_2\sin\hat{x}_3 \\ \sin\hat{x}_2\sin\hat{x}_3 & x_1\cos\hat{x}_2\sin\hat{x}_3 & x_1\sin\hat{x}_2\cos\hat{x}_3 \\ \cos\hat{x}_2 & -x_1\sin\hat{x}_2 & 0 \end{bmatrix} \quad (3.109)$$

The base vectors of the coordinate system $(\hat{x}_1, \hat{x}_2, \hat{x}_3)$ with respect to the coordinate system $(\bar{x}_1, \bar{x}_2, \bar{x}_3)$ are given by

$$\hat{b}_i = \frac{\partial \bar{x}_j}{\partial \hat{x}_i} \bar{e}_j \quad \ldots\ldots\ldots\ldots\ldots\ldots\ldots\ldots \quad (3.110)$$

where $\hat{b}_i$ = base vector in coordinate direction $\hat{x}_i$.

$\bar{e}_j$ = unit vector in coordinate direction $\bar{x}_j$.

From Eqns. (3.108) and (3.109), the base vectors $\hat{b}_i$ are given by

$$\hat{b}_i = \sin\hat{x}_2 \cos\hat{x}_3 \bar{e}_1 + \sin\hat{x}_2 \sin\hat{x}_3 \bar{e}_2 + \cos\hat{x}_2 \bar{e}_3 \ldots \quad (3.111a)$$

$$\hat{b}_2 = \hat{x}_1 \cos\hat{x}_2 \cos\hat{x}_3 \bar{e}_1 + \hat{x}_1 \cos\hat{x}_2 \sin\hat{x}_3 \bar{e}_2 - \hat{x}_1 \sin\hat{x}_2 \bar{e}_3 \quad (3.111b)$$

$$\hat{b}_3 = -\hat{x}_1 \sin\hat{x}_2 \sin\hat{x}_3 \bar{e}_1 + \hat{x}_1 \sin\hat{x}_2 \cos\hat{x}_3 \ldots\ldots \quad (3.111c)$$

The metric tensor is determined from the dot products of the base vector as follows

$$\hat{g}_{ij} = \hat{b}_i \cdot \hat{b}_j \quad \ldots\ldots\ldots\ldots\ldots\ldots\ldots \quad (3.112)$$

where $\hat{g}_{ij}$ = component of the metric tensor

From Eqn. (3.112), the metric tensor is given by

$$\hat{g}_{ij} = \begin{bmatrix} 1 & 0 & 0 \\ 0 & (\hat{x}_1)^2 & 0 \\ 0 & 0 & (\hat{x}_1)^2 \sin^2 \hat{x}_2 \end{bmatrix} \quad \ldots\ldots\ldots \quad (3.113)$$

The tensorial components of the displacement field in the coordinate system $(\hat{x}_1, \hat{x}_2, \hat{x}_3)$ are given by

$$\hat{v}^i(\hat{x}_1,\hat{x}_2,\hat{x}_3) = \frac{\hat{u}^i(\hat{x}_1,\hat{x}_2,\hat{x}_3)}{\sqrt{g_{ii}}}, \text{ no sum on i} \quad \ldots\ldots\ldots \quad (3.114)$$

where $\hat{v}^i$ = components of the displacement tensor

$\hat{u}^i$ = physical components of the displacement tensor

To determine the displacement components $\bar{v}^k(\bar{x}_1,\bar{x}_2,\bar{x}_3)$, the transformation law for a contravariant tensor of order 1 is used. This transformation law is

$$\bar{v}^k(\bar{x}_1,\bar{x}_2,\bar{x}_3) = \hat{v}^i(\hat{x}_1,\hat{x}_2,\hat{x}_3)\,\frac{\partial \bar{x}_k}{\partial \hat{x}_i} \quad \ldots\ldots\ldots\ldots\ldots \quad (3.115)$$

From Eqns. (3.109), (3.113) and (3.115), the displacement components $\bar{v}^k(\bar{x}_1,\bar{x}_2,\bar{x}_3)$ are given by

$$\{\bar{v}\} = [T_L]^T \{u\} \quad \ldots\ldots\ldots\ldots\ldots\ldots \quad (3.116)$$

The vectors and matrix appearing in Eqn. (3.116) are given by

$$\{\bar{v}\} = \begin{Bmatrix} \bar{v}^1 \\ \bar{v}^2 \\ \bar{v}^3 \end{Bmatrix} = \begin{Bmatrix} \bar{u}_1 \\ u_2 \\ \bar{u}_3 \end{Bmatrix} \quad \ldots\ldots\ldots\ldots\ldots \quad (3.117a)$$

$$\{\hat{u}\} = \begin{Bmatrix} \hat{u}_1 \\ \hat{u}_2 \\ \hat{u}_3 \end{Bmatrix} \quad \ldots\ldots\ldots\ldots\ldots\ldots\ldots \quad (3.117b)$$

$$\{T^L\} = \begin{bmatrix} \sin\hat{x}_2 \cos\hat{x}_3 & \sin\hat{x}_2 \sin\hat{x}_3 & \cos\hat{x}_2 \\ \cos\hat{x}_2 \cos\hat{x}_3 & \cos\hat{x}_2 \sin\hat{x}_3 & -\sin\hat{x}_2 \\ -\sin\hat{x}_3 & \cos\hat{x}_3 & 0 \end{bmatrix} \quad \ldots\ldots \quad (3.117c)$$

In Eqns. (3.117) the physical components $\bar{u}_i$ are used in place of the tensor components $\bar{v}^i$. In a rectangular coordinate system, no distinction is made between the contravariant, covariant and physical components of a tensor.

The global coordinates, (x_1, x_2, x_3) are related to the local coordinates, $(\bar{x}_1, \bar{x}_2, \bar{x}_3)$, by the mapping

$$x_1 = \cos\beta_m \cos\psi_m \bar{x}_1 + -\sin\psi_m \bar{x}_2 - \sin\beta_m \cos\psi_m \bar{x}_3 \quad (3.118a)$$

$$x_2 = \cos\beta_m \sin\psi_m \bar{x}_1 + \cos\psi_m \bar{x}_2 + \sin\beta_m \sin\psi_m \bar{x}_3 \quad (3.118b)$$

$$x_3 = -\sin\beta_m \bar{x}_1 - \cos\beta_m \bar{x}_3 \quad (3.118c)$$

The Jacobian matrix [J] of the functions in Eqns. (3.118) is given by

$$[J] = \begin{bmatrix} \cos\beta_m \cos\psi_m & -\sin\psi_m & \sin\beta_m \cos\psi_m \\ \cos\beta_m \sin\psi_m & \cos\psi_m & \sin\beta_m \sin\psi_m \\ -\sin\beta_m & 0 & \cos\beta_m \end{bmatrix} \quad (3.119)$$

The displacement field in the global coordinate system may be determined from the transformation law applicable to a contravariant tensor of order one. This transformation is given by

$$v^i(x_1,x_2,s_3) = \bar{v}^j(\bar{x}_1,\bar{x}_2,\bar{x}_3) \frac{\partial x_i}{\partial x_j} \quad (3.120)$$

From Eqns. (3.119), the displacement components $v^i(x_1,x_2,x_3)$ are given by

$$\{v\} = [T_g]^T \{\bar{v}\} \quad (3.121)$$

The vectors and matrix appearing in Eqn. (3.121) are given below

$$\left\{v\right\} = \left\{\begin{matrix} v^1 \\ v^2 \\ v^3 \end{matrix}\right\} = \left\{\begin{matrix} u_1 \\ u_2 \\ u_3 \end{matrix}\right\} \quad \ldots\ldots\ldots\ldots\ldots\ldots \quad (3.122a)$$

$$\left\{\bar{v}\right\} = \left\{\begin{matrix} \bar{v}^1 \\ \bar{v}^2 \\ \bar{v}^3 \end{matrix}\right\} = \left\{\begin{matrix} \bar{u}_1 \\ \bar{u}_2 \\ \bar{u}_3 \end{matrix}\right\} \quad \ldots\ldots\ldots\ldots\ldots\ldots \quad (3.1.2b)$$

$$\left\{T_g\right\} = \begin{bmatrix} \cos\beta_m \cos\psi_m & -\sin\psi_m & \sin\beta_m \cos\psi_m \\ \cos\beta_m \sin\psi_m & \cos\psi_m & \sin\beta_m \sin\psi_m \\ -\sin\beta_m & 0 & \cos\beta_m \end{bmatrix} \ldots\ldots \quad (3.122c)$$

In Eqns. (3.122), the physical components of displacement are used since no distinction is made between the tensor and physical components in a rectangular coordinate system. When the displacement components $u_i(\hat{x}_1,\hat{x}_2,\hat{x}_3)$ are known, the global displacements $u_i(x_1,x_2,x_2)$ may be determined from Eqns. (3.116) and 3.121). The displacement components $u_i(x_1,x_2,x_3)$ are given by

$$\left\{u\right\} = [T_g]^T\,[T_L]^T\left\{\hat{u}\right\} \quad \ldots\ldots\ldots\ldots\ldots\ldots \quad (3.123)$$

3.5.2 Transformation of Strain Fields

The solution to the strain field resulting from three spheres in contact along an axis of symmetry is referenced to the coordinate system $(\hat{x}_1,\hat{x}_2,\hat{x}_3)$. To determine the strain field in the global coordinate system, (x_1,x_2,x_3), it is helpful to first determine the strain field in the local coordinate system, $(\bar{x}_1,\bar{x}_2,\bar{x}_3)$. The relation between the coordinate systems $(\hat{x}_1,\hat{x}_2,\hat{x}_3)$ and $(\bar{x}_1,\bar{x}_2,\bar{x}_3)$ is given by Eqns. (3.108). The Jacobian matrix [J] of the functions defined in Eqns. (3.108) is given by Eqns. (3.109). The metric tensor of the coordinate system $(\hat{x}_1,\hat{x}_2,\hat{x}_3)$ with respect to the coordinate system $(\bar{x}_1,\bar{x}_2,\bar{x}_3)$ is given by Eqn. (3.113). The tensorial components of the strain field in the coordinate system $(\hat{x}_1,\hat{x}_2,\hat{x}_3)$ are given by

$$\hat{e}^{ij}(\hat{x}_1,\hat{x}_2,\hat{x}_3) = \frac{\hat{\varepsilon}_{ij}(\hat{x}_1,\hat{x}_2,\hat{x}_3)}{\sqrt{g_{ii}}\ \sqrt{g_{jj}}}\ , \text{ no sum on i or j} \quad \ldots\ldots \quad (3.124)$$

where $\hat{e}^{ij}$ = components of the strain tensor

$\hat{\varepsilon}_{ij}$ = physical components of the strain tensor.

To determine the strain field $\bar{e}^{ij}(\bar{x}_1,\bar{x}_2,\bar{x}_3)$, the transformation law for a contravariant tensor of order two is used. This transformation law is

$$\bar{e}^{ij}(\bar{x}_1,\bar{x}_2,\bar{x}_3) = \hat{e}^{k\ell}(\hat{x}_1,\hat{x}_2,\hat{x}_3)\ \frac{\partial \bar{x}_i}{\partial \hat{x}_k}\ \frac{\partial \bar{x}_i}{\partial \hat{x}_\ell} \quad \ldots\ldots\ldots\ldots \quad (3.125)$$

From Eqns. (3.109), (3.124) and (3.125), the components of the strain tensor, $\bar{e}^{ij}(\bar{x}_1,\bar{x}_2,\bar{x}_3)$, are given by

$$[\bar{e}^{ij}] = [T_L]^T [\hat{\varepsilon}_{ij}] [T_L] \quad \ldots\ldots\ldots\ldots\ldots\ldots \quad (3.126)$$

The transformation matrix $[T_L]$ is given by Eqn. (3.117c). The matrices $[e^{ij}]$ and $[\varepsilon_{ij}]$ are given by

$$[\bar{e}^{ij}] = \begin{bmatrix} \bar{e}^{11} & \bar{e}^{12} & \bar{e}^{13} \\ \bar{e}^{21} & \bar{e}^{22} & \bar{e}^{23} \\ \bar{e}^{31} & \bar{e}^{32} & \bar{e}^{33} \end{bmatrix} = \begin{bmatrix} \bar{\varepsilon}_{11} & \bar{\varepsilon}_{12} & \bar{\varepsilon}_{13} \\ \bar{\varepsilon}_{21} & \bar{\varepsilon}_{22} & \bar{\varepsilon}_{23} \\ \bar{\varepsilon}_{31} & \bar{\varepsilon}_{32} & \bar{\varepsilon}_{33} \end{bmatrix} \quad \ldots\ldots \quad (3.127a)$$

$$[\hat{\varepsilon}_{ij}] = \begin{bmatrix} \hat{\varepsilon}_{11} & \hat{\varepsilon}_{12} & \hat{\varepsilon}_{13} \\ \hat{\varepsilon}_{21} & \hat{\varepsilon}_{22} & \hat{\varepsilon}_{23} \\ \hat{\varepsilon}_{31} & \hat{\varepsilon}_{32} & \hat{\varepsilon}_{33} \end{bmatrix} \quad \ldots\ldots\ldots\ldots\ldots\ldots \quad (3.127b)$$

In Eqn. (3.127a) the physical components may be used in place of the tensor components, since the strain tensor, $[\bar{e}^{ij}]$, is referenced to the rectangular coordinate system, $(\bar{x}_1, \bar{x}_2, \bar{x}_3)$.

The relationships between the global coordinates, (x_1, x_2, x_2) and the local coordinates, $(\bar{x}_1, \bar{x}_2, \bar{x}_3)$, are given by Eqns. (3.118). The Jacobian matrix [J] of the functions given by Eqns. (3.118) is given by Eqn. (3.119). To determine the strain field in the global coordinate system, the following transformation law for a second order tensor will be used.

$$\bar{e}^{ij}(x_1, x_2, x_3) = \bar{e}^{k\ell}(\bar{x}_1, \bar{x}_2, \bar{x}_3) \frac{\partial x_i}{\partial \bar{x}_k} \frac{\partial x_j}{\partial \bar{x}_e} \quad \ldots\ldots\ldots\ldots \quad (3.128)$$

From Eqns. (3.119) and (3.128), the strain field $e^{ij}(x_1, x_2, x_3)$ is given by

$$[e^{ij}] = [T_G]^T [\bar{e}^{ij}] [T_G] \quad \ldots \quad (3.129)$$

The matrices $[T_G]$ and $[\bar{e}^{ij}]$ are given by Eqn. (3.122c) and Eqn. (3.127a), respectively. The strain field $[\bar{e}^{ij}]$ is given by

$$[e^{ij}] = \begin{bmatrix} e^{11} & e^{12} & e^{12} \\ e^{21} & e^{22} & e^{23} \\ e^{31} & e^{32} & e^{33} \end{bmatrix} = \begin{bmatrix} \varepsilon_{11} & \varepsilon_{12} & \varepsilon_{13} \\ \varepsilon_{21} & \varepsilon_{22} & \varepsilon_{23} \\ \varepsilon_{31} & \varepsilon_{32} & \varepsilon_{33} \end{bmatrix} \quad \ldots \quad (3.130)$$

In Eqn. (3.130), the physical components of the strain tensor may be used as the tensor components since the strain field is referenced to the rectangular coordinate system (x_1,x_2,x_3). Combining Eqns. (3.126) and (3.129), the strain field $[e^{ij}]$ is given by

$$[e^{ij}] = [T_G]^T [T_L]^T [\hat{\varepsilon}_{ij}] [T_L] [T_G] \quad \ldots \quad (3.131)$$

The matrices $[T_L]$, $[T_G]$ and $[\hat{\varepsilon}_{ij}]$ are given by Eqns. (3.117c), (3.122c) and 3.127b), respectively.

3.5.3 Transformation of Stress Fields

The stress fields in the rectangular coordinate systems $(\bar{x}_1,\bar{x}_2,\bar{x}_3)$ and (x_1,x_2,x_3) are determined in the same manner as the strain fields. Both the stress and strain tensors are second order and will transform in the same manner. Therefore, the results determined for the strain fields in section 3.5.2 may be used to determine the stress fields in the rectangular coordinate systems $(\bar{x}_1,\bar{x}_2,\bar{x}_3)$ and(x_1,x_2,x_3). From

these results, the stress fields are given by

$$[\bar{\tau}^{ij}] = [T_L]^T [\hat{\sigma}_{ij}] [T_L] \quad \ldots\ldots\ldots\ldots\ldots\ldots \quad (3.132)$$

$$[\tau^{ij}] = [T_G]^T [\bar{\tau}^{ij}] [T_G] \quad \ldots\ldots\ldots\ldots\ldots\ldots \quad (3.133)$$

The matrices $[T_L]$ and $[T_G]$ are given by Eqn. (3.117c) and Eqn. (3.122c), respectively. The matrices $[\bar{\tau}^{ij}]$ and $[\tau^{ij}]$ are given by

$$[\bar{\tau}^{ij}] = \begin{bmatrix} \bar{\tau}^{11} & \bar{\tau}^{12} & \bar{\tau}^{13} \\ \bar{\tau}^{21} & \bar{\tau}^{22} & \bar{\tau}^{23} \\ \bar{\tau}^{31} & \bar{\tau}^{32} & \bar{\tau}^{33} \end{bmatrix} = \begin{bmatrix} \bar{\sigma}_{11} & \bar{\sigma}_{12} & \bar{\sigma}_{13} \\ \bar{\sigma}_{21} & \bar{\sigma}_{22} & \bar{\sigma}_{23} \\ \bar{\sigma}_{31} & \bar{\sigma}_{32} & \bar{\sigma}_{33} \end{bmatrix} \quad \ldots\ldots \quad (3.134)$$

$$[\tau^{ij}] = \begin{bmatrix} \tau^{11} & \tau^{12} & \tau^{13} \\ \tau^{21} & \tau^{22} & \tau^{23} \\ \tau^{31} & \tau^{32} & \tau^{33} \end{bmatrix} = \begin{bmatrix} \sigma_{11} & \sigma_{12} & \sigma_{13} \\ \sigma_{21} & \sigma_{22} & \sigma_{23} \\ \sigma_{31} & \sigma_{32} & \sigma_{33} \end{bmatrix} \quad \ldots\ldots \quad (3.135)$$

In Eqns. (3.134) and (3.135), the physical components of the stress tensor may be used for the tensor components, since the stress fields are referenced to rectangular coordinate systems. Combining Eqn. (3.132) and Eqn. (3.133), the stress field in the global coordinates (x_1, x_2, x_3) is given by

$$[\bar{\tau}_{ij}] = [T_G]^T [T_L]^T [\hat{\sigma}_{ij}] [T_L] [T_G] \quad \ldots\ldots\ldots\ldots\ldots \quad (3.136)$$

The matrices $[T_L]$ and $[T_G]$ are given by Eqn. (3.117c) and Eqn. (3.122c), respectively.

3.5.4 Solution for a Sphere with an Arbitrary Number of Contacts

The results of Sections 3.5.1, 3.5.2 and 3.5.3 will be used to obtain the displacement, strain and stress fields for a sphere subject to an arbitrary number of contacts with adjoining spheres. Restrictions which are imposed on these solutions are listed below.

1. The contacts on the sphere appear in pairs along an axis of symmetry as shown in Fig. 3.9
2. The forces transmitted through the contacts are such that the sphere is in static equilibrium.

Subsections 3.51, 3.52 and 3.53 provide the displacement, strain and stress fields referenced to a global coordinate system. These fields were developed for the case of one pair of contacts along an axis of symmetry as appearing in Fig. 3.9 If a sphere has a number of these contact pairs, the displacement, strain and stress fields resulting from these contacts may all be referenced to the global coordinate system. The displacement, strain and stress fields resulting from all contacts are then found by adding the individual fields. Superposition of these individual fields yields the following total displacement, total strain and total stress fields.

$$\{u\}_T = \sum_{m=1}^{\frac{n_c}{2}} [T_g]_m^T [T_L]_m^T \{\hat{u}\}_m \quad \ldots\ldots\ldots\ldots\ldots\ldots \quad (3.137a)$$

$$[e^{ij}]_T = \sum_{m=1}^{\frac{h_c}{2}} [T_G]_m^T [T_L]_m^T [\hat{\varepsilon}_{ij}]_m [T_L]_m [T_G]_m \quad \ldots\ldots\ldots \quad (3.137b)$$

$$[\tau^{ij}]_T = \sum_{m=1}^{\frac{n_c}{2}} [T_G]_m^T [T_L]_m^T [\hat{\sigma}_{ij}]_m [T_L]_m [T_G]_m \quad \ldots\ldots \quad (3.137c)$$

where n_c = total number of contacts on the sphere.

In Eqns. (3.137), the subscript T is used to denote the total displacement, strain and stress fields. The subscript m denotes quantities resulting from the pair of contacts, m.

The quantities appearing in Eqns. (3.137) may be put in terms of the local coordinate system and global coordinate system shown in Fig. 3.9 and Fig. 3.10 respectively. The total displacement, strain and stress fields may be written as follows

$$\{u\}_t = \begin{Bmatrix} u_x \\ u_y \\ u_z \end{Bmatrix} \quad \ldots\ldots\ldots\ldots\ldots\ldots\ldots\ldots \quad (3.138a)$$

$$[e^{ij}]_T = \begin{bmatrix} \varepsilon_{xx} & \varepsilon_{xy} & \varepsilon_{xz} \\ \varepsilon_{yx} & \varepsilon_{yy} & \varepsilon_{yz} \\ \varepsilon_{zx} & \varepsilon_{zy} & \varepsilon_{zz} \end{bmatrix} \quad \ldots\ldots\ldots\ldots\ldots\ldots \quad (3.138b)$$

$$[\tau^{ij}]_T = \begin{bmatrix} \sigma_{xx} & \sigma_{xy} & \sigma_{xz} \\ \sigma_{yx} & \sigma_{yy} & \sigma_{yz} \\ \sigma_{zx} & \sigma_{zy} & \sigma_{zz} \end{bmatrix} \quad \ldots\ldots\ldots\ldots\ldots\ldots \quad (3.138c)$$

In Eqns. (3.138), the global coordinate system (x, y, z) is referenced.

the displacement, strain and stress fields resulting from contact m are given by

$$\{u\}_m = \begin{Bmatrix} u_\rho \\ u_\phi \\ u_\theta \end{Bmatrix}_m \quad \ldots\ldots\ldots\ldots\ldots\ldots\ldots\ldots\ldots\ldots \quad (3.139a)$$

$$[\hat{\varepsilon}^{ij}]_m = \begin{bmatrix} \varepsilon_{\rho\rho} & \varepsilon_{\rho\phi} & \varepsilon_{\rho\theta} \\ \varepsilon_{\phi\rho} & \varepsilon_{\phi\phi} & \varepsilon_{\phi\theta} \\ \varepsilon_{\theta\rho} & \varepsilon_{\theta\phi} & \varepsilon_{\theta\theta} \end{bmatrix}_m \quad \ldots\ldots\ldots\ldots\ldots\ldots \quad (3.139b)$$

$$[\hat{\varepsilon}^{ij}]_m = \begin{bmatrix} \sigma_{\rho\rho} & \sigma_{\rho\phi} & \sigma_{\rho\theta} \\ \sigma_{\phi\rho} & \sigma_{\phi\phi} & \sigma_{\phi\theta} \\ \sigma_{\theta\rho} & \sigma_{\theta\phi} & \sigma_{\theta\theta} \end{bmatrix}_m \quad \ldots\ldots\ldots\ldots\ldots\ldots \quad (3.139c)$$

The fields $\{u\}_m$, $[\hat{\varepsilon}_{ij}]_m$ and $[\hat{\sigma}_{ij}]_m$ are determined from the results given in Section 3.4. These fields are referenced to the spherical coordinate system $(\rho_m, \phi_m, \theta_m)$ shown in Fig. 3.9 . The transformation matrix, $[T_G]$, is given by

$$[T_G] = \begin{bmatrix} \cos\beta_m \cos\psi_m & -\sin\psi_m & \sin\beta_m \cos\psi_m \\ \cos\beta_m \cos\psi_m & \cos\psi_m & \sin\beta_m \sin\psi_m \\ -\sin\beta_m & 0 & \cos\beta_m \end{bmatrix} \quad \ldots\ldots \quad (3.140)$$

The angles β_m and ψ_m define the position of the local rectangular coordinate system, (x_m, y_m, z_m) relative to the global coordinate system,

(x, y, z). These angles are shown in Fig. 3.10. The transformation matrix, $[T_L]$, is given by

$$[T_L] = \begin{bmatrix} \sin\phi_m \cos\theta_m & \sin\phi_m \sin\theta_m & \cos\phi_m \\ \cos\phi_m \cos\theta_m & \cos\phi_m \cos\theta_m & -\sin\phi_m \\ -\sin\theta_m & \cos\theta_m & 0 \end{bmatrix} \quad \ldots\ldots (3.141)$$

The angles ϕ_m and θ_m are shown in Fig. 3.9. These angles are part of the spherical coordinate system, $(\rho_m, \phi_m, \theta_m)$. They define a point in the sphere relative to the local coordiante system, (x_m, y_m, z_m) for contact m.

In order to evaluate the total displacement, strain and stress fields at any point (x, y, z), the local coordinates must be determined from the global coordinates. This is necessary since the solutions provided in Section 3.4 are in terms of the local coordinates $(\rho_m, \phi_m, \theta_m)$ The following equations are used to determine the local coordinates (x_m, y_m, z_m) and $(\rho_m, \phi_m, \theta_m)$ when the global coordinates (x, y, z) are known.

$$\begin{Bmatrix} x_m \\ y_m \\ z_m \end{Bmatrix} = \begin{bmatrix} \cos\beta_m \cos\psi_m & \cos\beta_m \sin\psi_m & -\sin\beta_m \\ -\sin\psi_m & \cos\psi_m & 0 \\ \sin\beta_m \cos\psi_m & \sin\beta_m \sin\psi_m & \cos\beta_m \end{bmatrix} \begin{Bmatrix} x \\ y \\ z \end{Bmatrix} \quad \ldots (3.142)$$

$$\rho_m = \sqrt{x^2 + y^2 + z^2} \quad \ldots\ldots (3.143a)$$

$$\sin\phi_m = \frac{\sqrt{x_m^2 + y_m^2}}{\rho} \quad \ldots\ldots (3.143b)$$

$$\cos\varphi_m = \frac{z_m}{\rho} \quad \ldots\ldots\ldots\ldots\ldots\ldots\ldots\ldots\ldots\ldots \quad (3.143c)$$

$$\sin\theta_m = \frac{y_m}{\sqrt{x_m^2 + y_m^2}} \quad \ldots\ldots\ldots\ldots\ldots\ldots\ldots\ldots\ldots\ldots \quad (3.143d)$$

$$\cos\theta_m = \frac{x_m}{\sqrt{x_m^2 + y_m^2}} \quad \ldots\ldots\ldots\ldots\ldots\ldots\ldots\ldots\ldots\ldots \quad (3.143e)$$

From Eqns. (3.142) and (3.143) the total displacement, strain and stress fields may be evaluated for any point (x, y, z).

CHAPTER 4

EFFECTIVE MODULI OF AN IDEALIZED SOLID - FLUID SYSTEM

4.1 Effective Moduli

The effective moduli of heterogeneous materials are those moduli reflecting the average stress-strain properties of the materials. These moduli take into account the properties and the geometry of all the phases and their interaction. The effective moduli are determined by considering a small but representative sample of the heterogeneous materials. The size of the representative sample is chosen so that the behavior of this sample does not change when the sample size is increased. Therefore, the effective moduli determined for the sample may be used to represent the entire heterogeneous material. The two approaches that are used to determine the effective moduli are volumetric averaging and energy methods.

4.1.1 Volumetric Averaging Approach

The volumetric averaging approach derives effective material properties by considering a representative volume element of the material. The stress or displacement fields in this representative volume element are macroscopically homogeneous. The volume averaged stress is defined as

$$\langle \sigma_{ij} \rangle = \frac{1}{V} \int_V \sigma_{ij} \, dV \qquad (4.1)$$

where $\langle \sigma_{ij} \rangle$ = volume averaged stress field

σ_{ij} = stress field occurring in the different phases of the material

V = total volume of representative sample

In Eqn. (4.1), Cartesian tensor notation has been used. This notation will be used periodically, and the rule that a repeated tensor implies summation is applicable. The volume averaged strain is defined as

$$\langle \varepsilon_{ij} \rangle = \frac{1}{V} \int_V \varepsilon_{ij} \, dV \qquad (4.2)$$

where $\langle \varepsilon_{ij} \rangle$ = volume averaged strain field

ε_{ij} = strain field occurring in the different phases of the materials

Both of the integrals appearing in Eqns. (4.1) and (4.2) are taken over the representative volume of the material. The effective moduli are defined through the following equation.

$$\langle \sigma_{ij} \rangle = \bar{C}_{ijk\ell} \langle \varepsilon_{k\ell} \rangle \qquad (4.3)$$

where $\bar{C}_{ijk\ell}$ = effective moduli tensor

The Eqn. (4.3) is the general anisotropic form of the linear, volume averaged, stress-strain relations. In order to use Eqn. (4.3) to determine the effective moduli of a heterogeneous material, the stress and strain fields occurring in all phases must be known and the integrals in Eqns. (4.1) and (4.2) performed.

4.1.2. Energy Methods

When using an energy approach, the effective moduli are determined through energy equivalence. A representative sample of the heterogeneous material is considered to be subjected to a macroscopically homogeneous stress or deformation field. The sum of the strain energies for all the phases of the neterogeneous material is then made equivalent to that occurring in a homogeneous material with moduli, $C_{ijk\ell}$. This relationship is given by

$$\int_V \varepsilon_{ij} \sigma_{ij} \, dV = \langle \varepsilon_{ij} \rangle \langle \sigma_{ij} \rangle \, V \qquad (4.4)$$

where σ_{ij} = stress field

ε_{ij} = strain field

V = total volume of representative sample.

The volume averaged stress, $\langle\sigma_{ij}\rangle$, and the averaged volume strain, $\langle\varepsilon_{ij}\rangle$, are determined from Eqns. (4.1) and (4.2), respectively. Substituting Eqn. (4.3) into Eqn. (4.4) yields the following

$$\int_V \sigma_{ij}\ \varepsilon_{ij}\ dV = \bar{C}_{ijk\ell}\ \langle\varepsilon_{ij}\rangle\ \langle\varepsilon_{k\ell}\rangle\ V \qquad (4.5)$$

The integral appearing in Eqn. (4.5) is taken over the entire representative volume. As in the volumetric averaging approach, the stress fields, σ_{ij}, and the strain fields, ε_{ij}, must be known for the different phases of the heterogeneous material before Eqn. (4.5) may be evaluated.

4.2 Volumetric Averaging Approach to Determining the Effective Bulk Modulus of an Idealized Solid-Fluid System

The solid-fluid system to be considered is a heterogeneous material consisting of a number of solid spheres in contact, surrounded by a fluid phase. Such a system is shown in Fig. 4.1. The following assumptions are used in the determination of the effective bulk modulus.

1. The spheres contained in the system consist of isotropic, linearly elastic materials.
2. The spheres contained in the system are in static equilibrium.
3. The contacts on a particular sphere occur in pairs, directed along an axis passing through the sphere.
4. The surface displacements or surface tractions resulting from a pair of contacts are axisymmetric with respect to an axis passing through the center of the contact region.
5. The solid-fluid system behaves as an isotropic, linearly elastic

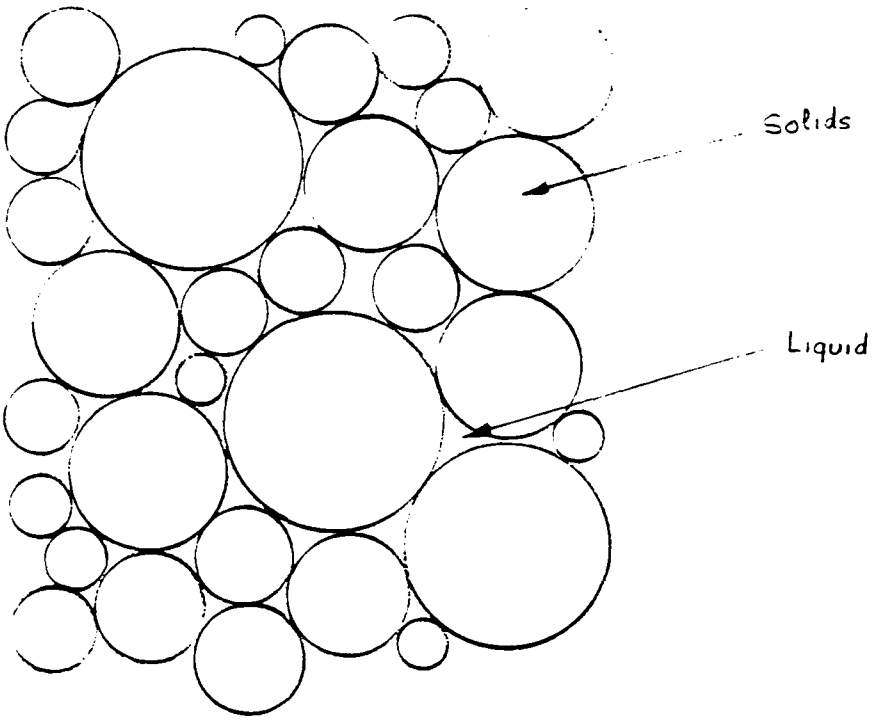

FIG 4.1

material macroscopically.

6. The void space between spheres in the system is completely filled with only one type of fluid.

For an isotropic, linearly elastic material, only two material constants are needed to relate the force field to the displacement field. For this case, Eqn. (4.3) reduces to

$$\langle \sigma_{ij} \rangle = 2\bar{G} \langle \varepsilon_{ij} \rangle + \bar{\lambda} \langle \varepsilon_{kk} \rangle \delta_{ij} \tag{4.6}$$

where $\langle \sigma_{ij} \rangle$ = volume averaged stress tensor

$\langle \varepsilon_{ij} \rangle$ = volume averaged strain tensor

$\bar{G}, \bar{\lambda}$ = effective Lame constants

δ_{ij} = Kronecker delta = $\begin{cases} 0 & i \neq j \\ 1, & i = j \end{cases}$

Another relationship may be obtained by contracting the i and j indices in Eqn. (4.6). This contracted form is given by

$$\langle \sigma_{kk} \rangle = 3 \bar{K} \langle \varepsilon_{kk} \rangle \tag{4.7}$$

where $\bar{K} = \frac{2}{3} \bar{G} + \bar{\lambda}$

the term $\bar{K}$, appearing in Eqn. (4.7), is the effective bulk modulus. The quantities $\langle \sigma_{kk} \rangle$ and $\langle \varepsilon_{kk} \rangle$, appearing in Eqn. (4.7), are determined from Eqn. (4.1) and (4.2), respectively. These quantities are given by

$$\langle \sigma_{kk} \rangle = \frac{1}{V} \int_V \sigma_{kk} \, dV \tag{4.8a}$$

$$\langle \varepsilon_{kk} \rangle = \frac{1}{V} \int_V \varepsilon_{kk} \, dV \tag{4.8b}$$

where σ_{kk} = trace of the stress tensor

ε_{kk} = trace of the strain tensor

V = representative volume

The integrals appearing in Eqns. (4.8) are taken over the volumes of both the solid and the fluid phases of the heterogeneous material. Due to this, the integrals appearing in Eqns. (4.8) may be rewritten as follows.

$$\langle \sigma_{kk} \rangle = \frac{1}{V} \left[\int_{V_s} \sigma_{kk}^{s} \, dV + \int_{V_f} \sigma_{kk}^{f} \, dV \right] \tag{4.9a}$$

$$\langle \varepsilon_{kk} \rangle = \frac{1}{V} \left[\int_{V_s} \varepsilon_{kk}^{s} \, dV + \int_{V_f} \varepsilon_{kk}^{f} \, dV \right] \tag{4.9b}$$

where V_s = volume of the solid phase of the heterogeneous material

V_f = volume of the liquid phase of the heterogeneous material

The superscripts s and f appearing in Eqns. (4.9) are used to denote the solid and fluid phases, respectively. Combining Eqns. (4.7) and (4.9), the following expressions for the effective bulk modulus, K, is obtained

$$3\bar{K} = \frac{\frac{1}{V} \left[\int_{V_s} \sigma_{kk}^{s} \, dV + \int_{V_f} \sigma_{kk}^{f} \, dV \right]}{\frac{1}{V} \left[\int_{V_s} \varepsilon_{kk}^{s} \, dV + \int_{V_f} \varepsilon_{kk}^{f} \, dV \right]} \tag{4.10}$$

To evaluate Eqn. (4.10) a representative volume of the solid-fluid system is considered. This representative volume is taken as the smallest possible sample which still exhibits the same behavior as the entire system. Due to this, the effective bulk modulus, $\bar{K}$, found by performing the integrals in Eqn. (4.10) over this representative volume, will be applicable to the entire system. In determining the effective bulk modulus, $\bar{K}$, the stress and the displacement fields occurring in the representative volume will be considered

to be macroscopically homogeneous.

The representative volume will contain N solid spheres. The spheres are considered to be isotropic, linearly elastic materials. They may have different radii and material constants. These spheres constitute the solid phase of the heterogeneous material shown in Fig. 4.1. In Eqn. (4.10), the integrals taken over the solid phase of the representative volume are written as follows.

$$\frac{1}{V}\int_{V_s}\sigma_{kk}^{s}\,dV = \frac{1}{V}\sum_{i=1}^{N}\int_{V_s^i}(\sigma_{kk}^{s})_i\,dV \qquad (4.11a)$$

$$\frac{1}{V}\int_{V_s}\varepsilon_{kk}^{s}\,dV = \frac{1}{V}\sum_{i=1}^{N}\int_{V_s^i}(\varepsilon_{kk}^{s})_i\,dV \qquad (4.11b)$$

where $(\sigma_{kk}^{s})_i$ = trace of the stress tensor for sphere i.

$(\varepsilon_{kk})_i$ = trace of the strain tensor for sphere i.

In Eqns. (4.11) the integrals appearing in the summations are taken over the volume of sphere i, V_s^i. Due to the first four of the assumptions made concerning the solid-fluid system, the results in Section 3.3 may be used to determine (σ_{kk}^{s}) and (ε_{kk}^{s}). From Section 3.3, the solution, [S], to the displacement, strain or stress fields for a sphere undergoing axisymmetric surface tractions or axisymmetric surface displacements are given by

$$[S] = \sum_{n=1}^{\infty} a_{-n-1}[A_{-n-1}] + \sum_{n=0}^{\infty} b_{-n-2}[B_{-n-2}] \qquad (4.12)$$

where [S] = solution to the displacement, strain, or stress field

$[A_{-n-1}]$ = component solution to the displacement, strain or stress field

$[B_{-n-2}]$ = component solution to the displacement, strain or stress field

a_{-n-1} = constant of superposition

b_{-n-2} = constant of superposition

The component solutions, $[A_{-n-1}]$ and $[B_{-n-2}]$, can be determined from Eqns. (3.46) and (3.53), respectively. The constants of superpositions, a_{-n-1} and b_{-n-2}, are determined from the specified boundary conditions on the sphere. Evaluating $(\sigma_{kk}^{s})_i$ and $(\varepsilon_{kk}^{s})_i$ corresponding to the component solution $[A_{-n-1}]$ gives the following

$$(\sigma_{kk}^{s})_i^{A_{-n-1}} = 0 \tag{4.13a}$$

$$(\varepsilon_{kk}^{s})_i^{A_{-n-1}} = 0 \tag{4.13b}$$

In Eqns. (4.13), the superscript A_{-n-1} is used to denote quantities which are determined from the component solution $[A_{-n-1}]$. Evaluating $(\sigma_{kk}^{s})_i$ and $(\varepsilon_{kk}^{s})_i$ corresponding to the component solution $[B_{-n-2}]$ yields the following

$$(\sigma_{kk}^{s})_i^{B_{-n-2}} = 2(n+1)(2n+3)(1+\nu_i)\,\rho^n P_n \tag{4.14a}$$

$$(\varepsilon_{kk}^{s})_i^{B_{-n-2}} = (n+1)(2n+3)\,\frac{(1-2\nu_i)}{G_i}\,\rho^n P_n \tag{4.14b}$$

where ν_i = Poisson's ratio for sphere i.

G_i = shear modulus of sphere i.

ρ = distance from the origin to a point in sphere i.

In Eqns. (4.14), the superscript B_{-n-2} is used to denote quantities determined from the component solution $[B_{-n-2}]$. Combining Eqns. (4.12) through (4.14) yields the following for $(\sigma_{kk}^{s})_i$ and $(\varepsilon_{kk}^{s})_i$, when there is one pair of contacts on sphere i.

$$(\sigma_{kk}^{s})_i = 2 \sum_{n=1}^{\infty} (b_{-n-2})_i (n+1)(2n+3)(1-\nu_i) \rho^n P_n \quad \ldots\ldots\ldots \quad (4.15a)$$

$$(\varepsilon_{kk}^{s}) = \frac{1}{G_i} \sum_{n=1}^{\infty} (b_{-n-2})_i (n+1)(2n+3)(1-2\nu_i) \rho^n P_n \quad \ldots\ldots\ldots \quad (4.15b)$$

The subscript i is used on the constant of superposition, b_{-n-2}, since its value will depend on sphere i and the spheres making contact with sphere i. This dependence is shown in Section 3.1 where the Hertz contact problem is discussed. The quantities $(\sigma_{kk}^{s})_i$ and $(\varepsilon_{kk}^{s})_i$ are invariant with respect to coordinate directions. Therefore, for a sphere with M contacts, (σ_{kk}^{s}) and (ε_{kk}^{s}) are given by

$$(\sigma_{kk}^{s})_i = 2 \sum_{n=1}^{N} \left[(\bar{b}_{-n-2})_i + \sum_{k=1}^{\frac{M_i}{2}} (b_{-n-2})_i^k \right] (n+1)(2n+3)(1+\nu_i) \rho^n P_n \quad (4.16a)$$

$$(\varepsilon_{kk}^{s})_i = \frac{1}{G_i} \left[(\bar{b}_{-n-2})_i + \sum_{k=1}^{\frac{M_i}{2}} (b_{-n-2})_i^k \right] (n+1)(2n+3)(1-2\nu_i) \rho^n P_n \quad (4.16b)$$

where M_i = number of contacts on sphere i.

In Eqns. (4.16), the superscript k has been used on the constant of superposition, b_{-n-2}, since this quantity will change for the different contacts, occurring on a single sphere. The constant of superposition, $\bar{b}_{-n-2}$, results from the application of a radial pressure to the surface of sphere i. Substituting Eqns. (4.16) into Eqns. (4.11) and performing the indicated integration yields the following

$$\frac{1}{V}\int_{V_s} \sigma_{kk}^{s}\, dV = \frac{1}{V}\sum_{i=1}^{N} 8\pi \left[(\bar{b}_{-2})_i + \sum_{k=1}^{\frac{M_i}{2}} (b_{-2})_i^k \right] (1+\ _i) R_i^3 \qquad (4.17a)$$

$$\frac{1}{V}\int_{V_s} \varepsilon_{kk}^{s}\, dV = \frac{1}{V}\sum_{i=1}^{N} \frac{4\pi}{G_i} \left[(\bar{b}_{-2})_i + \sum_{k=1}^{\frac{M_i}{2}} (b_{-2})_i^k \right] (1-2\nu_i) R_i^3 \qquad (4.17b)$$

where R_i = the radius of sphere i.

To determine the integrals involving σ_{kk}^{f} and ε_{kk}^{f}, which appear in Eqn. (4.10), the fluid pressure in the representative volume is denoted as $\bar{\sigma}_u$. The quantities σ_{kk}^{f} and ε_{kk}^{f} are related to $\bar{\sigma}_u$ by

$$\sigma_{kk}^{f} = 3\,\bar{\sigma}_u \qquad , \ldots\ldots\ldots\ldots\ldots\ldots \quad (4.18a)$$

$$\varepsilon_{kk}^{f} = -\int_{o}^{\bar{\sigma}u} \frac{dP}{K_f(P,T)} = e_f \ldots\ldots\ldots\ldots \quad (4.18b)$$

where P = fluid pressure

K_f = bulk modulus of the flued

T = temperature

In Eqns. (4.18) the fluid pressure, $\bar{\sigma}_u$, is interpreted to be a compressive stress and therefore its magnitude is negative. This

pressure is also a gauge pressure meaning that if the fluid pressure is atmospheric, $\bar{\sigma}_u$ is equal to zero. The Eqn. (4.18) states that in general, the bulk modulus of a fluid, K_f, is not constant. It may vary with the pressure and temperature. The lower limit of the integral appearing in Eqn. (4.18b) indicates that the fluid will be considered to be unstrained at zero gauge pressure. Henceforth, the volumetric strain of the fluid, ε^f_{kk}, will be denoted by e_f. Substitution of Eqns. (4.18) into the integrals given in Eqn. (4.10) yields the following.

$$\frac{1}{V} = \int_{V_f} \sigma^f_{kk} \, dV = 3 \, C_f \, \bar{\sigma}_u \quad \ldots\ldots\ldots\ldots \quad (4.19a)$$

$$\frac{1}{V} = \int_{V_s} \varepsilon^f_{kk} \, dV = C_f \, e_f \quad \ldots\ldots\ldots\ldots \quad (4.19b)$$

where $C_f = \dfrac{V_f}{V}$

V = representative volume

V_f = volume of fluid present in the representative volume

$\bar{\sigma}_u$ = fluid pressure in representative volume

e_f = volumetric strain of the fluid in the representative volume

The term, C_f, appearing in Eqns. (4.19) is the volume fraction of the voids containing fluid, in the solid-fluid system. Combining Eqns.

(4.10), (4.17) and (4.18) given the following expression for the effective builk modulus of the solid-fluid system under consideration.

$$3\bar{K} = \frac{\frac{1}{V}\sum_{i=1}^{N} 8\pi \left[(\bar{b}_{-2})_i + \sum_{k=1}^{\frac{M_i}{2}} (b_{-2})_i^k\right] (1+\nu_i)\, R_i^3 + 3\, C_f\, \bar{\sigma}_u}{\frac{1}{V}\sum_{i=1}^{N} \frac{4\pi}{G_i} \left[(\bar{b}_{-2})_i + \sum_{k=1}^{\frac{M_i}{2}} (b_{-2})_i^k\right] (1-2\nu_i)\, R_i^3 + C_f\, e_f} \qquad (4.20)$$

The Eqn. (4.20) gives the effective bulk modulus, K, of a solid-fluid system composed of a number of isotropic, linearly elastic spheres in contact and surrounded by a fluid phase. The assumptions made in arriving at Eqn. (4.20) are listed at the beginning of this section. Most of these assumptions were made so that the results from Section 3.2 could be used. To evaluate Eqn. (4.20), a knowledge of the sizes, material properties, number of contacts, location of contacts, forces on contacts and the materials in contact have to be known. It is unlikely that these variables would be known in a deterministic form. Therefore, the evaluation of Eqn. (3.20) would require statistical data. In the next subsection some simplications will be made concerning the solid-fluid system, which will allow an evaluation of Eqn. (4.20).

From Eqn. (4.20) some observations can be made concerning the effective bulk modulus, $\bar{K}$. For the case when the value of $\bar{\sigma}_u$ is zero gauge pressure, Eqn. (4.20) shows that the effective bulk modulus depends only on the material properties and geometries of the spheres

included in the solid-fluid system. The same results is obtained by having the volume fraction of the voids in the system, C_f, equal to zero. Although the two cases listed above give the same result, the manner in which these results were obtained are different. For the case of zero gauge pressure the solution for a sphere in contact with two adjacent spheres must be considered. This solution allows the sphere in contact to deform freely into the surrounding void space for conditions of zero gauge pressure. The effect of this is to consider that the air in the voids does not contribute to the stiffness of the solution. The Eqn. (4.20) would yield a different result if $\bar{\sigma}_u$ was an absolute pressure. Under these conditions the term e_f would still be zero and the contribution of $\bar{\sigma}_u$ in the numerator of Eqn. (4.20) would be negligible. For this case when the volume of voids is equal to zero, the system would only contain the solid phase so that the effective bulk modulus, $\bar{K}$, would depend only on the material properties and geometries of spheres in the system. In this case the system would consist of only spheres such that all the void space being occupied by a sphere of proper size. Another case to consider is when $|\bar{\sigma}_u| > 0$, and the fluid phase is incompressible. For this case the volumetric strain of the fluid phase, e_f, is zero. To study the effect of the incompressible fluid phase, it is recognized that the terms appearing in the numerator and the denominator of Eqn. (4.20), will have negative values when the solid-fluid system is in compression. Due to this, Eqn. (4.20) shown that the effective bulk modulus, $\bar{K}$, increases as $|\bar{\sigma}_u|$ increases, for a constant volume of solids and voids. This shows that a non-zero pressure in an incompressible fluid phase serves as a

restraint against volume deformation. This is reasonable since an incompressible fluid phase should increase the stiffness of the system and the fluid pressure, $\bar{p}_u$, should exist for such a fluid. For the limiting case when the solid phase is absent in the system, Eqn. (4.20) shows that the effective bulk modulus, $\bar{K}$, becomes infinite. This is reasonable since the system contains only an incompressible fluid phase. For a compressible fluid phase in the solid-fluid system, the volumetric strain of the fluid phase, e_f, will be non-zero. In the limiting case when the system contains only a compressible fluid, the effective bulk modulus, $\bar{K}$, in Eqn. (4.20) is a function of the bulk modulus of the fluid. This dependence is apparent from Eqn. (4.18b). For the case of a fluid with a constant bulk modulus, Eqns. (4.18b) and (4.20) show that the effective bulk modulus, $\bar{K}$, is equal to the bulk modulus of the fluid.

The effective bulk modulus given by Eqn. (4.20) was determined by considering a small representative sample of the solid-fluid system. The macroscopic system will be made up of a number of these small representative samples. If the displacement or the stress fields vary with the position in the macroscopic sample, the effective bulk modulus will vary with position. This occurs due to the fact that the constant of superposition, b_{-2}, is dependent on the boundary conditions present on the contacts between spheres. These boundary conditions change with the force or displacement, on the contact.

4.2.1 Effective Bulk Modulus of a Solid-Fluid System Consisting of Equal Spheres Arranged in Ideal Packing Configurations, and Surrounded by a Fluid.

Restrictions concerning the geometry and material properties of

the solid phase present in the solid-fluid system will be made. These restrictions will allow Eqn. (4.20) to be evaluated in the absence of statistical data. The restrictions on the solid phase of the system are as follows.

1. The spheres in the solid phase of the system are of equal radii.
2. The material properties of the solid phase are constant.
3. The spheres in the solid phase are arranged in ideal packing configurations.

With these restrictions Eqn. (4.20) is rewritten as follows.

$$3\bar{K} = \frac{6(1+\nu_s)\,C_s\left[\bar{b}_{-2}\sum_{k=1}^{\frac{M}{2}}(b_{-2})^k\right] + 3\,C_f\,\bar{\sigma}_u}{\frac{3}{G_s}(1-2\nu_s)\,C_s\left[\bar{b}_{-2}+\sum_{k=1}^{\frac{M}{2}}(b_{-2})^k\right] + C_f e_f} \quad \ldots\ldots \quad (4.21)$$

where $\bar{K}$ = effective bulk modulus

C_s = volume fraction of the solid phase

C_f = volume fraction of the fluid phase

$\bar{\sigma}_u$ = fluid pressure

e_f = volumetric strain of fluid

G_s = shear modulus of solid phase

ν_s = Poisson's ratio for the solid phase

M = the number of contacts on one sphere

$\bar{b}_{-2}$ = the constant of superposition resulting from a uniform radial pressure on the surface of the sphere

$(b_{-2})^k$ = the constant of superposition for contact k.

The restrictions on the solid-fluid system requires that all spheres are in static equilibrium, and that the contacts on a particular sphere occur in pairs along an axis passing through the origin of the sphere. Furthermore, all spheres contained in the system are of equal radii and have the same material properties. These restrictions allow the use of the results given in Section 3.4, to determine the constant of superposition, b_{-2}. The results contained in this section contain values of b_{-2} for the boundary conditions on a single sphere resulting from Hertzian contact with surrounding spheres and an uniform radial pressure applied on the surface of the sphere. The effective bulk modulus, K, given by Eqn. (4.21) will be determined for the cases when the displacements or stresses are specified on the boundary of the representative sample.

4.2.1.1 Displacements Specified on the Boundary of a Representative Sample of a Granular System

The effective bulk modulus, $\bar{K}$, will be determined for the case when the displacements are specified on the boundary of a representative volume element. The rectangular coordinate system, (x, y, z) is used to define a point in the representative volume. The representative volume will be subjected to a macroscopically homogeneous displacement field. The displacement field to be imposed is given below

$$u_x(x) = x\,\varepsilon_{xx} \tag{4.22a}$$

$$u_y(y) = y\,\varepsilon_{yy} \tag{4.22b}$$

$$u_z(z) = z\,\varepsilon_{zz} \tag{4.22c}$$

where u_x = the displacement in the x coordinate direction

u_y = the displacement in the y coordinate direction

u_z = the displacement in the z coordinate direction

ε_{xx} = strain in the x coordinate direction

ε_{yy} = strain in the y coordinate direction

ε_{zz} = strain in the z coordinate direction

The strain field appearing in Eqns. (4.22) is assumed to be constant with respect to the location within the representative volume. The displacement vector at any point, (x, y, z), within the representative volume is given by

$$\vec{u} = u_x(x)\,\hat{e}_x + u_y\,\hat{e}_y + u_z\,\hat{e}_z \quad \ldots\ldots\ldots\ldots \quad (4.23)$$

where u = the displacement vector

$\hat{e}_x$ = the unit vector in the x coordinate direction

$\hat{e}_y$ = the unit vector in the y coordinate direction

$\hat{e}_z$ = the unit vector in the z coordinate direction

Substitution of Eqns. (4.22) into Eqn. (4.23) gives the following displacement vector in terms of the strain field

$$\vec{u} = x\,\varepsilon_{xx}\,\hat{e}_x + y\,\varepsilon_{yy}\,\hat{e}_y + z\,\varepsilon_{zz}\,\hat{e}_z \quad \ldots\ldots\ldots \quad (4.24)$$

To determine the displacement vector at a point of contact between two spheres, it will be assumed that this vector is determined by evaluating Eqn. (4.24) at the coordinates of the contact. A typical sphere contained in the representative volume element, with the origin at point (x_o, y_o, z_o), is shown in Fig. 4.2. In Fig. 4.2, the sphere is shown in contact with two adjacent spheres. The local coordinate directions, $\bar{x}$, $\bar{y}$, $\bar{z}$, shown in Fig. 4.2 are parallel to the x, y and z coordinate directions, respectively. The local coordinate system (x_m, y_m, z_m), is positioned so that the z_m axis is directed through the origin of the sphere and contact pair m. The angles β_m and ψ_m define the position of the local coordinate system (x_m, y_m, z_m), relative to the coordinate system $(\bar{x}, \bar{y}, \bar{z})$. The contacts occurring along the z_m axis are labeled as contact 1 and contact 2, as shown in Fig. 4.2. The coordinates of the center of contact 1 in reference to the coordinate system, (x, y, z) are given by

$$x_1 = x_o + R \sin\beta_m \cos\psi_m \tag{4.25a}$$

$$y_1 = y_o + R \sin\beta_m \sin\psi_m \tag{4.25b}$$

$$z_1 = z_o + R \cos\psi_m \tag{4.25c}$$

where x_1 = x coordinate of the center of contact 1

y_1 = y coordinate of the center of contact 1

z_1 = z coordinate of the center of contact 1

R = radius of the sphere

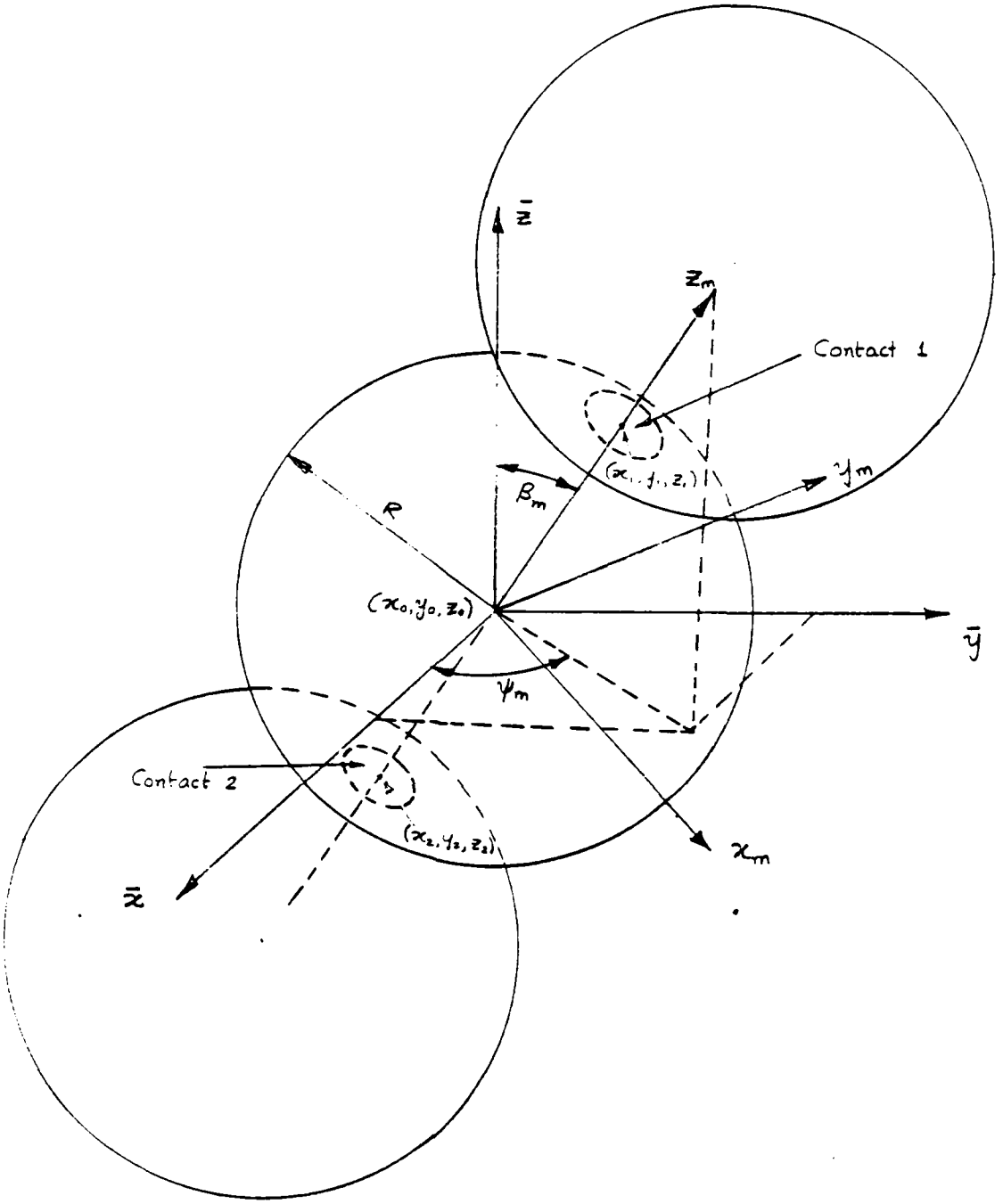
$\bar{z}$
z_m
Contact 1
(x_1, y_1, z_1)
y_m
β_m
R
(x_0, y_0, z_0)
$\bar{y}$
ψ_m
Contact 2
(x_2, y_2, z_2)
x_m
$\bar{x}$

FIG 4.2

In a similar manner, the coordinates of the center of contact 2, in reference to the coordinate system, (x,y,z), are given by

$$x_2 = x_o - R \sin\beta_m \cos\psi_m \quad \ldots\ldots\ldots\ldots\ldots\ldots \quad (4.26a)$$

$$y_2 = y_o - R \sin\beta_m \sin\psi_m \quad \ldots\ldots\ldots\ldots\ldots\ldots \quad (4.26b)$$

$$z_2 = z_o - R \cos\beta_m$$

Using Eqn. (4.24), the displacement vector may be evaluated for the points (x_1,y_1,z_1) and (x_2,y_2,z_2). The displacement vector at point (x_1, y_1,z_1) is given by

$$u_1 = (x_o + R \sin\beta_m \cos\psi_m)\ \hat{\varepsilon}_{xx}\ \hat{e}_x$$

$$+ (y_o + R \sin\beta_m \sin\psi_m)\ \varepsilon_{yy}\ \hat{e}_y$$

$$+ (z_o + R \cos\psi_m)\ \varepsilon_{zz}\ \hat{e}_z \quad \ldots\ldots\ldots\ldots\ldots\ldots \quad (4.27)$$

The displacement vector evaluated at point (x_2,y_2,z_2) is given by

$$\vec{u}_2 = (x_o - R \sin\beta_m \cos\psi_m)\ \varepsilon_{xx}\ \hat{e}_x$$

$$+ (y_o - R \sin\beta_m \sin\psi_m)\ \varepsilon_{yy}\ \hat{e}_y$$

$$+ (z_o - R \cos\psi_m)\ \varepsilon_{zz}\ e_z \quad \ldots\ldots\ldots\ldots\ldots\ldots \quad (4.28)$$

In Eqns. (4.27) and (4.28), the subscripts 1 and 2 denote the displacement vectors at contacts 1 and 2, respectively. The magnitudes of the displacements in the positive z_m coordinate direction may be determined for contact, 1 and 2 by taking the dot product of the displacement vectors at these contacts, with a unit vector in the positive z_m coordiante direction. The unit vector in the positive z_m coordinate direction, $\hat{e}_{zm}$, is given by

$$\hat{e}_{zm} = \sin\beta_m \cos\psi_m \hat{e}_x + \sin\beta_m \sin\psi_m \hat{e}_y + \cos\beta_m \hat{e}_z \quad . \quad (4.29)$$

The displacement at contact 1 in the positive z_m coordinate direction is given by

$$u^1_{zm} = \vec{u}_1 \cdot \hat{e}_{zm} = \varepsilon_{xx}(x_o + R \sin\beta_m \cos\psi_m)\sin\beta_m \cos\psi_m$$

$$+ \varepsilon_{yy}(y_o + R \sin\beta_m \sin\psi_m) \sin\beta_m \sin\psi_m$$

$$+ \varepsilon_{zz}(Z_o + R \cos\beta_m) \cos\beta_m \quad . \quad . \quad . \quad . \quad . \quad . \quad . \quad . \quad . \quad . \quad . \quad (4.30)$$

where u^1_{zm} = the displacement at contact 1 in the positive z_m coordinate direction.

The displacement at contact 2 in the positive z_m coordinate direction is given by

$$u^2_{zm} = \vec{u}_2 \cdot \hat{e}_{zm} =$$

$$\varepsilon_{xx} (x_o - R \sin\beta_m \cos\psi_m) \sin\beta_m \cos\psi_m$$

$$+ \varepsilon_{yy} (y_o - R \sin\beta_m \sin\psi_m) \sin\beta_m \sin\psi_m$$

$$+ \varepsilon_{zz} (z_o - R \cos\beta_m) \cos\beta_m \quad \ldots\ldots\ldots\ldots \quad (4.31)$$

where u^2_{zm} = the displacement at contact 2 in the positive z_m coordinate direction.

Having determined the displacements in the positive z_m coordinate directions for contacts 1 and 2, the change in the diameter of the sphere along the z_m coordinates axis is given by

$$\Delta u_{zm} = u^1_{zm} - u^2_{zm} = 2R\ \varepsilon_{xx} \sin^2\beta_m \cos^2\psi_m + 2R\ \varepsilon_{yy} \sin^2\beta_m \sin^2\psi_m$$

$$2R\ \varepsilon_{zz} \cos^2\beta_m \quad \ldots\ldots\ldots\ldots\ldots\ldots \quad (4.32)$$

where Δu_{zm} = the change in the dimension of the sphere along the axis z_m.

The Eqn. (4.32) gives the change in the diameter of a sphere resulting from contact pair m, directed along an axis passing through the origin of the sphere, as shown in Fig. 4.2. The position of this axis with respect to a global coordinate system, (x,y,z), is defined by the

angles β_m and ψ_m. If the spheres shown in Fig. 4.2 are all of the same radii and material properties, then the deformation occurring at the center of each contact would be equal. The magnitude of this displacement would be half of that given by Eqn. (4.32). This magnitude is given by

$$\bar{u}_m = R\,[\varepsilon_{xx} \sin^2\beta_m \cos^2\psi_m + \varepsilon_{yy} \sin^2\beta_m \sin^2\psi_m + \varepsilon_{zz} \cos^2\beta_m] \quad (4.33)$$

where $\bar{u}_m$ = the displacement at the center of either contact for contact pair m.

The direction of the displacement given in Eqn. (4.33) is toward the origin of the sphere if $\bar{u}_m$ is negative, and away from the origin of the sphere if $\bar{u}_m$ is positive. The result given by Eqn. (4.33) will be used to determine the effective bulk modulus, $\bar{k}$, for the case when the displacements are known on the boundaries of the representative volume element.

For the case when the displacements are known on the boundaries of the representative volume element, Eqn. (4.21) is written as

$$3\,\bar{k} = \frac{6\,(1+\nu_s)C_s\left[\bar{b}^u_{-2} + \sum_{m=1}^{\frac{M}{2}} (b^u_{-2})_m\right] + 3\,C_f\,\bar{\sigma}_u}{\frac{3}{G_s}(1-2\nu_s)C_s\left[\bar{b}^u_{-2} + \sum_{m=1}^{\frac{M}{2}} (b^u_{-2})_m\right] + C_f\,e_f} \quad (4.34)$$

All the terms appearing in Eqn. (4.34) have the same definitions as in Eqn. (4.21), except that the superscript, u, has been used on the constants, $\bar{b}_{-2}$ and $(b_{-2})_m$, to indicate that these constants are determined for the case when surface displacements on a sphere are specified. From Section 3.2, the constant of superposition, b^u_{-2}, is given by

$$b^u_{-2} = \frac{G\,\xi^u_o}{(1-2\nu)R} \quad \ldots\ldots\ldots\ldots\ldots\ldots\ldots\ldots \quad (4.35)$$

where R = radius of sphere

G = shear modulus of sphere

ν = Poisson's ratio for sphere.

The constant ξ^u_o, appearing in Eqn. (4.35) is determined from the displacement boundary conditions on a sphere. ~~Two cases of boundary conditions on a sphere.~~ Two cases of boundary conditions exist on the sphere. The first is the displacements resulting from contacts with adjacent spheres and the second due to the displacements from a uniform radial fluid pressure acting on the sphere.

The constant ξ^u_o has been determined for the displacement boundary conditions resulting from the contact of a sphere with two adjacent spheres, along an axis passing through the origin of the sphere. For this case the constant ξ^u_o is

$$\xi^u_o = K^u\,\bar{\xi}^u_o \quad \ldots\ldots\ldots\ldots\ldots\ldots\ldots\ldots \quad (4.36)$$

the terms K^u and $\bar{\xi}_o^u$ are given by

$$K^u = \frac{3(1-\nu^2)R^2F}{8\,a^3\,E} \quad \ldots\ldots\ldots\ldots\ldots\ldots \quad (4.37)$$

$$\xi_o^u = \frac{-(2\sin^2\phi'-1)\sin^2\phi'}{2} + \frac{(1-\cos^4\phi')}{4} \quad \ldots\ldots\ldots \quad (4.38)$$

where F = the force transmitted through the contact

R = radius of sphere

a = radius of the contact area

$\phi' = \sin^{-1}\left(\frac{a}{R}\right)$

The Eqns. (3.16a) and (3.20) may be combined to determine the radius of contact, a. For spheres of equal radii and material properties, the radius of contact, a, is given by

$$a = \sqrt[3]{\frac{3(1-\nu^2)RF}{4E}} \quad \ldots\ldots\ldots\ldots\ldots\ldots \quad (4.39)$$

Substitution of Eqn. (4.39) into Eqn. (4.37) yields the following value for k^u

$$k^u = \frac{R}{2} \quad \ldots\ldots\ldots\ldots\ldots\ldots\ldots\ldots \quad (4.40)$$

Combining Eqns. (4.35), (4.36) and (4.40), the constant of superposition, b^u_{-2}, can be determined for one pair of contacts on a sphere. This result is given by

$$b^u_{-2} = -\frac{G\,\bar{\xi}_o^u}{2(1-2\nu)} \quad \ldots\ldots\ldots\ldots\ldots\ldots \quad (4.41)$$

The term ξ_o^u appearing in Eqn. (4.41) is given by Eqn. (4.38). This term is a function of the angle defining the contact area, ϕ'. The angle, ϕ', may be related to the displacement at the center of the contact. This relationship is determined from Eqns. (3.16) and is given by

$$\phi' = \sin^{-1}\left(\frac{a}{R}\right) = \sin^{-1}\left(\sqrt{|\bar{u}|/R}\right), \quad (0 \leq \phi' \leq \pi/2) \quad . \quad . \quad (4.42)$$

where $\bar{u}$ = dispacement at the center of the contact area

R = the radius of the sphere.

The absolute value of u is used in Eqn (4.42) since $\phi' \geq 0$. The value of u for a pair of contacts on a sphere is determined from Eqn. (4.33). This value of u is an approximation but should be sufficient for the determination of the effective bulk modulus, $\bar{k}$.

The value of ξ_o^u for the surface displacements resulting from a uniformly applied radial pressure on a sphere may be determined from Section 3.4.3. This value is given by

$$\xi_o^u = \frac{(1-2\nu)R\,\bar{\sigma}_u}{2G(1+\nu)} \quad . \quad (4.43)$$

where $\bar{\sigma}_u$ = fluid pressure on sphere

Substitution of Eqn. (4.43) into Eqn. (4.35), gives the constant of superposition, b_{-2}^u, for a sphere subjected to a uniformly applied radial pressure. This constant is given by

$$b_{-2}^{\bar{u}} = \frac{\bar{\sigma}_u}{2(1+\nu)} \quad \ldots\ldots\ldots\ldots\ldots\ldots\ldots\ldots \quad (4.44)$$

Substitution of Eqns. (4.41) and (4.44) into Eqn. (4.34) yields the following for the effective bulk modulus.

$$3\bar{k} = \frac{\frac{-3(1+\nu_s)\, G_s\, C_s}{(1-2\nu_s)} \left[\sum_{m=1}^{\frac{M}{2}} (\xi_o^u)_m \right] + 3\bar{\sigma}_u}{\frac{3}{2} C_s \left[\sum_{m=1}^{\frac{M}{2}} (\xi_o^u)_m \right] + \frac{3(1-2\nu_s) G_s\, \bar{\sigma}_u}{2G_s(1+\nu_s)} + C_f\, e_f} \quad \ldots \quad (4.45)$$

where $\bar{k}$ = effective bulk modulus

C_s = volume fraction of solids in the solid-fluid system

C_f = volume fraction of fluid in the solid-fluid system

G_s = shear modulus of the solid phase

ν_s = Poisson's ratio of the solid phase

$\bar{\sigma}_u$ = fluid pressure

e_f = volumetric strain of the fluid phase.

ξ_o^u = constant determined from displacement boundary conditions on sphere

M = number of contacts on a single sphere.

The effective bulk modulus, $\bar{k}$, given in Eqn. (4.45) is for use when the displacements are specified on the boundaries of the solid-fluid system. The simpliciations used to arrive at Eqn. (4.45) from Eqn. (4.20) were that the spheres in the system are of equal radii and have

the same material properties. These spheres are situated in ideal packing configurations.

To evaluate Eqn. (4.45), the volume fractions and material properties of the solid and fluid phases must be known. The term, ξ_o^u, must be known for each contact pair occurring on a sphere in the solid-fluid system. This constant may be obtained when the displacement, $\bar{u}$, of the center of the contact region is known. To determine the displacement, $\bar{u}$, Eqn. (4.33) is used. The displacement, $\bar{u}$, is the displacement normal to the region of contact. This displacement was determined by treating the solid-fluid system as a continuum undergoing macroscopically homogeneous displacements of the form given in Eqn. (4.42). The displacement vector at a point in this continuum was taken to be that occurring on a contact at this point. The magnitude of the displacement vector normal to the region of contact was taken as $\bar{u}$. This value of $\bar{u}$ is an approximation. Any displacements on the region of contact which are tangential to this region have been neglected.

The angles, θ_m and ψ_m, defining the location of pairs of contacts with respect to a global coordinate system, must be known to evaluate the sum involving the term ξ_o^u.

4.2.1.2 Surface Tractions Specified on the Boundary of the Representative Sample.

The effective bulk modulus, $\bar{k}$, will be determined for the case when the surface tractions are specified on the boundary of a representative volume element. The representative volume element will be subjected to a macroscopically homogeneous stress field. The stress field to be applied to the representative volume is given by

$$\sigma_{xx}(x) = \sigma_{xx} \quad \ldots \quad (4.46a)$$

$$\sigma_{yy}(y) = \sigma_{yy} \quad \ldots \quad (4.46b)$$

$$\sigma_{zz}(z) = \sigma_{zz} \quad \ldots \quad (4.46c)$$

where σ_{xx} = the stress normal to the xz-plane

σ_{yy} = the stress normal to the xz-plane

σ_{zz} = the stress normal to the yz-plane

The stress field given by Eqns. (4.46) is constant with respect to position within the representative volume element.

An arbibitrary plane cut through the representative volume is shown in Fig. 4.3. The unit normal vector to this plane is designated as $\hat{n}$. The angles α_x, α_y and α_z define the position of the unit normal vector, $\hat{n}$, to the x, y and z axes, respectively. The stress vector, $\vec{T}$, on this plane is given by

$$\vec{T} = \sigma_{xx} \cos\alpha_x \, e_x + \sigma_{yy} \cos\alpha_y \, e_y + \sigma_{zz} \cos\alpha_z \, e_z \quad \ldots \quad (4.47)$$

where $\hat{e}_x$ = the unit vector in the x coordinate direction

$\hat{e}_y$ = the unit vector in the y coordinate direction

$\hat{e}_z$ = the unit normal vector in the z coordinate direction.

The unit normal vector, n, to the plane shown in Fig. 4.3 is given by

$$\hat{n} = \cos\alpha_x \, \hat{e}_x + \cos\alpha_y \, \hat{e}_y + \cos\alpha_z \, \hat{e}_z \quad \ldots \quad (4.48)$$

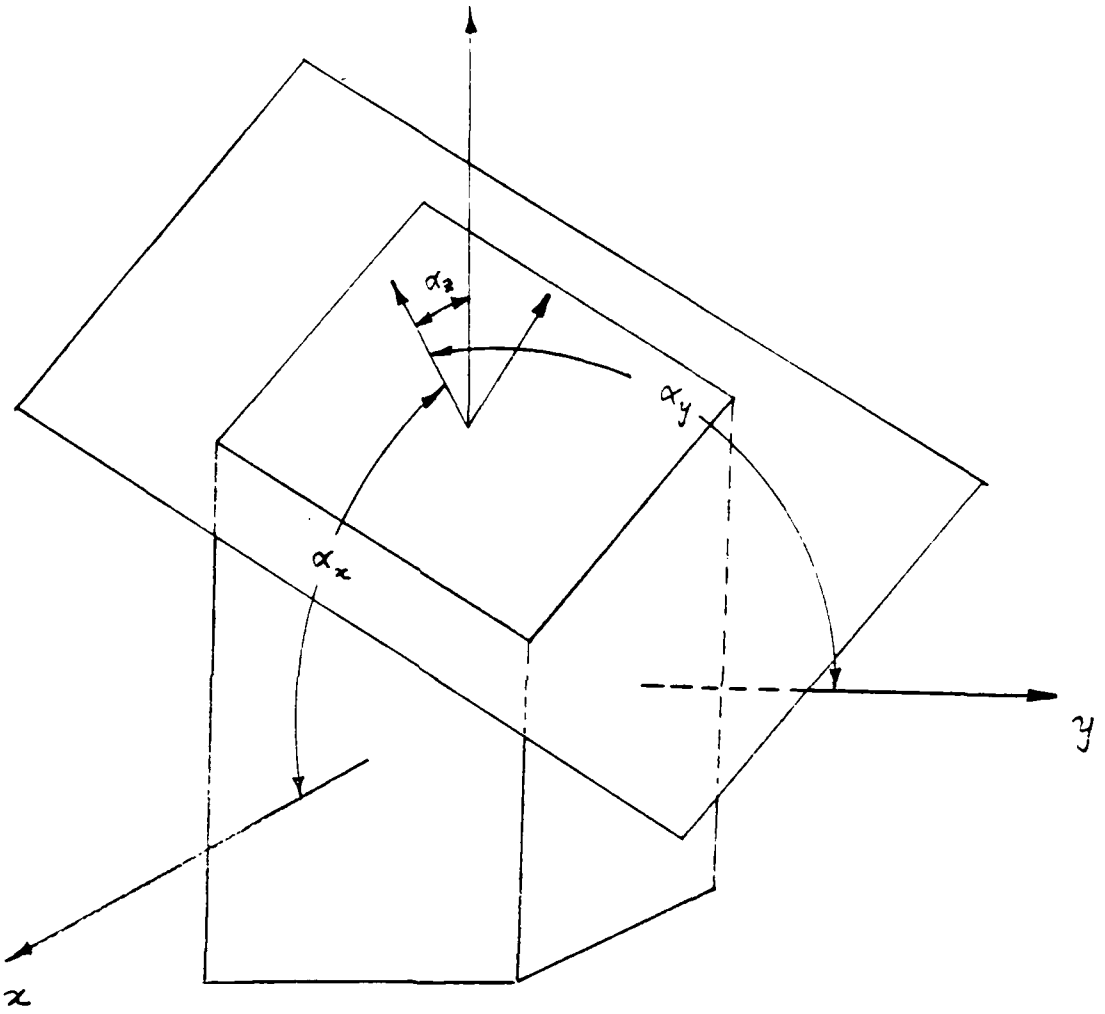

FIG 4.3

The normal stress on the plane is determined by the dot product of the stress vector, $\bar{T}$, with the unit normal vector, $\hat{n}$. Performing this operation, the normal stress is given by

$$\sigma_n = \sigma_{xx} \cos^2\alpha_x + \sigma_{yy} \cos^2\alpha_y + \sigma_{zz} \cos^2\alpha_z \quad . \quad . \quad . \quad . \quad . \quad . \quad (4.49)$$

The normal stress given by Eqn. (4.49) was determined by treating the representative volume element as a continuum subjected to the stress field given by Eqn. (4.46). The plane intersecting the representative volume, shown in Fig. 4.3, will contain a number of contact regions present in the solid-fluid system. These contact regions are formed as the spheres in this system are compressed together under the action of the stress field given by Eqns. (4.46). Such a contact region is shown in Fig. 4.4. The normal force transmitted through this contact region will be determined as the product of the normal stress acting on the plane containing the contact region and an area contained in the plane. In Fig. 4.4, the rectangular coordinate system, (x_m, y_m, z_m), is positioned such that the z_m axis is directed through the centers of the contact regions for contact pair m and the origin of the sphere. The coordinate system (x_m, y_m, z_m) is defined relative to the coordinate system $(\bar{x}, \bar{y}, \bar{z})$ by the angles β_m and ψ_m. The coordinates, $\bar{x}$, $\bar{y}$ and $\bar{z}$ are parallel to the global coordinates x, y and z, respectively. In Fig. 4.4, the plane containing one of the contact regions for contact pair m is shown. The unit normal vector to this plane is given by

$$\hat{n} = \sin\beta_m \cos\psi_m \hat{e}_x + \sin\beta_m \sin\psi_m \hat{e}_y + \cos\beta_m \hat{e}_y \quad . \quad . \quad . \quad (4.50)$$

where $\hat{e}_x$ = unit vector in the x coordinate direction

$\hat{e}_y$ = unit vector in the y coordinate direction

$\hat{e}_z$ = unit vector in the z coordinate direction.

The stress vector occurring on the plane shown in Fig. 4.4 is given by

$$\vec{T} = \sigma_{xx} \sin\beta_m \cos\psi_m \hat{e}_x + \sigma_{yy} \sin\beta_m \sin\psi_m \hat{e}_y + \sigma_{zz} \cos\beta_m \hat{e}_z \quad . \quad (4.51)$$

The stress components, σ_{xx}, σ_{yy} and σ_{zz}, appearing in Eqn. (4.51) are those applied to the boundaries of the representative volume element. The normal stress on the plane defined by the unit normal vector appearing in Eqn. (4.50) is determined as the dot product of the vectors given in Eqns. (4.50) and (4.51). This normal stress is given by

$$\sigma_n^m = \sigma_{xx} \sin^2\beta_m \cos^2\psi_m + \sigma_{yy} \sin^2\beta_m \sin^2\psi_m + \sigma_{zz} \cos^2\beta_m \quad . \quad . \quad . \quad . \quad (4.52)$$

where σ_n^m = the normal stress on the plane containing the contact regions for contact pair m.

The force transmitted through a contact region contained in the plane subjected to the normal stress, σ_n^m, is given by

$$F_m(\beta_m, \psi_m) = \sigma_n^m(\beta_m, \psi_m) \, A_m \quad . \quad . \quad . \quad . \quad . \quad . \quad . \quad . \quad . \quad . \quad . \quad . \quad . \quad . \quad . \quad (4.53)$$

where A_m = area of the plane containing the contact region which transmits normal stress σ_n^m through the contact region.

In Eqn. (4.53) F_m is the force transmitted through a contact contained in the plane defined by the unit normal vector given in Eqn. (4.50). The normal stress, σ_n^m, appearing in Eqn. (4.53) is given by Eqn. (4.52). To determine the force, F_m, transmitted through a pair of contacts m, it will be assumed that the spheres which are intersected by a particular plane carry the same loads as the contact regions contained in the place. Therefore, the normal stress occurring on a plane will be transmitted evenly through the spheres and contact regions intersected by the plane. The area A_m appearing in Eqn. (4.53) is given by

$$A_m = \frac{[2(1+\sqrt{3})R][2\sqrt{2}R]}{3\sqrt{3}} = \frac{4\sqrt{2}(1+\sqrt{3})R^2}{3\sqrt{3}} \quad \ldots (4.54)$$

From Eqn. (4.53), the force transmitted through contact A is given by

$$F_m = \frac{4\sqrt{2}(1+\sqrt{3})R^2\,\sigma_n^m}{3\sqrt{3}} \quad \ldots\ldots\ldots\ldots (4.55)$$

The normal stress, σ_n^m, is given by Eqn. (4.52). This normal stress depends on the angles, β_m and ν_m, defining the contact orientation with respect to the global coordinate system, (x,y,z). A particular sphere in the system under consideration will normally be subjected to many contacts. The force, F_m, transmitted through a contact will depend on the contact orientation and the area, A_m.

The value of F_m is an approximation to the actual force transmitted through a contact. The contact forces occurring in many systems of spheres situated in ideal packing configurations, may not be determined from the equations of static equilibrium. Due to this the approximation of the contact force, F_m, given by Eqn. (4.53) will be used. This approximation will be used to determine the effective bulk modulus, $\bar{K}$, for the case when surface tractions are known on the representative volume element.

For the case when surface tractions are specified on the boundaries of a ~~the~~ representative volume element, Eqn. (4.21) is written as follows.

$$3\bar{K} = \frac{6(1+\nu_s)C_s\left[\bar{b}^{\sigma}_{-2} + \sum_{k=1}^{\frac{M}{2}} (b^{\sigma}_{-2})_k\right] + 3\,C_f\,\bar{\sigma}_u}{\frac{3}{G_s}(1-2\nu_s)C_s\left[\bar{b}^{\sigma}_{-2} + \sum_{k=1}^{\frac{M}{2}} (b^{\sigma}_{-2})_k\right] + C_f\,e_f} \qquad (4.56)$$

All the terms appearing in Eqn. (4.56) have the same meaning as those appearing in Eqn. (4.21). The superscript, σ, has been used on the constants, $\bar{b}_{-2}$ and $(b_{-2})_k$, to indicate that these constants are determined for the case when the surface tractions have been specified on the boundaries of the representative volume element. In Section 3.2, the constant of superposition, b^{σ}_{-2}, was determined. This constant is given by

$$\bar{b}^{\sigma}_{-2} = \frac{\xi^{\sigma}_o}{2(1+\nu)} \qquad (4.57)$$

where ν = poison's ratio for the spheres.

The constant, ξ_o^σ, appearing in Eqn. (4.57) is determined from the surface tractions present on a particular sphere. Two types of boundary conditions will exist on the spheres in the solid-fluid system under consideration. The first of these boundary conditions are the surface tractions resulting from contacts with adjacent spheres. The second boundary condition is due to a uniform fluid pressure acting on the surface of the sphere.

The constant, ξ_o^σ, has been determined for the surface tractions which result when a sphere is in contact with two adjacent spheres. The contacts made with the two adjacent spheres are along an axis which passes through the center of the sphere. For this case the constant ξ_o^σ is

$$\xi_o^\sigma = k^\sigma \bar{\xi}_o^\sigma \quad \ldots\ldots\ldots\ldots\ldots\ldots\ldots\ldots \quad (4.58)$$

The terms k^σ and $\bar{\xi}_o^\sigma$, appearing in Eqn. (4.45) are given as follows.

$$k^\sigma = \frac{3FR}{2\pi a^3} \quad \ldots\ldots\ldots\ldots\ldots\ldots\ldots\ldots \quad (4.59)$$

$$\bar{\xi}_o^\sigma = -\left[\frac{\sin^3 \flat'}{4} + \frac{\cos^2 \flat' \sin \flat'}{8} - \frac{\cos^4 \flat'}{8} \ln\left(\frac{1+\sin \flat'}{\cos \flat'}\right)\right] \quad (4.60)$$

where F = the force transmitted through the contact

R = radius of the sphere

a = radius of the contact area

$\flat' = \sin^{-1}\left(\frac{a}{R}\right)$

The Eqn. (4.39) gives the relationship between the radius of the contact region, a, and the force transmitted through the contact, F. Using this relationship the constant, k^{σ}, given by Eqn. (4.59) may be rewritten as

$$k^{\sigma} = \frac{2E}{\pi(1-\nu^2)} \quad \ldots\ldots\ldots\ldots\ldots\ldots\ldots\ldots\ldots\ldots \quad (4.61)$$

where E = modulus of elasticity for the sphere

Combining Eqns. (4.57), (4.58), and (4.61), the constant of superposition, b_{-2}^{σ}, is given by

$$b_{-2}^{\sigma} = \frac{2G}{\pi(1-\nu^2)} \bar{\xi}^{\sigma} \quad \ldots\ldots\ldots\ldots\ldots\ldots\ldots\ldots\ldots\ldots \quad (4.62)$$

where G = the shear modulus of the sphere

The quantity, $\bar{\xi}_o^{\sigma}$, appearing in Eqn. (4.62) is given by Eqn. (4.60). From Eqn. (4.60) it is seen that $\bar{\xi}_o^{\sigma}$ is a function of the angle, ϕ', defining the contact region. This angle may be related to the force, F, transmitted through the contact through Eqn. (4.39). This relationship is given by

$$\phi' = \sin^{-1}\left(\sqrt[3]{\frac{3(1-\nu)\ F}{8\ G\ R^2}}\right) \quad \ldots\ldots\ldots\ldots\ldots\ldots\ldots \quad (4.63)$$

The approximation given by Eqn. (4.53) will be used to determine F, which is required in order to evaluate the effective bulk modulus, $\bar{K}$.

The value of ξ_o^{σ}, determined for the case when a uniform rdial pressure is acting on the surface of a sphere was determined in Section 3.4.3. This value is given by

$$\xi_o^{\sigma} = \bar{\sigma}_u \quad \ldots\ldots\ldots\ldots\ldots\ldots\ldots\ldots\ldots\ldots \quad (4.64)$$

where $\bar{\sigma}_u$ = fluid pressure on the sphere

Substitution of Eqn. (4.64) into Eqn. (4.57) gives the constant of superposition, $\bar{b}_{-2}^{\sigma}$, appearing in Eqn. (4.56). This constant is given by

$$b_{-2}^{\sigma} = \frac{\bar{\sigma}_u}{2(1+\nu)} \quad \ldots\ldots\ldots\ldots\ldots\ldots\ldots\ldots\ldots\ldots \quad (4.65)$$

Substitution of Eqns. (4.62) and (4.64) into Eqn. (4.56) yields the following expression for the effective bulk modulus.

$$3\bar{K} = \frac{-\dfrac{12\, G_s\, G_s}{(1-\nu)}\left[\sum_{k=1}^{\frac{M}{2}} (\bar{\xi}_o^{\sigma})_k\right] + 3\,\bar{\sigma}_u}{\dfrac{-6(1-2\nu_s)C_s}{(1-\nu_s^{\,2})}\left[\sum_{k=1}^{\frac{M}{2}} (\bar{\xi}_o^{\sigma})_k\right] + \dfrac{3(1-2\nu_s)C_s\bar{\sigma}_u}{3\,G_s(1+\nu_s)} + C_f\, e_f} \quad \ldots \quad (4.66)$$

Where $\bar{K}$ = effective bulk modulus

C_s = volume fraction of the solids in the solid-fluid system

C_f = volume fraction of the fluid in the solid-fluid system

G_s = shear modulus of the solid phase

ν_s = Poisson's ratio of the solid phase

σ_u = fluid pressure

$\bar{e}_f$ = volumetric strain of the fluid phase

$\bar{\xi}_o^{\sigma}$ = constant determined from the stress boundary conditions on a single sphere

M = number of contacts on a single sphere.

The Eqn. (4.65) gives the effective bulk modulus, $\bar{K}$, of a system comprised of a number of equal spheres, in ideal packing configurations, with the surrounding void space being filled with a fluid phase. The effective bulk modulus, $\bar{K}$, given by Eqn. (4.65) is used when the normal stresses are known on the boundaries of a representative volume element. To use Eqn. (4.65), the volume fractions of the solid and liquid phases present in the system must be known. The constants, $\bar{\xi}_o^{\sigma}$, must be determined for every contact pair occurring on a single sphere in the system. To determine these constants the force, F_m, occurring on a contact pair m is approximated by Eqn. (4.53) The approximation to the force, F_m, was arrived at by considering the solid-fluid system to be a continuum. The normal stress acting on a plane containing a particular contact region was determined and then the contact was said to carry a portion of this normal stress. Any tangential shear stresses acting on the plane containing the contact region were neglected so that the solutions given in Chapter 3 , could be used in determining the effective bulk modulus.

4.2.2 Discussion of the Effective Bulk Modulus Determined from the Volume Averaged Approach

In the previous two subsections of this chapter, the effective bulk modulus, $\bar{K}$, for an idealized solid-fluid system was determined using a volume averaged approach. The idealized solid-liquid system under consideration consists of a number of spheres in contact surrounded by a fluid phase. In order to obtain a simple expression for the effective bulk modulus, $\bar{K}$, of such a system some restrictions on the geometry and material properties of the spheres in the system had to be imposed. These restrictions are as follows:

1. All the spheres in the system have the same material properties.
2. The spheres in the system are of equal radii.
3. The spheres in the system exist in ideal packing configurations.

The first of these restrictions is the most reasonable with respect to modeling actual systems. The second and third restrictions are less realistic with respect to modeling actual systems. In some cases all the spheres in a solid-fluid system may be of equal radii thus making the second restriction valid. The third restriction which requires the spheres in the solid-fluid system to exist in ideal packing configurations is the most unreasonable. In actual systems composed of spheres in contact, the spheres will be arranged in a random order. In such a system it would be impossible to identify the locations of the contacts present on a single sphere so that statistical data of some form would be required to evaluate the effective bulk modulus. By restricting the spheres in the solid-fluid system to be of

equal radii and arranged in ideal packing configurations, the location of the contacts on a single sphere within the system may be identified. This allows for the determination of the effective bulk modulus without the use of statistical data. In fact, the three restrictions thus far mentioned allows the determination of the effective bulk modulus by considering only one sphere and its interactions with adjacent spheres and the fluid phase present in the solid-fluid system.

Other restrictions were imposed on the stresses and displacements occurring on the regions of contact between adjacent spheres. These restrictions are as follows.

1. The contacts on a particular sphere appear in pairs with each pair occurring along an axis passing through the origin of the sphere.
2. The stresses and displacements occurring on a particular region of contact are axisymmetric with respect to an axis passing through the center and perpendicular to the region of contact.
3. The displacements and stresses normal to the region of contact may be determined from Hertz contact theory.

The purpose of these restrictions was to allow the use of the solutions given in Chapter 3 , in determining the effective bulk modulus. Any non-symmetric displacements or stresses, tangential to the region of contact have been neglected in the determination of the effective bulk modulus of the idealized solid-fluid system.

Using the restrictions thus far mentioned, the effective bulk modulus, $\bar{K}$, of the idealized solid-fluid system was determined for two types of boundary conditions present on a representative volume ele-

ment. The first of the boundary conditions to be considered, corresponded to the case when the displacements are specified on the surface of the representative volume element. The displacement occurring on a particular contact was approximated by treating the solid-liquid system as a continuum. The displacement on a particular contact was then determined as the displacement occurring in a continuum at the location of the contact. This type of approximation is used because the actual value of the displacement on a particular contact is indeterminate for many ideal packing configurations. For the case of a simple cubic packing configuration, the actual displacements occurring on the contacts may be determined. The approximation used to determine the displacement on a contact, yields the actual displacement for this case. The second type of boundary conditions which were considered, corresponded to the case when the surface tractions are specified on the surface of the representative volume element. For this case the force transmitted through a particular contact was again approximated by considering the solid-fluid system to be a continuum. The normal stress acting over a portion of the place containing a particular contact region is taken to be the force transmitted through the contact. This approach to determine the contact forces yields the actual value of this force for the case of a simple cubic packing configuration.

The expressions for the effective moduli obtained in the previous two subsections represent very idealized conditions as apparent from the restrictions and approximations used in the derivation. In using these expressions to determine the effective moduli for an actual solid-fluid system, the accuracy of the value obtained for the effec-

tive bulk modulus should improve as this system becomes better represented by the idealized solid-liquid system. Predictions of the effective bulk modulus should improve for hydrostatic stress states. This is because there would be no shear stresses developed in the idealized solid-liquid system. Any shear stresses which develop due to non-hydrostatic stress states have been neglected in the determination of the effective moduli. By the same reasoning, the predictions of the effective bulk modulus should improve when the displacement components are all of equal magnitude.

4.3 Energy Approach for Determining Bounds on the Effective Bulk Modulus

The theorems of minimum potential energy and minimum complementary energy will be used to determine upper and lower bounds on the effective bulk modulus of an idealized solid-fluid system. These theorems and their use in determining upper and lower bounds for the effective bulk modulus will be discussed below.

To discuss the theorems of minimum potential energy and minimum complementary potential energy, an elastic body in static equilibrium is considered. The boundary conditions prescribed on such a body are given by

$$T_i = \sigma_{ij} n_j \qquad \text{on } S \quad \ldots\ldots\ldots\ldots\ldots\ldots \quad (4.66a)$$

$$\bar{u}_i = u_i \qquad \text{on } S \quad \ldots\ldots\ldots\ldots\ldots\ldots \quad (4.66b)$$

where σ_{ij} = stress tensor

u_i = components of displacement vector

n_j = components of the unit outward normal vector on the surface

T_i = components of the stress vector on the surface

$\bar{u}_i$ = components of the displacement vector on the surface

S_σ = surface over which T_i is prescribed

S_u = surface over which $\bar{u}_i$ is prescribed

Cartesian tensor notation is used in Eqns. (4.66) and will continue to be used in this section. The potential energy functional is defined as follows:

$$U = \int_V W(\varepsilon_{ij})\, dV - \int_V F_i u_i\, dV - \int_{S_\sigma} T_i u_i\, dS \quad \ldots . (4.67)$$

where F_i = components of the body force vector.

In Eqn. (4.67) the term $W(\varepsilon_{ij})$ is called the strain energy function. This function is given by

$$W(\varepsilon_{ij}) = 1/2\ C_{ijk\ell}\ \varepsilon_{k\ell}\varepsilon_{ij} \quad \ldots \ldots \ldots \ldots \ldots \quad (4.68)$$

where $C_{ijk\ell}$ = elastic stiffness tensor

$k\ell$ = strain tensor

Admissible displacement fields, $\hat{u}_i$, are defined as any continuous displacement fields satisfying the boundary condition given by Eqn. (4.66b), but otherwise arbitrary. Under these restrictions the theorem

of minimum potential energy says that of all the admissible displacement fields, $\hat{u}_i$, the one that satisfies the equations of equilibrium is that which results in a stationary value of the potential energy functional. This may be written as

$$\hat{U}_\varepsilon = U_\varepsilon \geq 0 \quad \ldots\ldots\ldots\ldots\ldots\ldots\ldots\ldots \quad (4.69)$$

where $\hat{U}_\varepsilon$ = the potential energy functional evaluated for any admissible displacement field

U_ε = the potential energy functional evaluated for the displacement field which satisfies the equations

In using Eqn. (4.69) to determine bounds of the effective bulk modulus of a composite material, the body force components, F_i, will be considered to be zero and the boundary conditions will be such that displacements are prescribed over the entire surface of the body under consideration. For this special case the potential energy functional given by Eqn. (4.67) reduces to

$$U_\varepsilon = \int_V W(\varepsilon_{ij})\, dV \quad \ldots\ldots\ldots\ldots\ldots\ldots\ldots\ldots \quad (4.70)$$

The Eqn. (4.70) gives the strain energy of the body under consideration. Therefore, for this special case the theorem of minimum potential reduces to a minimization of the strain energy stored in the body.

In discussing the theorem of minimum complementary energy, an elastic body in static equilibrium is considered. The boundary conditions on this body are those given by Eqns. (4.66). The complementary energy functional is defined as

$$U_\sigma = \int_V W(\sigma_{ij})\, dV - \int_{S_U} \sigma_i \bar{u}_i\, dS \quad \ldots\ldots\ldots\ldots (4.71)$$

The term $W(\sigma_{ij})$ appearing in Eqn. (4.71) is the strain energy function expressed in terms of stresses. This function is given by

$$W(\sigma_{ij}) = \frac{1}{2} S_{ijk\ell}\, \sigma_{k\ell}\, \sigma_{ij} \quad \ldots\ldots\ldots\ldots\ldots\ldots (4.72)$$

where $S_{ijk\ell}$ = tensor of elastic compliances

The stress field, σ_{ij}, appearing in Eqn. (4.71) and Eqn. (4.72) is admissible when the boundary conditions given by Eqn. (4.66a) and the equations of equilibrium, are satisfied. Under these restrictions the theorem of minimum complementary energy says that of all the admissible stress fields, the one which satisfies the compatibility equations is that which results in a stationary value of the complementary energy functional. This statement may be written mathematically as

$$\hat{U}_\sigma - U_\sigma \geq 0 \quad \ldots\ldots\ldots\ldots\ldots\ldots (4.73)$$

where $\hat{U}_\sigma$ = the complementary energy functional evaluated for any admissible stress field

U_σ = the complementary energy functional evaluated for the stress field which satisfies the compatibility equations.

In using Eqn. (4.73) to determine bounds on the effective bulk modulus of a composite material, the surface tractions will be prescribed over the entire surface of the body under consideration. For this special case the complementary energy functional is given by

$$U_\sigma = \int_V W(\sigma_{ij})\, dV \quad \ldots\ldots\ldots\ldots\ldots\ldots \quad (4.74)$$

The Eqn. (4.74) is an expression for the strain energy of the body under consideration. Thus, when surface tractions are prescribed over the entire surface of the body, the theorem of minimum complementary energy reduces to a minimum principle for the strain energy.

4.3.1 Upper and Lower Bounds of the Effective Bulk Modulus

The theorems of minimum potential energy and minimum complementary energy will be used to determine upper and lower bounds on the effective bulk modulus for a composite system. The Eqn. (4.5) may be rewritten as

$$\frac{1}{2}\int_V \sigma_{ij}\,\varepsilon_{ij}\, dV = \frac{1}{2}\langle\sigma_{ij}\rangle\langle\varepsilon_{ij}\rangle V \quad \ldots\ldots\ldots\ldots\ldots \quad (4.75)$$

where $\langle\sigma_{ij}\rangle$ = volume averaged stress tensor

$\langle\varepsilon_{ij}\rangle$ = volume averaged strain tensor

σ_{ij} = infinitesimal stress tensor

ε_{ij} = infinitesimal strain tensor

V = total volume

The Eqn. (4.75) is a statement that the strain energy stored in the different phases of a is equal to the strain energy expressed in terms of volume averaged stress and strain. The integral appearing in Eqn. (4.75) is taken over all the phases contained in the composite material. If the volume averaged stress tensor, $\langle\sigma_{ij}\rangle$, or the volume averaged strain tensor, $\langle\varepsilon_{ij}\rangle$, are known from the macroscopic stress or strain states occurring in the composite material, then it follows from the minimum theorems of potential and complementary energy that

$$\frac{1}{2}\int_V \sigma_{ij}\varepsilon_{ij}\,dV \geq \langle\sigma_{ij}\rangle\langle\varepsilon_{ij}\rangle V \quad \ldots\ldots\ldots\ldots\ldots\ldots \quad (4.76)$$

The Eqn. (4.76) is applicable when either the surface displacements or the surface tractions have been specified over the entire boundary of the composite material. When the displacement field is specified on the boundaries of the composite material, then an admissible strain field, ε_{ij}, must be such that it satisfies the displacement boundary conditions. Then the stress field, σ_{ij}, is related to the strain field, ε_{ij}, by

$$\sigma_{ij} = C_{ijk\ell}\varepsilon_{ij} \quad \ldots\ldots\ldots\ldots\ldots\ldots\ldots\ldots \quad (4.77)$$

where $C_{ijk\ell}$ = tensor of elastic moduli.

When the surface tractions are specified on the boundaries of the composite material, then an admissible stress field, σ_{ij}, must satisfy these stress boundary conditions. Then the strain field, ε_{ij}, is related to the infinitesimal stress field, σ_{ij}, by

$$\varepsilon_{ij} = S_{ijk\ell}\sigma_{k\ell} \quad \ldots\ldots\ldots\ldots\ldots\ldots\ldots \quad (4.78)$$

where $S_{ijk\ell}$ = tensor of elastic compliances.

An upper bound on the effective bulk modulus, $\bar{K}$, may be determined by considering the composite material to be subjected to displacement boundary conditions which result in a uniform volume averaged strain tensor, $\langle\varepsilon_{ij}\rangle$. The displacement boundary conditions of this type are given by

$$\bar{u}_i = \frac{\langle\varepsilon_{kk}\rangle}{3}\bar{x}_i \quad \ldots\ldots\ldots\ldots\ldots\ldots\ldots \quad (4.79)$$

where: $\bar{u}_i$ = surface displacement components

$\langle\varepsilon_{kk}\rangle$ = the trace of the volume averaged strain tensor

$\bar{x}_i$ = rectangular Cartesian coordinates with respect to a system of axes, evaluated on the boundaries of the composite material

The volume averaged strain field, $\langle\varepsilon_{ij}\rangle$, resulting from the boundary conditions given by Eqn. (4.79) are given by

$$\langle\varepsilon_{ij}\rangle = \frac{\langle\varepsilon_{kk}\rangle}{3}\delta_{ij} \quad \ldots\ldots\ldots\ldots\ldots\ldots\ldots \quad (4.80)$$

where δ_{ij} = Kronecker delta = $\begin{cases} 1, & i=j \\ 0, & i\neq j \end{cases}$

If the composite material is an isotropic, linearly elastic material, then the volume averaged stress field, $\langle\sigma_{ij}\rangle$, occurring in the composite material is given by

$$\langle\sigma_{ij}\rangle = \bar{K}\,\langle\varepsilon_{ij}\rangle\,\delta_{ij} \quad \ldots\ldots\ldots\ldots\ldots\ldots\ldots\ldots \quad (4.81)$$

where $\bar{K}$ = the effective bulk modulus

Using Eqns. (4.76), (4.80), and (4.81), the upper bound on the effective bulk modulus is given by

$$\bar{K} \leq \bar{K}_u \quad \ldots\ldots\ldots\ldots\ldots\ldots\ldots\ldots\ldots\ldots \quad (4.82)$$

where $$\bar{K}_u = \frac{1}{\langle\varepsilon_{KK}\rangle^2 V}\int_V \sigma_{ij}\,\varepsilon_{ij}\,dV \quad \ldots\ldots\ldots\ldots\ldots\ldots \quad (4.83)$$

To evaluate Eqn. (4.83) an admissible form of the infinitesimal strain tensor, ε_{ij}, is required for all phases of the composite material. The infinitesimal stress tensor, σ_{ij}, for phase k is given by

$$\sigma_{ij} = \frac{E_k}{(1+\nu_k)}\,\varepsilon_{ij} + \frac{\nu_k E_k}{(1+\nu_k)(1-2\nu_k)}\,\varepsilon_{KK}\,\delta_{ij} \quad \ldots\ldots\ldots \quad (4.84)$$

where E_k = the elastic modulus of phase k

ν_k = Poisson's ratio for phase k.

A lower bound on the effective bulk modulus, $\bar{K}$, may be found by

considering the case when the composite material is subjected to a hydrostatic stress state. The surface tractions for such a case are given by

$$T_i = \frac{\langle \sigma_{KK} \rangle}{3} n_i \quad \ldots\ldots\ldots\ldots\ldots\ldots\ldots\ldots \quad (4.85)$$

where T_i = the components of the surface stress vector

n_i = outward normal to the surface

$\langle \sigma_{KK} \rangle$ = trace of the volume averaged stress tensor.

The surface tractions given by Eqn. (4.85) result in a constant stress field throughout the composite material. The volume averaged stress tensor is given by

$$\langle \sigma_{ij} \rangle = \frac{\langle \sigma_{KK} \rangle}{3} \delta_{ij} \quad \ldots\ldots\ldots\ldots\ldots\ldots\ldots\ldots \quad (4.86)$$

Considering the composite to be an isotropic, linearly elastic material, then the volume averaged strain tensor is given by

$$\langle \varepsilon_{ij} \rangle = \frac{\langle \sigma_{KK} \rangle}{9\bar{K}} \delta_{ij} \quad \ldots\ldots\ldots\ldots\ldots\ldots\ldots\ldots \quad (4.87)$$

where $\bar{K}$ = the effective bulk modulus

Using Eqns. (4.76, (4.86), and (4.87), the lower bound on the effective bulk modulus is given by

$$K \geq K_L$$

where

$$\bar{K}_L = \frac{\langle \sigma_{KK} \rangle^2 V}{9 \int_V \sigma_{ij} \varepsilon_{ij} \, dV} \quad \ldots\ldots\ldots\ldots\ldots\ldots\ldots\ldots \quad (4.88)$$

In order to evaluate Eqn. (4.88) an admissible form of the infinitesimal stress tensor must be known for each phase contained in the composite material. The infinitesimal strain tensor, ε_{ij}, for phase k is then given by

$$\varepsilon_{ij} = \frac{(1+\nu_k)}{E_k} \sigma_{ij} - \frac{\nu_k}{E_k} \sigma_{KK} \delta_{ij} \quad \ldots\ldots\ldots\ldots\ldots\ldots \quad (4.89)$$

where E_k = the elastic modulus of phase k

ν_k = Poisson's ratio for phase k.

To summarize, bounds on the effective bulk modulus, $\bar{K}$, are given by

$$\bar{K}_L \leq \bar{K} \leq \bar{K}_u \quad \ldots\ldots\ldots\ldots\ldots\ldots\ldots\ldots \quad (4.90)$$

In Eqn. (4.90), $\bar{K}_L$ is given by Eqn.(4.88) and $\bar{K}_u$ is given by Eqn. (4.83).

4.3.2 Upper and Lower Bounds on the Effective Bulk Modulus of an Idealized Solid-Fluid System

The general form of the upper and lower bounds on the effective bulk modulus have been determined in Section 4.3.1. In order to evaluate the expressions for the upper and lower bounds the phase geometry and phase material properties must be specified. The remainder of this section will be concerned with evaluating the expressions for the upper and lower bounds for an idealized solid-fluid system.

The idealized solid-fluid system to be considered is composed of spheres arranged in ideal packing configurations and surrounded by a fluid phase. The spheres in this assemble will all have the same material properties and will be of equal radii. The results for a sphere subjected to axisymatric surface displacements or surface tractions, determined in Chapter 3 will be employed to determine the bounds on the effective bulk modulus. Use of these solutions requires the following assumptions concerning the contacts between adjacent spheres.

1. The contacts on a particular sphere occur in pairs with each contact directed along an axis which passes through the origin of the sphere.
2. The sphere is in static equilibrium with negligible body forces.
3. No non-axisymetric surface tractions or displacements, occur on the region of contact between two adjacent spheres.

The first of these assumptions is satisfied automatically by considering only spheres in ideal packing configurations. The geometry for a pair of contacts is shown in Fig. 4.4. The third assumption is reasonable since the bounds on the effective bulk modulus are determined for the cases of the representative volume element undergoing either a uniform strain state or a hydrostatic stress state. For the case of the representative volume element subjected to a state of uniform strain, Eqn. (4.33) gives the following approximation for the displacement, $\bar{u}$, occurring at the center of a contact between adjacent spheres contained in the system.

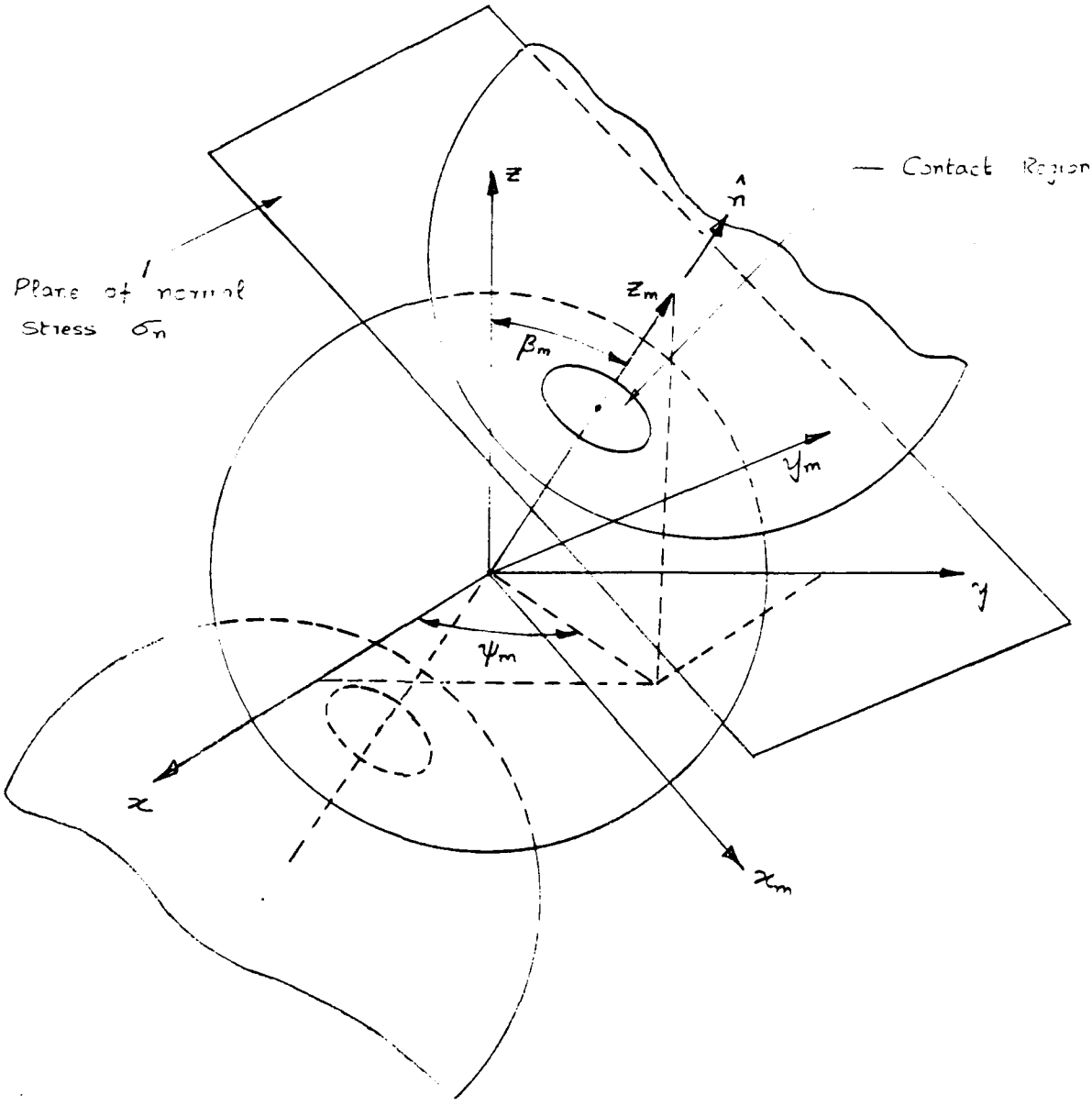
— Contact Region
Plane of normal Stress σ_n
z
$\hat{n}$
z_m
β_m
y_m
y
ψ_m
x
x_m

FIG 4.4

$$\bar{u} = \frac{R\langle \varepsilon_{kk} \rangle}{3} \quad \ldots \ldots \ldots \ldots \ldots \ldots \ldots \quad (4.91)$$

where R = the radius the spheres in the solid-fluid system

$\langle \varepsilon_{kk} \rangle$ = the trace of the volume averaged strain tensor.

For the case of the representative volume element subjected to a state of hydrostatic stress, Eqns. (4.52 and (4.53) give the following approximation for the force transmitted through a contact between adjacent spheres contained in the system.

$$F = \frac{\langle \sigma_{kk} \rangle}{3} A_m \quad \ldots \ldots \ldots \ldots \ldots \ldots \ldots \quad (4.92)$$

where A_m = the area which transmits the stress normal to the contact region through the contact.

$\langle \sigma_{kk} \rangle$ = the trace of the volume averaged stress tensor.

The area, A_m, appearing in Eqn. (4.92) will depend on the packing configuration and the orientation of the particular contact with respect to the global coordinate system for the representative volume element. To simplify the determination of the bounds on the effective bulk modulus it will be assumed that the force acting on all contacts in the system will be of one magnitude. The magnitude of this force is given by

$$F = \frac{\langle \sigma_{kk} \rangle}{3} \bar{A}_m \quad \ldots \ldots \ldots \ldots \ldots \ldots \ldots \quad (4.93)$$

where $\bar{A}_m$ = an average area which transmits the stress normal to the contact region through the contact.

The approximations to the displacement at the center of a contact and the force transmitted through a contact, given by Eqn. (4.91) and Eqn. (4.93), respectively, will be used to determine the bounds on the effective bulk modulus.

To determine the bounds on the effective bulk modulus the integral appearing in Eqn. (4.83) and Eqn. (4.88) must be determined. The integral appearing in Eqn. (4.83) is used to determine the upper bound, on the effective bulk modulus. This integral must be determined for the case when the displacements are specified on the surface of the representative volume elements. The displacements being specified on the surface of the representative volume element are given by Eqn. (4.79). The integral appearing in Eqn. (4.88) is used to determine the lower bound on the effective bulk modulus. This integral must be determined for the case when the stresses are specified on the surface of the representative volume element. The surface tractions to be specified are given by Eqn. (4.86). The integral to be determined can be written as

$$\int_V \sigma_{ij}\varepsilon_{ij}\, dV = \int_{V_s} \overset{s}{\sigma}_{ij}\,\overset{s}{\varepsilon}_{ij}\, dV + \int_{V_f} \overset{f}{\sigma}_{ij}\,\overset{f}{\varepsilon}_{ij}\, dV \quad . \quad . \quad . \quad (4.94)$$

where V = total volume of the representative sample

V_s = volume of the solid phase

V_f = volume of the liquid phase

σ_{ij} = infinitesimal stress tensor

ε_{ij} = intinitesimal strain tensor

The superscripts, s and f, appearing in Eqn. (4.94) are used to denote quantities for the solid and fluid phases, respectively. From the results of Section 4.3.1, the integral taken over the fluid phase is given by

$$\int_{V_f} \sigma_{ij}^f \varepsilon_{ij}^f \, dV = \bar{\sigma}_u \, e_f \, V_f \quad \ldots\ldots\ldots\ldots\ldots\ldots \quad (4.95)$$

where e_f = the volumetric strain of the fluid phase

$\bar{\sigma}_u$ = the fluid pressure

When the fluid pressure, $\bar{\sigma}_u$, is known, the volumetric strain of the fluid phase, e_f, is determined by

$$e_f = \int_0^{\bar{\sigma}_u} \frac{dP}{K_f} \quad \ldots\ldots\ldots\ldots\ldots\ldots \quad (4.96)$$

where P = pressure

K_f = the bulk modulus of the fluid phase

The fluid pressure, $\bar{\sigma}_u$, appearing in Eqn. (4.95) and Eqn. (4.96) is taken to be negative for gauge pressures, P, greater than zero.

The solid phase of the representative volume element will be comprised of a number of spheres in contact. The spheres in the system bill be subjected to loads resulting from contacts with adjacent spheres as well as from the fluid pressure. Using the principle of superposition, the integral taken over the solid phase which appears in Eqn. (4.97) is written as

$$\int_{V_s} \sigma_{ij}^{s} \varepsilon_{ij}^{s} \, dV = \int_{V_s} [\sigma_{ij}^{c} + \sigma_{ij}^{p}] \, [\varepsilon_{ij}^{c} + \varepsilon_{ij}^{p}] \, dV \quad \ldots\ldots\ldots \quad (4.97)$$

In Eqn. (4.97), the superscripts c and p are used to denote the stress and strain fields occurring within a sphere, which result from contacts with adjacent spheres and the fluid pressure, respectively. The results for a sphere subjected to a uniform radial pressure are given in Section 3.4.3. Using this solution, σ_{ij}^{p} and ε_{ij}^{p} are given as

$$\sigma_{ij}^{p} = \bar{\sigma}_u \, \delta_{ij} \quad \ldots\ldots\ldots\ldots\ldots\ldots \quad (4.98)$$

$$\varepsilon_{ij}^{p} = \frac{1}{3 K_s} \bar{\sigma}_u \, \delta_{ij} \quad \ldots\ldots\ldots\ldots\ldots\ldots \quad (4.99)$$

where $\bar{\sigma}_u$ = the fluid pressure

K_s = the bulk modulus of the solid phase

δ_{ij} = Kronecker delta

Substitution of Eqns. (4.98) and (4.99) into Eqn. (4.94) yields

$$\int_{V_s} \sigma_{ij}^{s}\, \varepsilon_{ij}^{s}\, dV = \int_{V_s} \sigma_{ij}^{c}\, \varepsilon_{ij}^{c}\, dV + \frac{\bar{\sigma}_u}{3\, K_s} \int_{V_s} \sigma_{kk}^{c}\, dV$$

$$+ \bar{\sigma}_u \int_{V_s} \varepsilon_{kk}^{c}\, dV + \frac{V_s\, (\sigma_u)^2}{K_s} \quad \ldots\ldots\ldots\ldots\ldots\ldots \quad (4.100)$$

The terms σ_{kk}^{c} and ε_{kk} are invariant with respect to coordinate systems. Because of this the integrals containing these terms may be performed without transforming the solutions for the stress and strain fields due to a particular contact into one global coordinate system. The integral containing these terms were determined in Section 4.2.1. The values of these integrals are given by

$$\int_{V_s} \sigma_{kk}^{c}\, dV = 3\,(1+\nu_s)\, C_s\, M\, b_{-2}\, V \quad \ldots\ldots\ldots\ldots\ldots\ldots \quad (4.101)$$

$$\int_{V_s} \varepsilon_{kk}^{c}\, dV = \frac{3(1-2\nu_s) C_s\, M\, b_{-2}\, V}{2\, G_s} \quad \ldots\ldots\ldots\ldots\ldots\ldots \quad (4.102)$$

where M = the number of contacts between a particular sphere and adjacent spheres

C_s = the volume fraction of the solids contained in the system

G_s = the shear modulus of the solid phase

AD-A189 727 MICROMECHANICS MODELS FOR UNSATURATED SATURATED AND DRY SANDS(U) WISCONSIN UNIV-MADISON J K JEYAPALAN ET AL 25 JAN 88 AFOSR-TR-88-0154 AFOSR-84-0090 3/3

UNCLASSIFIED F/G 8/10 NL

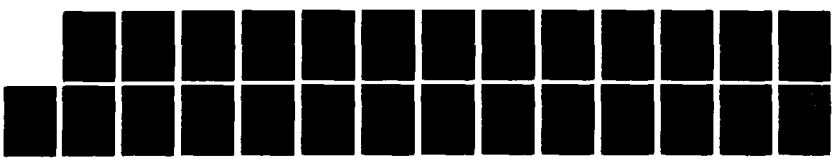

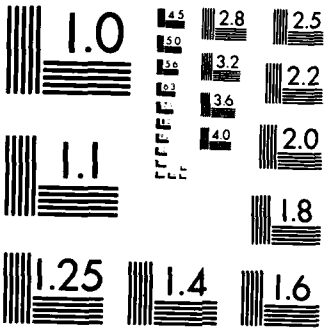

MICROCOPY RESOLUTION TEST CHART
NATIONAL BUREAU OF STANDARDS-1963-A

Following the above approach would yield for energy functionals

$$U_c^u = U_c^u (M, \beta_m, \psi_m, \phi', \nu_s) \qquad (4.103)$$

where M = the number of contacts on a particular sphere

β_m, ψ_m = the angles defining the position of contact m with respect to a global coordinate system

ϕ' = the angle defining the region of contact on a sphere

ν = Poisson's ratio for the sphere

For spheres arranged in a particular ideal packing configuration, the number of contacts on a particular sphere, N, and the angles β_m and ψ_m, are known. Therefore for a particular ideal packing configuration, the quantities, U_c^u and U_c^σ, may be presented as a family of curves for different values of ϕ' and ν_s.

The expressions for the upper and lower bounds on the effective bulk modulus, $\bar{K}$, may now be determined. The upper bound on the effective bulk modulus, $\bar{K}_u$, is determined for the case when the displacements are specified on the representative volume element. Combining Eqns. (4.41), (4.83), 4.94), 4.95), (4.100), (4.101), and (4.102)

gives the

$$\bar{K}_u = \frac{K_1 u}{K_2 u} \qquad (4.104)$$

The values of K_1^u and K_2^u are given by

$$\bar{K}_1^u = 4(1+\nu_s)\, C_s\, \sigma_u \quad 3\, K_s\, M\, \xi_o^u + 2\, \sigma_u$$

$$- \quad 2\, K_s ef \quad + 8(1+\nu_s)\, K_s\, \sigma_u\, ef$$

$$+ \quad 3(1-2\nu_s)\, C_s\, K_s\, U_c^u \tag{4.105}$$

$$\bar{K}_2 = 8(1k+\nu_s)\, C_s\, \langle \varepsilon_{kk} \rangle^2 \tag{4.106}$$

The lower bound on the effective bulk modulus, K_L, is determined from the case when the surface tractions are specified on the representative volume. Combining Eqs. (4.62), (4.88), (4.94), (4.95), (4.100), (4.101), and (4.102) gives the following for K_L,

$$\bar{K}_L = \frac{\bar{K}_1 L}{\bar{K}_2 L} \tag{4.107}$$

The values of $\bar{K}_1^L$ and $\bar{K}_2^L$ are given by

$$\bar{K}_1^L = \pi^2\, (1-\nu_s^2)^2 \quad s\, \langle \sigma_{kk} \rangle^2 \tag{4.108}$$

$$\bar{K}_2^L = 9 \left\{ \pi(1-\nu_s^2) \quad s \quad s\, \sigma_u \left[6\, (1-2\nu_s)\, M\, \xi_o^\sigma \right. \right.$$

$$\left. + \quad \pi(1-\nu_s^2)\, \sigma_u - \pi\, (1-\nu_s^2)\, ef \right] \tag{4.109}$$

$$+ 24\, (1-2\nu_s)\, (1+\nu_s)\, C_s\, K_s^2\, U_c^\sigma$$

In summary, the upper and lower bounds of the effective bulk modulus, $\bar{K}$, of the idealized solid¬fluid system under consideration are given by

$$\bar{K}_L = \leq \bar{K} \leq \bar{K}_u \tag{4.110}$$

The quantities, $\bar{K}_L$ and $\bar{K}_u$, are determined from Eqns. (4.101 to 4.106). The expressions for the upper and lower bounds show that the voids in the system have an effect on the effective bulk modulus when the fluid pressure is atmospheric. This was not the case for the effective bulk modulus determined from the volumetric averaging approach.

4.4 Effective Poisson's Ratio

In this section an effective Poisson's ratio, $\bar{\nu}$, will be determined for the idealized solid¬fluid system. This effective Poisson's ratio will be determined through the definition of this quantity. Poisson's ratio is defined as the negative of the ratio of lateral strain to longitudinal strain for a sample loaded along the longitudinal axis. Fig. 4.5 shows a sample undergoing uniaxial loading along the z axis. The dotted line shows the deformed shape of the sample due to the applied load. For the sample shown in Fig. 4.5, Poisson's ratio is determined as

$$\nu = \frac{\Delta_u / L_y}{\Delta_x / L_x} \tag{4.111}$$

where ν = Poisson's ratio

The effective Poisson's ratio for the solid¬fluid system can be determined in

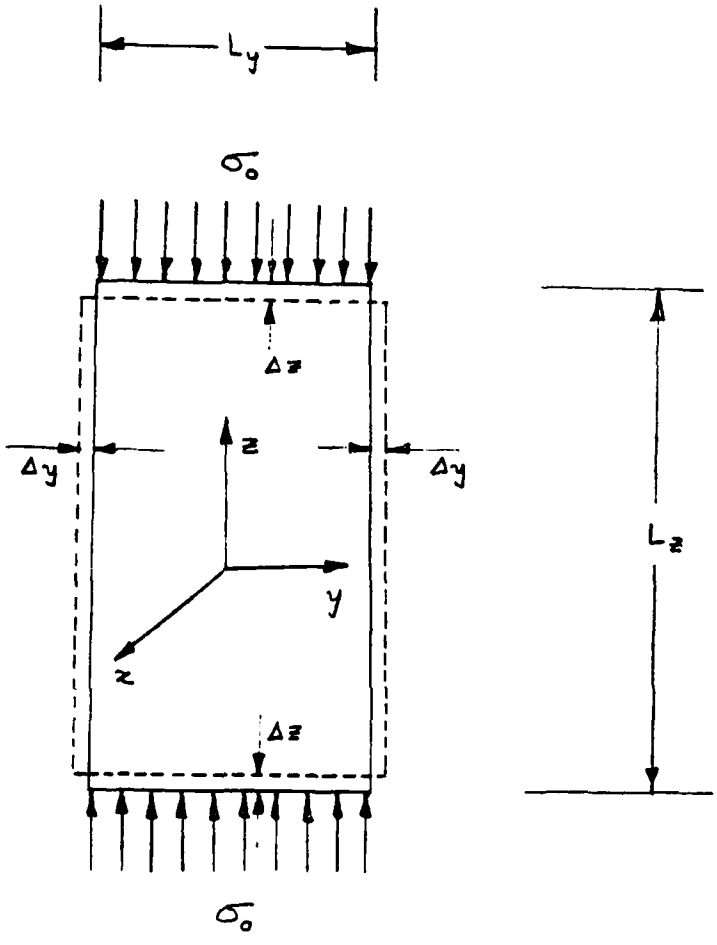

FIG. 45

the same manner as that given by Eqn. (4.111). The idealized solid-fluid system consists of a number of equal spheres arranged in ideal packing configurations. These spheres are surrounded by a fluid phase. The following assumptions are required in order to allow the determination of the effective Poisson's ratio,

1. The spheres in the system do not experience any rigid body motion.
2. Only normal forces are transmitted through contacts between adjacent spheres.
3. The fluid pressure in the system is at steady state conditions.

The first assumption is necessary so that the geometry of the spheres in the system remains known. The second assumption allows the use of the results given in Chapter 3 in determining the effective Poisson's ratio. The reason for the last assumption will be explained presently.

To determine the effective Poisson's ratio, the idealized solid-fluid system will be loaded in one direction only as shown in Fig. 4.6. The system may initially be stressed due to body forces. The effective Poisson's ratio will be determined from the displacements occurring in the system when the system is disturbed from its initial state. The addition of the stress, $\Delta\sigma_{zz}$, as shown in Fig. 4.6 may cause an increase in the fluid pressure as well as the stresses present in the spheres making up the solid phase. The effective Poisson's ratio of the system may be determined for the case when the fluid pressure has dissipated to its initial value (steady state condition). For this condition the additional stress, $\Delta\sigma_{zz}$, will be transferred to the solid phase and the effective Poisson's ratio may be determined by only considering this phase. If non-steady state conditions were considered, a sample of the material from within the system would be subjected to multi-axial stresses in reference to its initial state. Thus, the definition of Poisson's ratio could

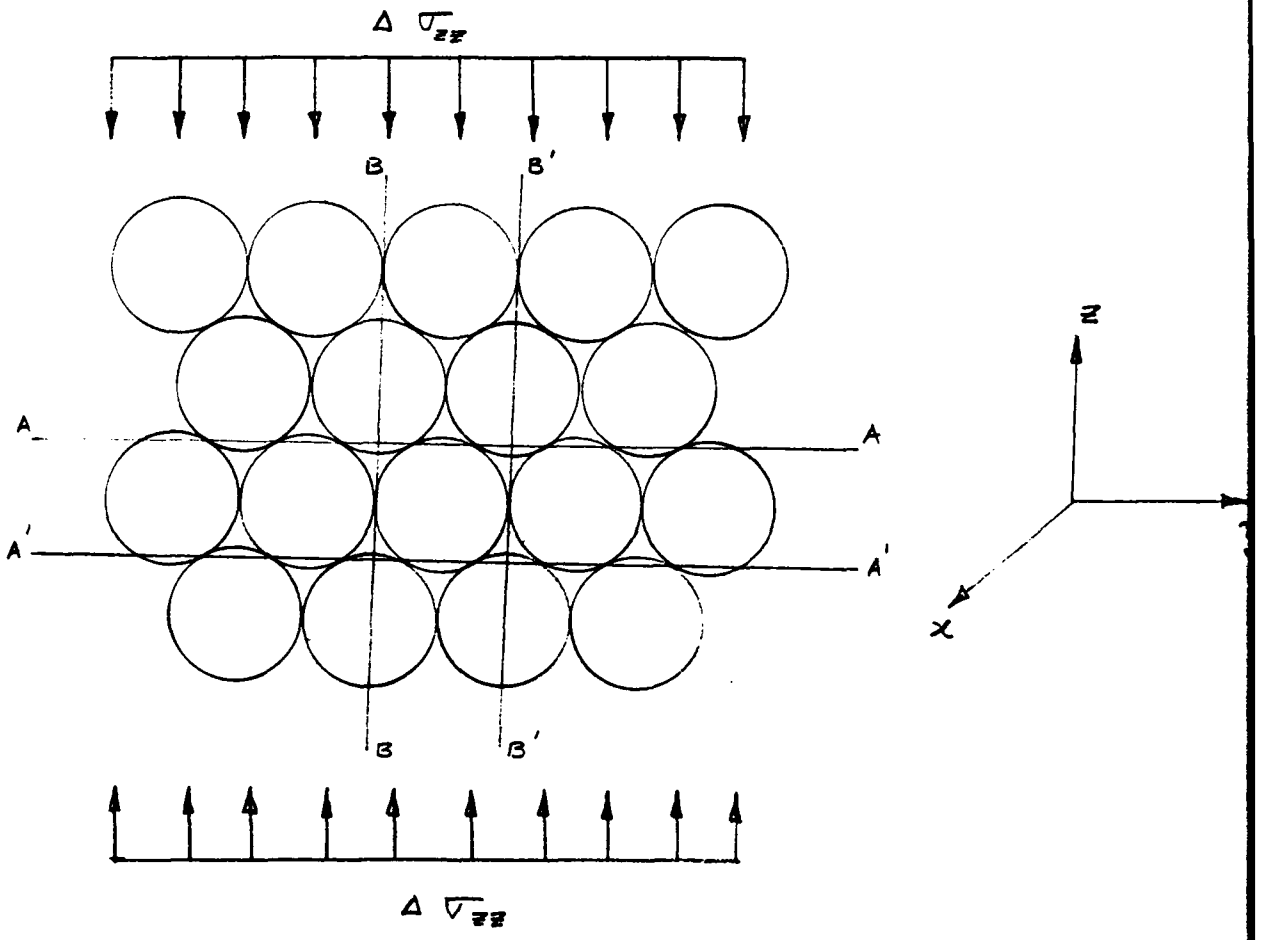

FIG 4.6

not be used to determine the effective Poisson's ratio. For steady state conditions, the change in stress on the system will be one directional and the definition of Poisson's ratio may be used to determine the effective Poisson's ratio. Under the loading shown in Fig. 4.6, the two planes, A¬A and A'¬A', will approach each other by some amount, while the two planes, B¬B and B'¬B', will move away from each other by some amount. These displacements may be determined from the results given in Chapter 3. From these displacements the effective Poisson's ratio may be determined. The change in the displacement vector at any point, (x, y, z), in the sphere, due to the addition load is given by

$$\left\{\Delta u\right\} = \left\{ \sum_{m=1}^{\frac{M^{\sigma}}{z}} [T_G]_m^T [T_L]_m^T \left[\left\{ \hat{u}^F \right\}_m - \left\{ \hat{u}^I \right\}_m \right] \right\}\Bigg|_{(x,y,z)} \qquad (4.112)$$

where M^{σ} = the number of contacts transmitting force

m = the contact of interest

In Eqn. (4.112), the superscripts F and I denote final and initial values of the displacement vector, in reference to a local spherical coordinate system, respectively. The symbol, Δ, appearing in this equation is used to denote the change in the displacement vector. The transformation matrices, $[T_G]$ and $[T_L]$, are given by Eqns. (3.140) and (3.141), respectively. The displacement vector, $\{\Delta u\}$, in reference to the global coordinate system is given by

$$\left\{\Delta u\right\} = \begin{Bmatrix} \Delta u_x \\ \Delta u_y \\ \Delta u_z \end{Bmatrix} \qquad (4.113)$$

The Eqn. (4.112) may be evaluated at contacts contained on the planes, A-A and A'-A', to determine the strain occurring between these planes. This strain is given by

$$\varepsilon_{zz} = \frac{\Delta u_z \big|_{C^\sigma}}{R \cos\beta_c} \qquad (4.114)$$

where C^σ = a contact which transmits force.

β_c = an angle defining the position of a contact transmitting force to the sphere

CHAPTER 5

EFFECTIVE MODULI OF AN IDEALIZED 3-PHASE SYSTEM

5.1 Introduction

In the previous chapter effective moduli for an idealized soil-water system was derived. This model may be applicable for a fully saturated system. In a partially saturated system where soil, water and air are in contact, previously derived moduli cannot be used. The compressible nature of the gaseous phase plays an important role. In this chapter an attempt is made to arrive at an effective moduli for the soil-water-air 3-phase system under idealized conditions. The approach used by Chang & Duncan (1974) is used in arriving at a compressibility parameter for this air-water system.

In this chapter, in the development of the effective moduli for a 3-phase system it is also assumed that the effective stress variation in a partially saturated granular void, changes with the degree of saturation.

5.2 The compressibility of the homogenized pore fluid of partially saturated soil

The compressibility of the homogenzied pore fluid $1/K_p$ is defined as the volumetric strain induced by a unit change in pore fluid pressure. It can be defined by the following equation

$$\frac{1}{K_p} = -\frac{d\,\varepsilon_p}{d\,\sigma_p} \qquad 5.1$$

where ε_p = volumetric strain of pore fluid

σ_p = pore fluid pressure

The homogenized pore fluid pressure can be expressed as a function of air pressure, water pressure and surface tension. It may be expressed

$$\sigma_p = f(\sigma_a , \sigma_w , T_c) \qquad 5.2$$

where σ_a = air pressure in the pore

σ_w = water pressure

T_c = surface tension

The compressibility of tne homogenized pore fluid, therefore, can be evaluated using the following eq.

$$K_p = \pi \left(\frac{\partial_f}{\partial\sigma_a} \cdot \frac{\partial\sigma_a}{\partial\varepsilon_p} + \frac{\partial_f}{\partial\sigma_w} \cdot \frac{\partial\sigma_w}{\partial\varepsilon_p} + \frac{\partial_f}{\partial T_c} \cdot \frac{\partial T_c}{\partial\varepsilon_p}\right) \qquad 5.3$$

If the form of Equation 5.3 is known, the compressibility of the homogenized pore fluid can be evaluated by knowing the changes in air pressure, water pressure, and tension due to unit change in volumetric strain. For the case in which the air bubbles are occluded, Eq. 5.3 reduced to:

$$K = \pi \frac{\partial\sigma_w}{\partial\varepsilon_p} \qquad 5.4$$

For this important practical case, the compressibility of the homogenized pore fluid can be evaluated using Boyle's law and Henry's law. This derivation is given in the following section.

Note that for clays with low degrees of saturation, open channels are likely

to be present. The behavior in such a case is extremely complicated. The approach here considers only granular soils.

5.3 Derivation of compressibility expression:

This derivation is based on Boyle's law and Henry's law.

Boyle's Law

Boyle's Law states that the product of pressure and volume of a gas is constant under constant temperature conditions:

Henry's Law

Henry's Law states that at a constant temperature, the weight of gas which can be dissolved in a given volume of liquid is directly proportional to the gas pressure.

Let V_d be the volume that would be occupied by the dissolved gas if it was extracted from the liquid and compressed to the pressure acting on the fluid. According to Boyle's and Henry's Laws this volume will be constant and thus independent of the pressure. V_d is only dependent on the volume of water and can be calculated as follows:

$$V_d = H\, V_w \qquad 5.5$$

where V_w is the volume of water, H is the coefficient of solubility. At 20°C, $H = 0.02$.

According to Dalton's division law, the saturated water vapor pressure in

the free air does not obey Boyle's Law. However, the saturated water vapor pressure is usually very small (Schuurman, 1966) and the influence can be disregarded.

According to Henry's Law, the volume of air dissolved in the water is proportional to the volume of water. The rate at which the air dissolves in the water depends on the air pressure. The time t necessary to dissolve the air for a unit change in pressure was shown by Beek (1963) to be

$$t = \frac{r^2}{D_f} \qquad 5.6$$

where D_f is the diffusion coefficient and r is the radius of the bubble. At 20°C, D_f is equal to 10^{-5} cm^2/sec. For small air bubbles, the time necessary to dissolve the air is very small. Therefore, it can be assumed that the air dissolves in the water instantaneously and that the water is always saturated with dissolved air.

As a result of the surface tension, T_c, the air pressure and the water pressure of an air-water mixture are not the same. The value of σ_w and σ_a are related by

$$\sigma_w = \sigma_a - \sigma_c \qquad 5.7$$

where σ_c is the capillary pressure due to surface tension. σ_c is usually expressed in terms of the meniscus radii, r_1, r_2, as shown in Fig. 5.1.

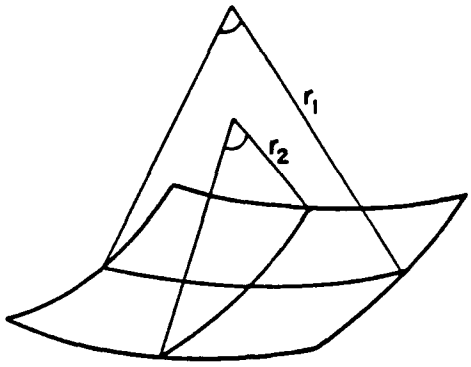

DOUBLY CURVED INTERFACE
BETWEEN AIR AND WATER

FIG. 5.1

$$\sigma_c = \frac{T_c}{r_1} + \frac{T_c}{r_2} \qquad 5.8$$

In a mixture of air and water, the bubbles do not necessarily all have the same shape and size. Therefore, it is assumed that:

$$\sigma_c = 2\,\frac{T_c}{R_c} \qquad 5.9$$

where R_c is the average capillary radius for the mixture of air and water. Generally, for soils with high degrees of saturation, the effect of σ_c is small.

If e_a is the volume of free air and e_s is the volume of dissolved air in the air-water mixture, then it follows from Boyle's and Henry's Law that

$$(e_a + e_s)\,(p_a + \sigma_a) = (e_{ao} + e_s)\,(p_a + \sigma_{ao}) \qquad 5.10$$

where p_a is atmospheric pressure, e_{ao} is the initial air volume and σ_{ao} is the initial air gauge pressure. Equation 5.10 can also be expressed as:

$$\sigma_a = \frac{(e_{ao} - e_a)P_a + (e_{ao} + e_a)\sigma_{ao}}{e_a + e_s} \qquad 5.11$$

Using expressions 5.7 and 5.11, the pore water pressure may be expressed as:

$$\sigma_w = \frac{(e_{ao} - e_a)p_a + (e_{ao} - e_s)\sigma_{ao}}{e_a + e_s} - \frac{2T_c}{R_c} \qquad 5.12$$

The compressibility of the air-water mixture is,

$$\frac{1}{K_p} = -\frac{d\varepsilon_p}{d\sigma_w} = -\frac{1}{(1+e_o)}\frac{d_{ea}}{d\sigma_w} \qquad 5.13$$

where e_o is the initial voids ratio.

$$\frac{d\sigma_w}{de_a} = -\frac{(e_{ao} + e_s)P_a + (e_{ao} + e_s)\sigma_{ao}}{(e_a + e_s)^2} + \frac{2T_c}{R_c^2}\frac{de_c}{de_a} \qquad 5.14$$

In terms of degree of saturation S and void ratio e

$$\frac{d\sigma_w}{de_a} = -\frac{(e_o - Se_o + HS_oe_o)(u_{ao} + P_a)}{(e - Se + HSe)^2} + \frac{2T_c}{R_c^2}\frac{dR_c}{dS}\frac{S}{e} \qquad 5.15$$

Substituting Eq. 5.13 into Eq. 5.15, the compressibility of the homogenized pore fluid can be expressed as:

$$\frac{1}{K_p} = \frac{\frac{1}{(1+e_o)}}{\frac{(e_o - Se_o + HS_oe_o(\sigma_{ao}+P_a)}{(e-Se+HSe)^2} - \frac{2t_c}{R_c^2}\frac{dR_c}{dS}\frac{S}{e}} \qquad 5.16$$

where K_p = Bulk modulus of the air-water moisture

e_a = initial voids ratio

S_o = initial degree of saturation

e = voids ratio

S = degree of saturation

H = Coeff. of solubility

T_c = Surface tension

R_c = Average capillary radius

σ_{ao} = initial gage air pressure

If the surface tension term in Eq. 16 is neglected, the equation reduces to a form similar to that suggested by Hilf (1948) and Skempton and Bishop (1954). The comparison between test data obtained by Mitchell et al., (1965) and the results predicted by Hilf's and Skempton and Bishop's equation is shown in Fig. 5.2.

Schuurman (1966) took surface tension into account by assuming that the air bubbles were all of equal size and spherical in shape. By this assumption, the value of R_c in Eq. 5.9 would be equal to the radius of the air bubbles. Taking the initial radius of air bubbles as R_o, the radius after a change in void ratio can be expressed as

$$R_c = R_o \left(\frac{e_a}{e_{ao}}\right)^{1/3}$$

By substituting this expression into Eq. 5.15, the compressibility of this air-water mixture can be calculated. A comparison between test data obtained by Mitchell et al. (1965) and the results predicted by Schuurman's equation is shown in Fig. 5.2.

It seems likely that the discrepancies between experimental data and the results predicted by Hilf's and Skempton and Bishop's equation are mainly due to the negligenece of the effect of surface tension. The discrepancies between the experimental data and the results predicted by Schuurman's equation are probably due to the assumption that all the bubbles are spherical and uniform, and that the total number of bubbles does not change during the compression of the soil.

A further consideration relative to surface tension effects is that the capillary pressure does not necessarily arise only from the bubbles. It can also arise from the other water surfaces exposed to air at the specimen boundaries. Therefore, it seems more reasonable to use an empirically determined average capillary radius R_c to simulate capillary effects.

It has been found that the calculated results agree quite well with the test by Mitchell et al. (1965) if it is assumed that the average capillary radius R_c and the degree of saturation are related as follows:

$$R_c = R_{cs}\left(\frac{S - S_f}{1 - S_f}\right) \qquad 5.19$$

where R_{cs} is the capillary radius at saturation. The comparison is shown in Fig. 5.3. S_f is the lowest degree of saturation at which the water begins to flow freely. S_f may be found from permeability tests for samples with different degrees of saturation. For the clay tested by Mitchell, et al., S_f was found to be zero. It was also found that the relation between the water pressure and the degree of saturation was approximated best by adopting a value of $2T_c/R_{cs}$ = 5 psi. At 20°C, the value of T_c is 74×10^{-6} kg/cm. The value of $2T_c/R_{cs}$ = 5 psi corresponds to an effective value of R_{cs} equal to 4.23×10^{-4} cm.

5.4 Effective Bulk modulus of a 3-phase system.

Previously an expression was derived for the effective bulk modulus of a saturated 2-phase soil-water system. The bulk modulus expression in Eqn. 4.66 is further modified here for a 3-phase soil-water-air system in light of the

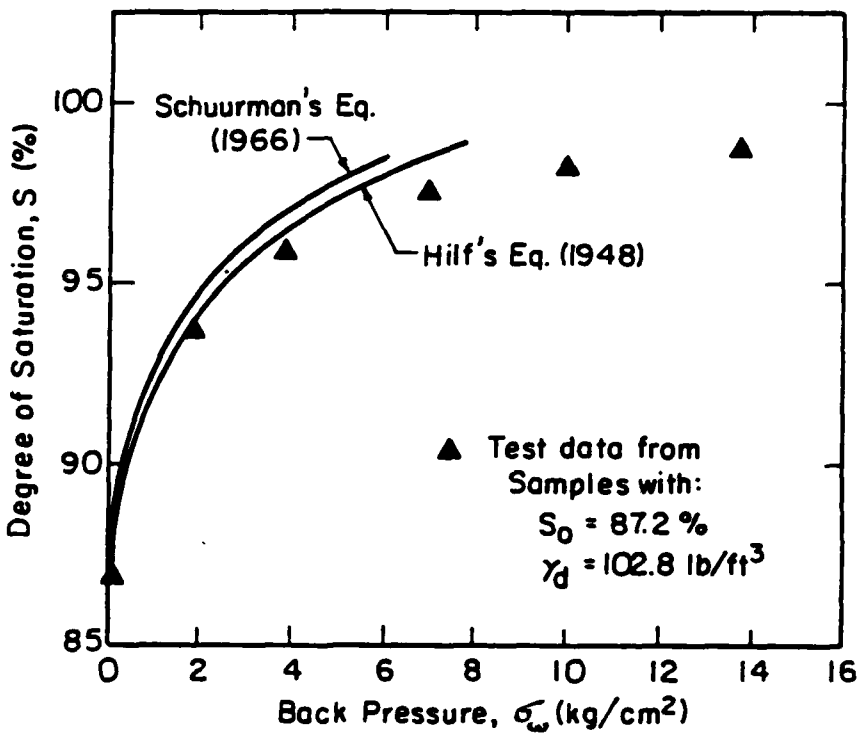

CALCULATED AND MEASURED VARIATIONS OF
DEGREE OF SATURATION WITH BACK PRESSURE

(Data from Mitchell, et al., 1965)

FIG. 5.2

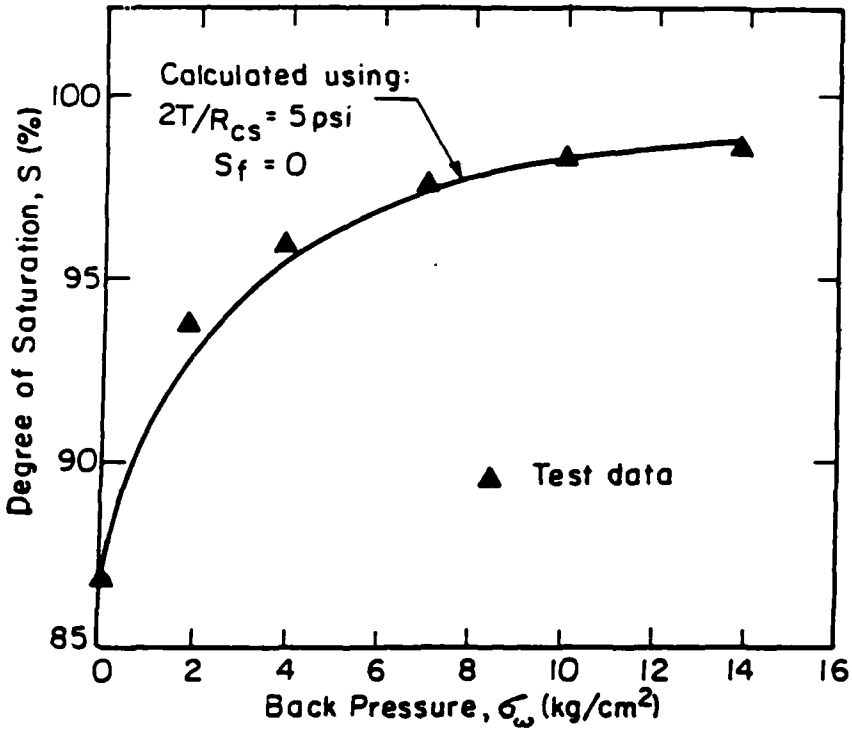

COMPARISON BETWEEN MEASURED VARIATION OF DEGREE OF SATURATION AND THAT CALCULATED ASSUMING

$$R_c = R_{cs} \frac{S - S_f}{1 - S_f}$$

(Data from Mitchell, et al., 1965)

FIG. 5.3

compressibility expression for a water-air mixture derived before.

In Eq. 4.66 the parameters affected by the degree of saturation are c_f, σ_u, e_f and ξ_o^σ.

Assuming that the pore pressure in partially saturated systems is directly related to the degree of saturation via χ ,where χ is an empirical parameter given in Fig. 5.4 in the relation

$$\sigma' = \sigma - \sigma_a + \chi\ (\sigma_a - \sigma_w) \qquad 5.18$$

The volumetric strain for a partially saturated system, e_f^*, can be determined from the following expression

$$e_f^* = \frac{\sigma_u^*}{K_p} \qquad 5.19$$

where K_p = Bulk modulus of the air-water mixture.

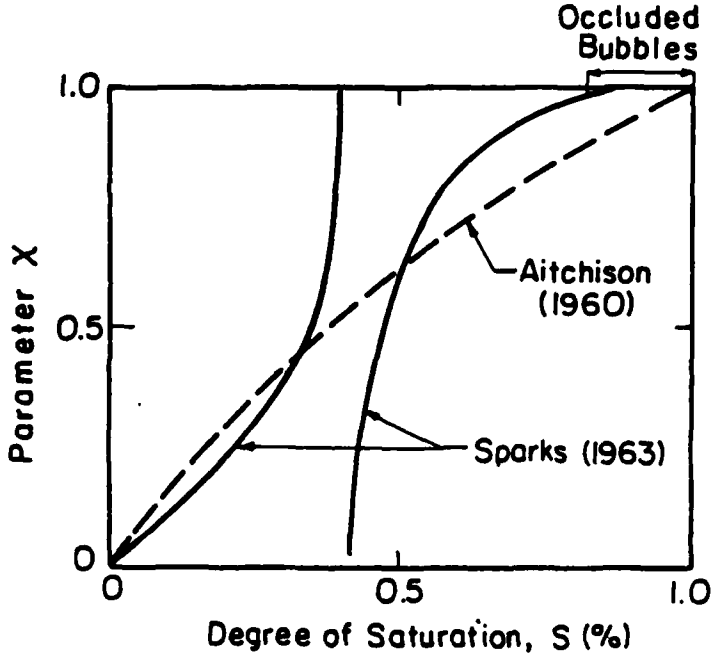

VARIATIONS OF χ WITH DEGREE OF SATURATION

FIG. 5.4

CHAPTER 6
CONCLUSIONS AND RECOMMENDATIONS

From this investigation, the following conclusions can be drawn:

1. The modelling of even saturated systems using the micromechanics approaches is quite complicated, and the degree of complexity is far greater with such approaches for partly saturated systems.

2. Numerous assumptions need to be made in order to arrive at the stress-strain response of partly saturated systems using the micromechanics-based models. However, one could obtain some insight into the fundamental behavior of partly saturated systems in this methodology.

3. The expressions developed for effective moduli, and the procedure outlined for poisson's ratio should be valuable in modelling behavior of partly saturated systems.

4. Although the immediate usefulness of this type of modelling approach may not be that evident, the long term potential for improving the understanding of the behavior of partly saturated soils is great.

The recommendations for futher research include the possible elimination of some of the assumptions based on experimental data, and validation of predictions by the newly developed models on various partly saturated systems using results from controlled experiments. Another useful further research effort would be to extend this work for time-dependent behavior and strain-rate dependent behavior.

References

1. Barder, L., Ismail, H. and Tong, "Plane Deformation of Granular Material at Low and High Pressures", Geotechnique 19, pp. 441-452, 1969.

2. Bhatt, J. J., Carroll, M. M. and Schatz, J. F., "A Spherical Model Calculation for Volumetric Response of Porous Rocks", J. Appl. Mech., 42, pp. 363-368, 1975.

3. Bokkovitch, T. R., "A Technique for Generating Pressure Volume Relationship and Failure Envelopes for Rocks", Lawrence Livermore Laboratory Report, UCRL-51441, Livermore, CA, 1973.

4. Carroll, M., and Hall, A.C., "Suggested Modification for the P-K Model for Porous Materials", J. App. Phys., Vol. 43, No. 2, pp. 759-761, 1972.

5. Carroll, M.M., and Holt, A. C., "Static and Dynamic Pore Collapse Relations for Ductile Porous Materials", J. Appl. Phys., Vol. 43, No. 4, pp. 1626-1636, 1972.

6. Chadwick, P., "Compression of a Spherical Shell of Work Hoardening Material", Ind. J. Mech. Sci.,5, pp. 165-182, 1963.

7. Chu, T. Y., and Hashin, Z., "Plastic Behavior of Composites and Porous Media Under Isotropic Stress, Ind. J. Engrg. Sci. 9, pp. 972-994, 1971.

8. Duncan, J. M. and Chang, Y-Y., "Non-Linear Analysis of Stress and Strain in Soils", J. Soil Mech. and Foundation Div., ASCE, Vol. 96, No. SM5, 1970.

9. Grydman, S., Zeitlin, J. G., and Alpan, I., "The Yieldikng Behavior of Particulate Media", Can. Geotech. J. 10, pp. 341-362, 1973.

10. Hashin, Z., "The Elastic Moduli of Hetregeneous Materials", J. Appl. Mech. 29, pp. 143-150, 19726

11. Hashin, Z., Mechanics of Composite Materials, Pergamon Press, 1970.

12. Herrmann, W., "Constitutive Equations for Compaction of Porous Materials", Symposium on Appl. Mech. Aspects of Nuclear Effects in Materials, ASME, Wiknter Ann. meeting, Nov. 28-Dec. 3, 1971, Washington, D.C.

13. Kakov, A.K. and Chakladev, A.C.D., "Deformation Theory of Hod-Pressing", J. Appl. Phys. 38, pp. 3223-3230, 1967.

14. Ko, H. Y., and Scott, R. F., "Deformation of Sand in Hydrostatic Compression", J. Soil Mech. Found. Div., ASCE 93, pp. 137-156, 1967.

15. Kreher, W., and H. G. Schopf, "Effective Elastic-Plastic Compressibility of Porous Bodies", Int. J. Solids Structures 9, pp. 1331-1348, 1973.

16. Mackenzie, J. K., "The Elastic Constants of a Solid Containing Spherical Holes", Proc. Phys. Soc. 863, pp. 2-11, 1950.

17. Mandl, A. and Luque, R. F., "Fully Developed Plastic Shear Flow of Granular Materials", Geotechnique 20, pp. 277-307, 1970.

18. O'Connell, R. J. and Budiansky, B., "Seismic Velocities in Dry and Saturated Craked Solids", J. Geophys. Res. 79, pp. 5412-5426, 1974.

19. Rowe, P. N., "The Stress-Dilatency Relation for Static Equilibrium of an Assembly of Particles in Contact", Proc. Royal Society of London, Ser. A, Vol. 269, pp. 50-527, 1962.

20. Schatz, J. F., Carroll, M. M., and Chung, D. H., "A Model for the Inelastic Volume Deformation in Dry Porous Rocks", EOS, Trans. Amer. Geop[hys. U. 56, pp. 1195, 1979.

21. Schofield, A., and Wroth, P., Critical State Soil Mechanics,McGraw Hill, London, 1961.

22. Sternberg, E., Eubanks, R. A., and Sadowsky, M. A., "On the Axisymmetric Problem of Elasticity, Theory for a Region Bounded by Two-Concentric Spheres".

23. Timoshenko, S. and Goodier, J. N., Theory of Elasticity, 2nd Ed., McGraw-Hill, New York, N.Y., 1951.

24. Torre, C., "Theorie Und Verhalten Zusammengeprebteer Pulver", Berg-U. Hultenmannische Monatshetic 93, 62, 1948.

25. Warren, N., and Anderson, O. L., "Elastic Properties of Granular Materials Under Uniaxial Compaction Cycle", J. Geophys. Res. 78, pp. 691-695, 1973.

26. Wilkins, J.K., "A Theory for Shear Strength of Rock Fill", Rock Mechanics 2, pp. 205-272, 1970.

END

DATE

3-88

DTIC